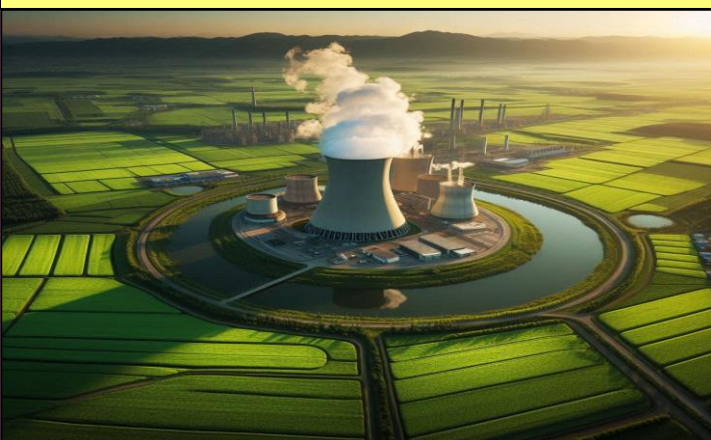


Peer-reviewed, Partially Open-access Journal

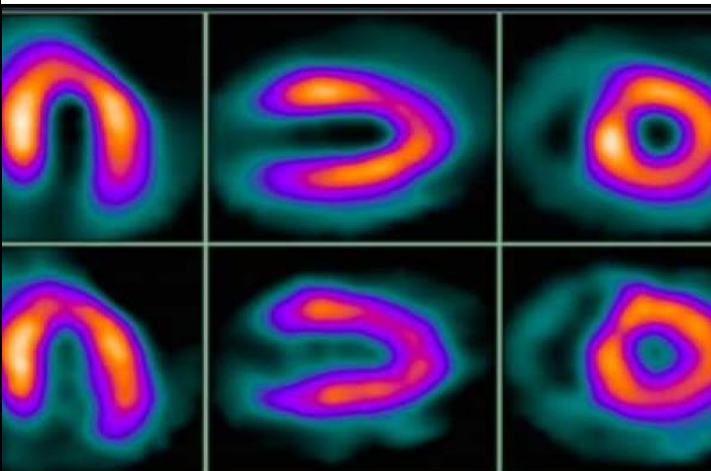
**Nuclear Reactor**



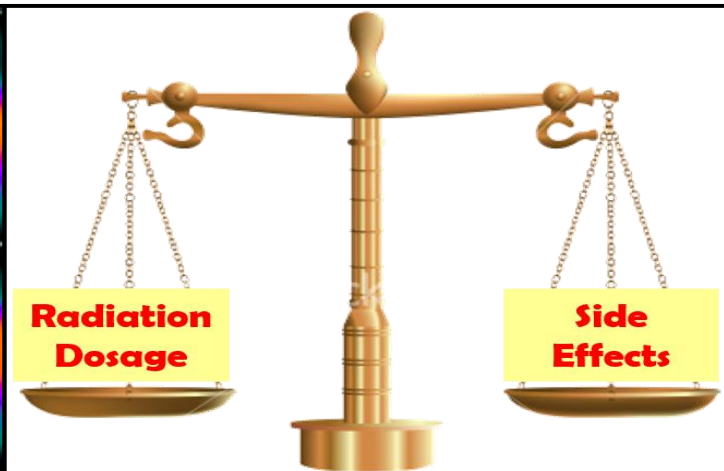
**Radiation therapy**



### **Nuclear Energy for Sustainable Development and Environmental Management**



**Myocardial Perfusion Scan for Heart Health**



**Radiation Safety : A Balance between Dose and Effects**

## **About CNS&E**

Current Natural Science & Engineering (CNS&E) Journal publishes new, innovative and cutting-edge research in Natural sciences including physical, chemical, biological, agricultural and environmental sciences, metrology, and other related interdisciplinary fields. Scientific research results in the form of high-quality manuscripts, review articles, mini-reviews, reports, news and short communications are highly welcome.

CNS&E is a partially Open Access, bimonthly, multidisciplinary journal published by the Vigyanvardhan Blessed Foundation (VBF), a non-profit organization working to disseminate science for the betterment of society.

**Scope:** CNS&E journal has a broad multidimensional scope. It publishes research in the areas of:

- Hydrogen & Renewable Energy
- Environmental Sciences & Hydroelectric Cell
- Artificial Intelligence Convergence in S&T
- Net Carbon Zero & Earth Sustainability
- Condensed Matter & Nanomaterials
- Health Science & Technology
- Nuclear Science: Health & Society
- Measurement Science & Industrial Research
- Digital & Sustainable Agriculture
- Smart Engineering Materials & Sensors

**Publication Policy:** The journal maintains integrity and high ethical values. Submitted manuscripts are peer-reviewed and evaluated for novel scientific content irrespective of its origin. The information about a submitted manuscript will be confidential and will not be disclosed other than Chief Editor, editorial staff, corresponding author, reviewers, and the publisher. The journal ensures that any unpublished work must not be used in Editor's, and reviewer's own research without the explicit written consent of the author(s).

**Publication Decisions:** The Chief Editor of the journal is responsible for deciding the publication or rejection of the submitted manuscript. The Chief Editor may take suggestion with other editors or reviewers in making decision.

**Publisher:** VB Foundation

## **CNS&E Editorial Board**

### **Chief Editor**

**Prof. (Dr.) R K Kotnala,**

Former Chairman NABL, Raja Ramanna Fellow DAE &  
Chief Scientist, CSIR-National Physical Laboratory

### **Senior Editors**

**Prof. A C Pandey**

Director, Inter University Accelerator  
Centre, New Delhi, India

**Prof. K K Pant**

Director IIT Roorkee, Uttarakhand, India

**Prof. R K Sinha** Vice Chancellor,

Gautam Buddha University, G Noida, India

**Prof. Bhanooduth Lalljee,**

President, Sustainable Agricultural  
Organisation, External Professor at the  
Mauritius Institute of Education (MIE) and  
JSS Academy, Mauritius.

### **Editors**

**Dr. Indra Mani**

Vice-Chancellor, Vasantrya Naik  
Marathwada Krishi Vidyapeeth,  
Maharashtra, India

**Prof Ajay Dhar**

Associate Director, Academy of Scientific  
and Innovative Research, AcSIR,  
Ghaziabad-UP, India

**Dr A K Srivastava**

Director, CSIR-Advanced Materials and  
Processes Research Institute, CSIR-  
AMPRI, Bhopal

**Dr. S K Jha**

Outstanding Scientist and Head, Radiation  
Protection Section (Nuclear Fuels) Health  
Physics Division & Professor, HBNI,  
Bhabha Atomic Research Centre, Mumbai.

**Dr. Nasimuddin**

Principal Scientist, Antenna and Optical  
Department, Institute for Infocomm  
Research; Agency for Science,  
Technology, and Research, Singapore.

### **Associate Editors**

**Prof. Kedar Singh**

Professor & Dean of School of Physical  
Sciences, Jawaharlal Nehru University,  
New Delhi, India

**Prof Rajesh Punia**

Head of Department, Department of  
Physics, MDU, Rohtak, India

**Dr Jyoti Shah**

DST-WoSA, CSIR-National Physical  
Laboratory, India

**Dr. Rakesh Kr Singh**

Academic Head, Aryabhata Center for  
Nano Science and Nano Technology,  
Aryabhata Knowledge University, Patna,  
India

## CNS&E Volume 1, Issue 5, October 2024

### Table of contents:

S. No.	Title and Author	Page No.
1.	<i>Chief Editor's Message</i> <b>Importance of Nuclear Energy to Accomplish Net Zero Carbon</b> Prof R K Kotnala	<b>360</b>
2.	<i>Guest Editorial</i> <b>Nuclear Energy's Role in Sustainability and Environmental Protection in India</b> Dinesh K Aswal and Anirudh Chandra	<b>361-370</b>
3.	<i>Preface to Special Theme</i> <b>Global Warming and Climate Change – Need of Nuclear Energy</b> S K Jha and S K Sahoo	<b>371-374</b>
4.	<b>Bandgap Engineering and Frequency Dispersive Dielectric Properties of Rare Earth (Sm<sup>3+</sup>) Modified Ba<sub>0.8</sub>Sr<sub>0.2</sub>TiO<sub>3</sub> Ceramics for Potential Use as an Optoelectronic Materials</b> Jyotirekha Mallick and Manoranjan Kar	<b>375-380</b>
5.	<b>Geometry Dependent Microwave Absorption Properties in Carbonaceous Materials over X-Band Frequencies (8.2-12.4 GHz) for Stealth Applications</b> Lokesh Saini, Priyambada Sahoo, Raj Kumar Jani, Ambesh Dixit	<b>381-392</b>
<b>Special Theme Manuscripts</b>		
6.	<b>Decentralized Clean Energy for Rural India: The Role of Small Modular Reactors</b> Anirudh Chandra* and D K Aswal	<b>393-405</b>
7.	<b>Uranium Mill Tailings Generation and Management Challenges</b> Pallavi Singhal, Sanjay. K. Jha	<b>406-415</b>

8.	<b>Spatial Distribution of Water Quality Parameters in a Mineralized Region of Rajasthan</b> V. K. Thakur, P. Lenka, Sumesh C. G., Gopal P. Verma, Aditi C. Patra	<b>416-420</b>
9.	<b>Modeling Cs-137 Migration in Groundwater due to Low Probability Event of Leaching from Near Surface Disposal Facility for Low Level Solid Radioactive Waste</b> Shelly Goel, Manish Chopra, R.B. Oza	<b>421-425</b>
10.	<b>Radon and Gamma Radiation Dose to the Population Residing Near the Uranium Mill Tailings Disposal Site in Uranium Mineralized Zone at Jaduguda</b> Gopal P. Verma, N. K. Sethy, Aditi C. Patra, V. N. Jha and K. A. Dubey	<b>426-433</b>
11.	<b>Thermodynamic and Kinetic Studies on the Pyrophoricity of Uranium Flakes</b> Saparya Chattaraj and P. Srinivasan	<b>434-441</b>

**Chief Editor's Message****Importance of Nuclear Energy to Accomplish Net Zero Carbon****Prof R K Kotnala**

FNASC, FIGU, FMSI

Chief Editor, Current Natural Sciences &amp; Engineering, Journal (CNS&amp;E)

**Prof R K Kotnala**

\* Corresponding author email: rkkotnala@gmail.com

The world is entangled with the urgent need for existing energy modes transition to clean energy for mitigating global warming and climate change. It ultimately demands to set stringent goals for achieving net zero carbon for each country. In this direction different approaches are being stipulated and one of the important options emerges as nuclear power, a compelling option for sustainable development. Unlike renewable energy sources such as solar, wind and nuclear energy which provides a continuous and reliable supply of electricity with minimal greenhouse gas emissions. On the other hand nuclear power plants operate with high capacity factor compared to variable renewable sources that depend on weather conditions and its reliability makes nuclear energy a strong candidate for baseload power. Moreover, nuclear energy's low carbon footprint and high energy density output makes it an attractive alternative to fossil fuels. Although, it is crucial to acknowledge the challenges associated with nuclear energy, including the safe management of nuclear waste, the risk of nuclear accidents, and the high upfront costs of building nuclear power plants. Hence, a balanced perspective on the future of nuclear energy and its potential to contribute to a sustainable future is to be adopted carefully. However, a periodic advancements in technology and stringent safety measures, modern Nuclear reactors are designed to minimize environmental impact and enhance safety.

However, nuclear radiations are being used carefully and responsibly as powerful tools in healthcare medical imaging (PET Scan), radiotherapy in cancer treatment, therapeutic usages and different industries as tracers. The other critical aspects of applications are in manufacturing, agriculture and in environmental monitoring which consists of radioactive tracers injected into water sources to track the movement of water underground or in rivers and tracers are used to study soil erosion rates and identify areas prone to erosion etc. In the interest of Researchers, Engineers and scientific community CNS&E Journal took an initiative to publish fifth issue with a special theme to address "Nuclear Energy for Sustainable Development and Environmental Management."

For this issue Dr D K Aswal, Director HSEG Bhabha Atomic Research Centre (BARC), Trombay has been invited to write a Guest Editorial on Nuclear Energy's Role in Sustainability and Environmental Protection in India and Dr S K Jha, Outstanding Scientist, BARC has been entrusted with Thematic Editorship.

Further, CNS&E journal is highly thankful to Dr D K Aswal, Dr S K Jha and the editors team of the journal for bringing out this issue. Nevertheless, Prof Nand Lal Singh NSUT, Delhi, Dr Amit Partap Singh, Indore and Dr Anurag Gaur, NSUT deserve a special thanks for their special efforts for the Journal.

**Guest Editorial**

**Nuclear Energy's Role in Sustainability and  
Environmental Protection in India**

**Dinesh K Aswal\* and Anirudh Chandra**

*Health, Safety and Environment Group  
Bhabha Atomic Research Center, Trombay, Mumbai 400085*

\* Corresponding author email: [dkaswal@yahoo.com](mailto:dkaswal@yahoo.com)



**Dr. D K Aswal**

The world today stands at a critical juncture, grappling with the profound and far-reaching impacts of climate change. The increasing frequency of extreme weather events, rising sea levels, and deteriorating ecosystems only serve to underscore the urgency of transitioning to a low-carbon economy. Governments across the globe are intensifying their climate policies, striving to meet the ambitious goals set forth in international agreements such as the Paris Agreement. Central to these efforts is the systematic decarbonization of national energy mixes [1], where nations are increasingly turning to green and clean technologies to power their economies and ensure sustainable electrification. In this global race to mitigate climate change, renewable energy sources like wind, solar, and hydropower are often highlighted as the vanguards of a sustainable future [2]. However, the challenge lies not only in generating sufficient clean energy but also in ensuring a reliable and continuous supply that can meet the growing demands of an energy-hungry world.

For India too, the stakes are particularly high. With a rapidly growing population and an expanding economy, the demand for energy is set to surge dramatically in the coming decades [3]. At the same time, India is committed to its nationally determined contributions (NDCs) under the Paris Agreement, aiming to reduce its greenhouse gas emissions intensity and increase the share of non-fossil fuel-based energy in its power generation capacity [4]. Balancing these competing priorities—meeting the burgeoning energy needs of its citizens and industries while adhering to climate goals—poses a formidable challenge.

In this context, nuclear energy offers a compelling solution. As a source of clean energy, nuclear power generates electricity with virtually no greenhouse gas emissions during operation [5]. Moreover, nuclear plants occupy less land and have a minimal ecological footprint compared to other large-scale energy sources [6]. With advancements in technology, modern nuclear reactors are safer, more efficient, and capable of playing a key role in India's energy mix. They can provide the continuous, large-scale power needed to support industrial growth, urbanization, and the rising aspirations of millions, all while contributing to the nation's climate objectives.

This editorial for the special issue on "Nuclear Energy for Sustainable Development and Environmental Management" highlights how nuclear power can push India toward a sustainable energy future, striking a balance between economic growth and environmental preservation.

### **Where does nuclear power stand in today's world?**

To understand the role of nuclear energy today, it is essential to look at both global and national perspectives. Nuclear power currently generates 2,602 TWh of electricity, accounting for nearly 9% of global electricity production [7]. With approximately 440 nuclear power plants in operation across 31 countries, the world has accumulated around 20,000 reactor years of operational experience [7]. This has been achieved through a period of rapid growth in the 60s to 80s, followed by a gradual stagnation and decline since the 90s and early 2000s. But in recent times, nuclear energy has seen a resurgence, driven by the volatility in energy markets, especially in Europe following Russia's invasion of Ukraine. This situation is further intensified by rising fossil fuel prices and the global push to meet climate change targets.

While the revival of nuclear power in developed economies of the Global North has been gradual, it is the developing economies of the Global South that are expected to drive nuclear growth in the coming years [8]. India and China stand out as countries that have consistently pursued civilian nuclear power programs over the decades, positioning themselves as key players in the future expansion of nuclear energy [9].

In India, nuclear power currently contributes about 1.8% of the country's installed power capacity and nearly 3% of its national electricity needs [10]. The country operates 23 nuclear power plants with an average capacity factor of 83% and an availability factor of 86% [11]. Recently, the newly commissioned 700 MWe units, KAPS 3 and 4 in Gujarat, have begun full-power operations, supplying electricity to the grid [12]. India's nuclear energy outlook is further strengthened by the core loading of the Prototype Fast Breeder Reactor (PFBR) at Kalpakkam [13] and its regulatory permission for first approach to criticality [14], marking the beginning of the long-anticipated second stage of India's three-stage nuclear program. With multiple projects in various stages of development [15] and several uranium supply agreements signed with countries like Uzbekistan, Kazakhstan, Russia, Canada, and France [16] [17], India is poised to significantly expand its nuclear power program in the coming decades.

### **How does nuclear energy enable sustainable development?**

Going forward in the nuclear journey, it is important to understand what makes this energy source so significant. Nuclear energy plays a crucial role in enabling sustainable development by offering a reliable, low-carbon energy source that supports economic growth, social well-being, and environmental protection (see **Error! Reference source not found.** for an illustrative understanding).

Sustainable development is about meeting the needs of the present without compromising the ability of future generations to meet their own needs [18]. In this context, nuclear energy is a key player, particularly in mitigating climate change. Nuclear power plants generate electricity with minimal direct emissions of carbon dioxide (CO<sub>2</sub>) [19], making them essential in strategies aimed at decarbonizing the energy sector. As countries transition away from fossil fuels, nuclear energy provides a stable and consistent power source that complements intermittent renewable energy sources like wind and solar, ensuring a reliable supply of electricity while reducing the overall carbon footprint.

The reliability and stability of nuclear power are significant advantages [20], especially when compared to some renewable energy sources that depend on weather conditions. Nuclear power plants operate continuously, providing a consistent and stable supply of electricity essential for supporting industrial activities, economic development, and essential services like healthcare and education. Furthermore, nuclear energy enhances energy security by reducing dependence



on imported fossil fuels [21], thereby reducing vulnerability to global energy market fluctuations and geopolitical risks, supporting long-term economic stability.

Nuclear energy also contributes to economic development and job creation [22]. The nuclear industry creates high-skilled jobs in engineering, construction, operations, and maintenance, offering higher wages and long-term career opportunities. This, in turn, drives economic expansion, increases productivity, and improves living standards. Additionally, nuclear power supports industrial growth by providing a reliable and affordable electricity source, critical for infrastructure development and overall economic growth.

From an environmental perspective, nuclear energy is beneficial due to its minimal land use and efficient resource utilization [6]. Nuclear power plants require significantly less land than many renewable energy sources, which helps preserve natural habitats and ecosystems, supporting biodiversity. Moreover, nuclear energy is highly energy-dense, meaning it produces a large amount of energy from a small amount of fuel, reducing the environmental impact associated with mining and resource extraction.

In the long term, nuclear energy supports sustainable development by future-proofing energy needs. As populations grow and energy demands increase, nuclear power offers a viable solution that can meet these demands without exacerbating environmental problems. Advances in technology have also led to effective waste management practices, including long-term storage solutions [23] and the potential for recycling nuclear fuel [24], ensuring that waste is managed safely and sustainably.

Finally, nuclear energy accommodates technological innovation. Continued research and development in nuclear technology, such as Small Modular Reactors (SMRs) and Generation IV reactors, are leading to safer, more efficient, and more flexible nuclear power options. These innovations address some challenges associated with traditional nuclear energy, such as high capital costs and safety concerns, making nuclear power an even more sustainable option. Moreover, nuclear energy can work synergistically with renewable energy sources, providing the consistent power needed to balance the intermittency of renewables, supporting the development of a more resilient and sustainable energy grid.

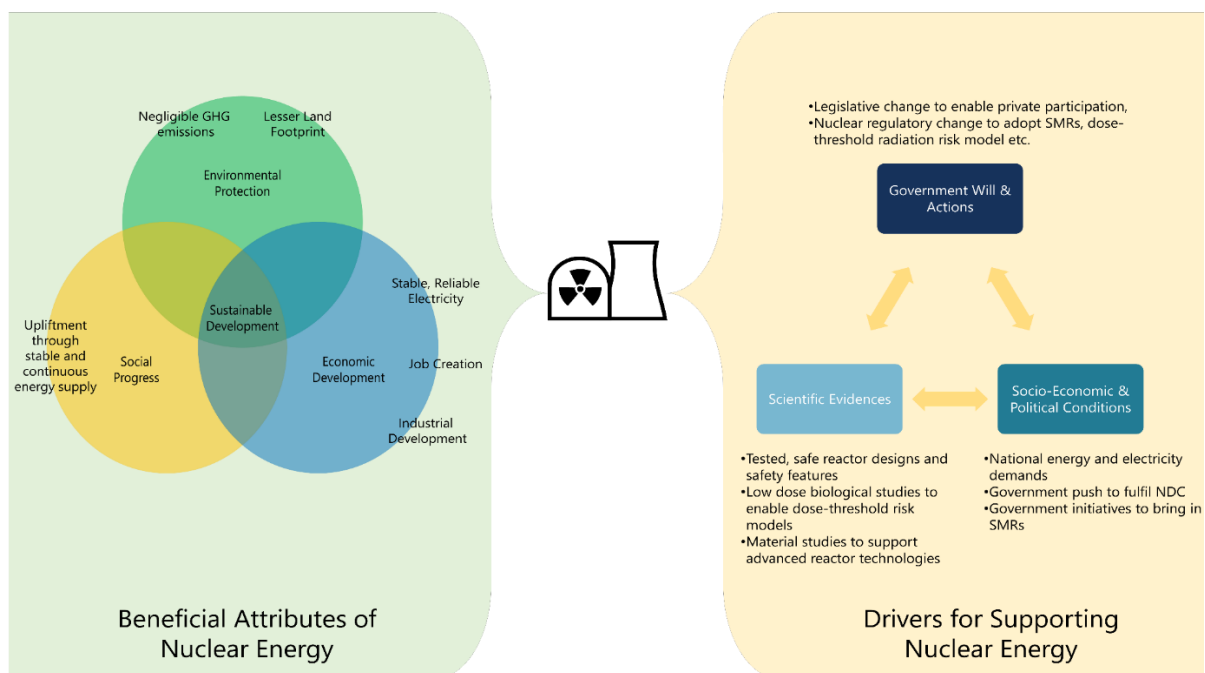


Figure 1. Illustrating the beneficial attributes of nuclear energy and what it would take to support its growth

## How does nuclear energy support environmental protection?

Nuclear energy plays a significant role in supporting environmental protection in several ways, primarily by reducing greenhouse gas (GHG) emissions, minimizing air pollution, conserving natural resources, and enabling land preservation.

Nuclear power plants generate large amounts of electricity with almost no direct GHG emissions. During operation, nuclear reactors emit negligible amounts of carbon dioxide (CO<sub>2</sub>) [19], making them one of the most effective tools for mitigating climate change. In India, the operating nuclear power plants have generated nearly 411 billion units of electricity, averting nearly 353 million tonnes of CO<sub>2</sub> equivalent to the environment [25]. This is particularly important as the global community and India strive to reduce carbon emissions to meet targets like those set by the Paris Agreement. Although nuclear energy does produce some emissions during the construction, operation, and decommissioning of plants, these emissions are comparable to those of renewable energy sources like wind and solar, and far lower than those from fossil fuel-based power generation [26].

Unlike coal, oil, or natural gas plants, nuclear power does not involve the combustion of fossil fuels. Therefore, it does not release harmful pollutants such as sulfur dioxide (SO<sub>2</sub>), nitrogen oxides (NO<sub>x</sub>), or particulate matter into the atmosphere. These pollutants are major contributors to air pollution, which can cause respiratory problems, cardiovascular diseases, and other health issues in humans, as well as harm ecosystems. By preventing the emission of SO<sub>2</sub> and NO<sub>x</sub>, nuclear power helps reduce the formation of acid rain and smog, both of which have detrimental effects on the environment, including damage to forests, soils, and water bodies.

Being a highly energy-dense source, nuclear power produces a large amount of energy from a small amount of fuel. For example, a single uranium fuel pellet, about the size of a fingertip, can produce as much energy as one ton of coal or 149 gallons of oil [27]. This efficiency reduces the need for extensive mining and extraction activities, which can have significant environmental impacts, including habitat destruction and water contamination. Therefore, the extent of mining and extraction activities for nuclear power is far less than for coal-based plants.

Nuclear power plants also require less land than renewable energy sources such as wind or solar farms. For example, a nuclear plant can produce the same amount of electricity as a solar farm covering hundreds of times more land area [28]. This means that nuclear energy can provide large-scale power without requiring large tracts of land, preserving natural habitats and ecosystems. Furthermore, with the advent of SMRs, the land requirement for nuclear power is further reduced.

Finally, though nuclear power generates radioactive waste, modern waste management techniques allow for its safe containment and storage. The volume of nuclear waste is relatively small compared to the waste produced by fossil fuel plants [29], which includes vast quantities of ash, sludge, and other byproducts that often end up in landfills or are released into the environment. Further, since India follows a closed fuel cycle, it is considered more sustainable in terms of waste management than open fuel cycle technologies in other countries [30]. And through advanced waste management techniques these wastes are stored deep below the earth's surface to minimize their environmental impact [31]. Also, efforts towards transmuting the radionuclides in these wastes to further reduce their harm, is being pursued in India [32].

### What can be done to support nuclear's growth in India?

The Indian government maintains a positive outlook on nuclear energy's role in facilitating a sustainable and clean transition away from fossil fuels. National economic models evaluating future energy needs across various human development scenarios emphasize the importance of nuclear power, alongside renewable sources, in replacing fossil-fuel-based plants [33]. Recent advancements, such as the addition of two new high-capacity nuclear power plants to the grid and the initiation of the second stage of India's three-stage nuclear program, highlight this commitment. Furthermore, increased governmental support for Small Reactors and Small Modular Reactors [34] highlights nuclear energy's anticipated critical role in driving India's future growth and development [33].

Therefore, it is now important to focus on the steps required to accelerate this growth. To ensure that the expansion of the domestic nuclear power industry aligns with the country's development needs, a range of supportive technological, economic, social, and policy-level changes are necessary (see for **Error! Reference source not found.** an illustrative understanding).

On the technological front, Pressurized Heavy Water Reactor (PHWR) technology is likely to remain the backbone of India's domestic nuclear expansion [35]. However, a few upcoming projects aim to introduce large-capacity Light Water Reactor technologies from international vendors [25]. To ensure a seamless and timely integration of these new technologies, it will be crucial to develop the necessary expertise within India's nuclear engineering and science communities. With the announcement of the Bharat Small Reactor (BSR) and Bharat Small Modular Reactors (BSMRs) [36], the Indian government is also emphasizing a shift towards advanced, Generation VI reactors aimed at delivering nuclear energy directly to industrial and residential users. For BSRs, the existing, proven 220 MWe PHWR technology will likely be adapted [37] with suitable modularity to enable factory fabrication. In the case of BSMRs, extensive research and planning will be required to select the most suitable design from the over 70 SMR options available globally [38], tailored to meet India's specific needs.

To support the expansion of India's nuclear power program, significant advancements in technology will be necessary within the domestic nuclear supply chain. Key components of the nuclear value chain, including manufacturers, suppliers, and service providers, will need to enhance their capabilities to handle increased demand and align with international standards [39]. This involves adopting cutting-edge technologies and implementing rigorous international quality assurance measures and certifications [40]. Improving technological capabilities will ensure that domestic suppliers can meet the growing needs of the nuclear program efficiently and reliably. It will also be crucial for these entities to stay competitive on a global scale by adhering to international best practices in quality and safety. This includes investing in state-of-the-art manufacturing processes, advanced materials, and precision engineering to produce components that meet global standards. Additionally, fostering strong partnerships with international organizations and participating in global supply chains can provide valuable insights and support in achieving these objectives.

The expansion of India's nuclear power program will also require substantial financial investments, as demonstrated by the recent budget allocation of nearly trillion rupees toward research and development in the domestic nuclear sector [41]. However, there is considerable potential for private investment in nuclear power production, which will likely materialize only after legislative changes are implemented. An example of this is the joint venture between Nuclear Power Corporation of India Ltd (NPCIL) and the National Thermal Power Corporation (NTPC) to develop the nuclear power project at Mahi Banswara in Rajasthan [42].

Additionally, the BSR and BSMR programs are expected to be largely funded through private investments [36], reflecting a growing trend towards leveraging private sector capital in the nuclear energy domain.

From an environmental perspective, it is crucial to reclassify the nuclear power industry based on its actual pollution emissions, in order to foster nuclear growth. Currently, the industry's classification as 'Red' in the Central Pollution Control Board's (CPCB) color-coded environmental permitting scheme [43] imposes unnecessary strictness and negatively impacts public perception. Given the decades of safe operation of domestic nuclear power plants and their minimal conventional and radiological emissions [44], it is appropriate to categorize them as 'Orange' or 'Green' under the CPCB framework. This reclassification would enhance public perception and facilitate the influx of both domestic private and international investment through sustainable financing frameworks. The existing practices of conducting environmental impact assessments (EIAs) and submitting periodic emissions reports to environmental and nuclear regulators will continue to ensure that nuclear power plants operate safely and within environmental standards, even under a revised classification.

As far as nuclear regulations are concerned, an expanding nuclear programme would mean greater more regulatory oversight. The introduction of new reactor technologies, such as SMRs necessitates evolving regulations to accommodate these advancements. But a specific area of concern is radiation health risk regulations. Currently, the framework is based on the linear no-threshold (LNT) radiation risk model, which is scientifically flawed [45]. Research has shown that low levels of radiation do not cause the harm predicted by the LNT model; rather, there may be a threshold below which health effects are minimal [46]. Updating regulations to incorporate a dose-threshold based approach could support the nuclear expansion program by relaxing several operational and design requirements [45]. This change would also enhance public perception by aligning regulations with current scientific understanding of low-dose radiation. Additionally, directing scientific research towards studying the effects of low doses of radiation on biological systems, through both experimental and theoretical approaches, would provide a more accurate basis for risk assessment and regulation [47]. This would go a long way in grounding the nuclear expansion in scientific principles and evidences.

Finally, public consensus on nuclear power projects is crucial. Achieving this consensus requires a comprehensive approach involving nationwide public awareness campaigns at local, state, and national levels. An effective strategy would be to integrate information about nuclear energy into school curricula at both state and central levels. This can help educate students from a young age about the benefits and safety of nuclear power, fostering a more informed and open-minded future generation. Additionally, hosting district-level meetings and community forums is crucial for directly addressing public concerns and dispelling misconceptions about nuclear energy. These meetings should be designed to provide clear, accurate information and offer a platform for residents to ask questions and express their views. Efforts should also include the development of transparent communication techniques and risk communication tools that simplify complex information. This approach helps convey the importance of having a nuclear power plant in the vicinity and addresses potential concerns about safety and environmental impact. By using accessible language and visual aids, public outreach can demystify nuclear energy and highlight its benefits, such as its role in reducing carbon emissions and ensuring a reliable energy supply.

## **Conclusion**

In summary, nuclear energy is poised to be a crucial component of India's clean energy transition. To fully realize its potential, it is essential to provide robust support across technical,

economic, legislative, social, regulatory, and policy dimensions. This special issue on "Nuclear Energy for Sustainable Development and Environmental Management" aims to offer valuable insights and timely information on these aspects. It will guide policymakers, technocrats, researchers, and students in developing a thorough understanding of why nuclear energy and its varied applications is vital for India's future energy landscape.

## References

- [1] R. J. Brecha, G. Ganti, R. D. Lamboll, Z. Nicholls, B. Hare, J. Lewis, M. Meinshausen, M. Schaeffer, C. J. Smith and M. J. Gidden, "Institutional decarbonization scenarios evaluated against the Paris Agreement 1.5 °C goal," *Nature Communications*, vol. 13, p. 4304, 2022.
- [2] L. S. Paraschiv and S. Paraschiv, "Contribution of renewable energy (hydro, wind, solar and biomass) to decarbonization and transformation of the electricity generation sector for sustainable development," *Energy Reports*, vol. 9, pp. 535-544, 2023.
- [3] Goldman Sachs, "How India could rise to the world's second-biggest economy," Goldman Sachs, 6 July 2023. [Online]. Available: <https://www.goldmansachs.com/intelligence/pages/how-india-could-rise-to-the-worlds-second-biggest-economy.html>. [Accessed 15 May 2024].
- [4] Cabinet, "Cabinet approves India's Updated Nationally Determined Contribution to be communicated to the United Nations Framework Convention on Climate Change," Press Information Bureau, 3 August 2022. [Online]. Available: <https://pib.gov.in/PressReleaseIframePage.aspx?PRID=1847812>. [Accessed September 2 2024].
- [5] International Energy Agency, *Nuclear Power in a Clean Energy System*, IEA, 2019.
- [6] E. Derr, "Nuclear Needs Small Amounts of Land to Deliver Big Amounts of Electricity," Nuclear Energy Institute, 29 April 2022. [Online]. Available: <https://www.nei.org/news/2022/nuclear-brings-more-electricity-with-less-land>. [Accessed 3 December 2023].
- [7] World Nuclear Association, "Nuclear Power in the World Today," 29 August 2024. [Online]. Available: <https://world-nuclear.org/information-library/current-and-future-generation/nuclear-power-in-the-world-today>. [Accessed 1 September 2024].
- [8] UN News, "'Without nuclear, it will be almost impossible to decarbonize by 2050', UN atomic energy chief," United Nations, 13 June 2024. [Online]. Available: <https://news.un.org/en/interview/2024/06/1151006>. [Accessed 1 September 2024].
- [9] M. Goh, "China and India will lead the world's nuclear power growth, experts say," CNBC, 7 November 2018. [Online]. Available: <https://www.cnbc.com/2018/11/08/china-india-will-lead-global-nuclear-power-production-growth-experts.html>. [Accessed 3 September 2024].
- [10] Ministry of Power, "National Power Portal," Government of India, [Online]. Available: <https://npp.gov.in/dashBoard/cp-map-dashboard>. [Accessed 19 August 2024].
- [11] NPCIL, "Plants Under Operation," NPCIL, [Online]. Available: [https://www.npcil.nic.in/content/302\\_1\\_AllPlants.aspx](https://www.npcil.nic.in/content/302_1_AllPlants.aspx). [Accessed 2 September 2024].

- [12] Press Trust of India, "India's second 700 MW nuclear power KAPS-4 plant starts operations at full capacity," *The Hindu*, 21 August 2024. [Online]. Available: <https://www.thehindu.com/news/national/indias-second-700-mw-nuclear-power-kaps-4-plant-starts-operations-at-full-capacity/article68549652.ece>. [Accessed 2 September 2024].
- [13] Express News Service, "Core loading of India's 1st indigenous nuclear reactor in Kalpakkam on Monday," *The New Indian Express*, 4 March 2024. [Online]. Available: <https://www.newindianexpress.com/states/tamil-nadu/2024/Mar/04/core-loading-of-indias-1st-indigenous-nuclear-reactor-in-kalpakkam-on-monday>. [Accessed 2 September 2024].
- [14] Department of Atomic Energy, "AERB Grants Permission for First Approach to Criticality of 500 MWe Prototype Fast Breeder Reactor," Press Information Bureau, 30 July 2024. [Online]. Available: <https://pib.gov.in/PressReleaseIframePage.aspx?PRID=2039099>. [Accessed 2 September 2024].
- [15] IAEA, "Power Reactor Information System (PRIS) - India," IAEA, 28 August 2024. [Online]. Available: <https://pris.iaea.org/PRIS/CountryStatistics/CountryDetails.aspx?current=IN>. [Accessed 23 August 2024].
- [16] R. Nayan, "Governing Uranium in India. DIIS Report 2015:02," Danish Institute for International Studies, Copenhagen, 2015.
- [17] Government of India, "Lok Sabha Questions & Answers - Unstarred Question No. 3525," Government of India, New Delhi, 2018.
- [18] IISD, "Sustainable Development," International Institute for Sustainable Development, [Online]. Available: <https://www.iisd.org/mission-and-goals/sustainable-development#:~:text=%22Sustainable%20development%20is%20development%20that,to%20meet%20their%20own%20needs.%22>. [Accessed 1 September 2024].
- [19] International Atomic Energy Agency, "Climate Change and Nuclear Power 2020," International Atomic Energy Agency, Vienna, 2020.
- [20] L. Johnson, "When it Comes to Reliability, Look No Further than Nuclear," Nuclear Energy Institute, 1 February 2024. [Online]. Available: <https://www.nei.org/news/2024/for-reliability-look-no-further-than-nuclear>. [Accessed 1 September 2024].
- [21] WNA, "Nuclear Power and Energy Security," World Nuclear Association, 16 April 2024. [Online]. Available: <https://world-nuclear.org/information-library/economic-aspects/nuclear-power-and-energy-security>. [Accessed 30 August 2024].
- [22] N. Watson and L. Ashton, "Towards a Just Energy Transition: Nuclear Power Boasts Best Paid Jobs in Clean Energy Sector," IAEA, 14 April 2022. [Online]. Available: <https://www.iaea.org/newscenter/news/towards-a-just-energy-transition-nuclear-power-boasts-best-paid-jobs-in-clean-energy-sector>. [Accessed 30 August 2024].
- [23] T. A. Kurniawan, M. H. D. Othman, D. Singh, R. Avtar, G. H. Hwang, T. Setiadi and W.-h. Lo, "Technological solutions for long-term storage of partially used nuclear waste: A critical review," *Annals of Nuclear Energy*, vol. 166, p. 108736, 2022.
- [24] L. Ashton, "When Nuclear Waste is an Asset, not a Burden," *IAEA Bulletin*, vol. 64, no. 3, September 2023.

- [25] Department of Atomic Energy, "Government has initiated steps to increase the nuclear power capacity from 7480 MW to 22480 MW by 2031-32, says Union Minister Dr Jitendra Singh," Press Information Bureau, 20 December 2023. [Online]. Available: <https://pib.gov.in/PressReleaseIframePage.aspx?PRID=1988863>. [Accessed 12 April 2024].
- [26] UNECE, "Carbon Neutrality in the UNECE Region: Integrated Life-Cycle Assessment of Electricity Sources; Updated Report," UNECE, Geneva, 2022.
- [27] NEI, "Nuclear Fuel," Nuclear Energy Institute, [Online]. Available: <https://www.nei.org/fundamentals/nuclear-fuel>. [Accessed 31 August 2024].
- [28] NEI, "Land Needs for Wind, Solar Dwarf Nuclear Plant's Footprint," Nuclear Energy Institute, 9 July 2015. [Online]. Available: <https://www.nei.org/news/2015/land-needs-for-wind-solar-dwarf-nuclear-plants>. [Accessed 31 August 2024].
- [29] V. Tsyplenkov, "Electricity production and waste management: Comparing the options," *IAEA Bulletin 4/1993*, vol. 4, pp. 27-33, 1993.
- [30] J. Donovan, "Shrinking nuclear waste and increasing efficiency for a sustainable energy future," *IAEA Bulletin*, vol. 61, no. 3, 2020.
- [31] WNA, "Storage and Disposal of Radioactive Waste," World Nuclear Association, 30 April 2024. [Online]. Available: <https://world-nuclear.org/information-library/nuclear-fuel-cycle/nuclear-waste/storage-and-disposal-of-radioactive-waste>. [Accessed 2 September 2024].
- [32] S. B. Degweker, P. V. Bhagwat, S. Krishnagopal and A. Sinha, "Physics and technology for development of accelerator driven systems in India," *Progress in Nuclear Energy*, vol. 101, pp. 53-81, 2017.
- [33] A. Garg, O. Patange, S. S. Vishwanathan, T. Nag, U. Singh and V. Avashia, "Synchronizing energy transitions toward possible Net Zero for India: Affordable and clean energy for all. A report prepared for Office of the Principle Scientific Advisor (PSA) to Government of India and Nuclear Power Corporation of India Limited (NPCIL)," Office of the Principle Scientific Advisor (PSA) to Government of India, New Delhi, 2024.
- [34] Department of Atomic Energy, " Union Minister Dr Jitendra Singh says, India taking steps for development of Small Modular Reactors (SMR), with up to 300 MW capacity to fulfill its commitment to Clean Energy transition," Press Information Bureau, 27 November 2022. [Online]. Available: <https://pib.gov.in/PressReleasePage.aspx?PRID=1879298>. [Accessed 19 August 2024].
- [35] Press Trust of India, "India to start construction of 10 'fleet mode' nuclear reactors from 2023," Live Mint, 27 March 2022. [Online]. Available: <https://www.livemint.com/news/india/india-to-start-construction-of-10-fleet-mode-nuclear-reactors-from-2023-11648394949101.html>. [Accessed 31 August 2024].
- [36] Press Trust of India, "Govt to open up nuclear power sector for private investments," ET Energy World, 24 July 2024. [Online]. Available: <https://energy.economictimes.indiatimes.com/news/power/govt-to-open-up-nuclear-power-sector-for-private-investments/111982069>. [Accessed 2 September 2024].
- [37] Swarajya Staff, "India's 220 MW PHWRs Get A Makeover As Bharat Small Reactors For Private Sector Use," Swarajya, 20 August 2024. [Online]. Available: <https://swarajyamag.com/infrastructure/indias-220-mw-phwrs-get-a-makeover-as-bharat-small-reactors-for-private-sector-use>. [Accessed 2 September 2024].

- [38] IAEA, "Advanced Reactor Information System," IAEA, [Online]. Available: <https://aris.iaea.org/>. [Accessed 2 September 2024].
- [39] D. K. Aswal and A. Chandra, "Key drivers for achieving India's 100 GW nuclear power ambition," *Current Science*, vol. 127, no. 4, pp. 1-3, 2024.
- [40] Larsen & Toubro, "The Nuclear Edge," Larsen & Toubro, [Online]. Available: <https://newsnviews.larsentoubro.com/Lists/Posts/Post.aspx?ID=709>. [Accessed 12 April 2024].
- [41] NDTV Newsdesk, "On India's Push For Nuclear Energy, An Update From Nirmala Sitharaman," NDTV, 26 July 2024. [Online]. Available: <https://www.ndtv.com/india-news/on-indias-push-for-nuclear-energy-an-update-from-nirmala-sitharaman-6195796>. [Accessed 1 September 2024].
- [42] Ministry of Power, "NTPC and NPCIL sign Agreement for joint development of Nuclear Power Plants," Press Information Bureau, 1 May 2023. [Online]. Available: <https://pib.gov.in/PressReleasePage.aspx?PRID=1921196>. [Accessed 2 August 2024].
- [43] Central Pollution Control Board, "Final Document on Revised Classification of Industrial Sectors Under Red, Orange, Green and White Categories," CPCB, New Delhi, 2016.
- [44] A. Vinod Kumar, A. K. Patra, S. N. Tiwari, A. Baburaja, Y. P. Gautam, B. Vijayakumar, T. Jesan, M. S. Vishnu, I. V. Saradhi, A. Chandra and D. K. Aswal, "Negligible radiological impact of Indian nuclear power plants on the environment and the public: Findings from a 20-year study," *Science of the Total Environment*, vol. 914, p. 169936, 2024.
- [45] D. K. Aswal and A. Chandra, "Revisiting radiation realities," *Current Science*, vol. 126, no. 3, p. 295, 2024.
- [46] R. K. Chaurasia, B. K. Sapra and D. K. Aswal, "Interplay of immune modulation, adaptive response and hormesis: Suggestive of threshold for clinical manifestation of effects of ionizing radiation at low doses?," *Science of the Total Environment*, vol. 917, p. 170178, 2024.
- [47] A. Chandra and D. K. Aswal, "Need of Quantum Biology to Investigate Beneficial Effects at Low Doses (< 100 mSv) and Maximize Peaceful Applications of Nuclear Energy," *MAPAN -Journal of Metrology Society of India*, vol. 39, pp. 5-24, 2023.
- [48] Press Information Bureau, "Dr Jitendra Singh says nuclear power capacity set to increase from 7480 MW to 22480 MW by 2031," Press Information Bureau, 20 July 2023. [Online]. Available: <https://pib.gov.in/PressReleasePage.aspx?PRID=1941010>. [Accessed 11 April 2024].



**Preface to Special Theme**

**Global Warming and Climate Change – Need of Nuclear Energy**

**S. K. Jha and S.K. Sahoo**

*Health Physics Division, Bhabha Atomic Research Center  
Trombay, Mumbai 400 085*

*Corresponding author Email: [skjha@barc.gov.in](mailto:skjha@barc.gov.in)*



**Dr. S K Jha**

Global warming and climate change are the central point of scientific discussion and research around the world in 21<sup>st</sup> Century, the endeavor to alleviate the adverse impacts. The looming crisis of rising of global mean surface temperature by 1.5 °C and/or 2 °C over and above the pre-industrial level compelled the international community to execute the Paris Agreement in 2015. This is an agreement negotiated by 196 countries emphasizing the exigency to reduce the emission intensity of greenhouse gases and adopt measures to mitigate the adverse effect on the ecosystem. Extreme temperatures; more intense and frequent storms, droughts & floods; ocean acidifications; warmer ocean; loss of biodiversity; disruption of crops and increased health risks are reported across the regions which reflects the adverse effects of global warming and climate change. Intensity, frequency and scale of these man-made risks are going to follow an upward trend till the reduction of emissions of greenhouse gases to limit the anticipated temperature rise [1].

India, in the Asian region, is particularly vulnerable to the impacts of global warming climate change, as the region has the longer coastline, incredibly diverse and often unique marine environments, many large coastal population centres (mega-cities) and already suffers from frequent storms and floods when compared to other regions in the world. Growth in trade in fisheries resources, expansion of aquaculture production, mining and agriculture all these activities have impacted on the health and sustainability of coastal resource.

Our climate depends on the Earth's temperature. Due to rapidly increasing concentrations of carbon dioxide (CO<sub>2</sub>) and other greenhouse gases in the atmosphere, the temperature of the planet is rising quickly compared with relatively stable temperatures throughout the past millennium. Atmospheric carbon dioxide concentrations remained relatively constant at around 280 parts per million (ppm) for at least a thousand years, but concentrations have risen since the mid-1700s, presently reaching around 421 ppm as on 2022. The increasing use of fossil fuels for energy generation and transport purposes means carbon dioxide is the most critical greenhouse gas. Although India's carbon dioxide emissions increased by a whopping 5.9 percent in post-COVID phase, with those from coal growing 10.2 percent.

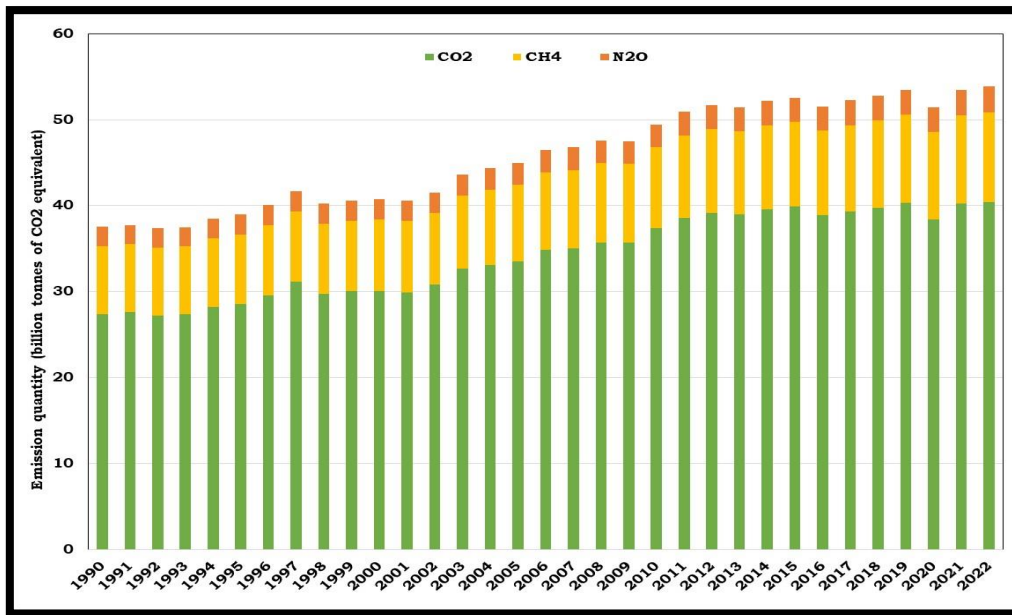


**Fig.1. Global greenhouse gases emission quantity (billion tonnes of CO<sub>2</sub> equivalent)**

Anthropogenic sources of carbon dioxide, methane and nitrous oxide are the predominant components of greenhouse gases which is responsible for global warming and climate change. From the Fig.1, it may be observed that globally carbon dioxide in the range of 30 – 40 billion tonnes while 8- 10 and 2 – 3 billion tonnes equivalent to CO<sub>2</sub> of methane and nitrous oxide emitted per year [2]. The corresponding percentage contribution observed to be around 75%, 20% and 5% w.r.t. CO<sub>2</sub>, CH<sub>4</sub> and NO<sub>2</sub>, respectively. Therefore, globally the prime focus on carbon dioxide and efforts to reduce the emission intensity of it. However, it is pertinent to underscore here the global warming potential (GWP) of different greenhouses gases considering the radiative efficiency and atmospheric lifetime. Though the emission quantity of methane and nitrous oxide is much lesser than that of carbon dioxide but the global warming potential of both these gases is 21 and 310, respectively [3].

In addition to this context, multiple anthropogenic sources like electricity & heat, transport, manufacturing & construction, agriculture, industry, energy production, etc. contribute to the global emission of carbon dioxide. The percentage contribution of various anthropogenic sources is given in Fig. 3 and clearly shows that 70% of global carbon dioxide emission is shared by four sources [2]. Global atmospheric average carbon dioxide concentration in the last century is depicted in Fig. 4 [2]. It is, therefore, efforts made globally to reduce the carbon dioxide emission intensity of these sources fueled by fossil fuels. Nuclear energy and renewable energy sources are best possible options to meet the net carbon zero.

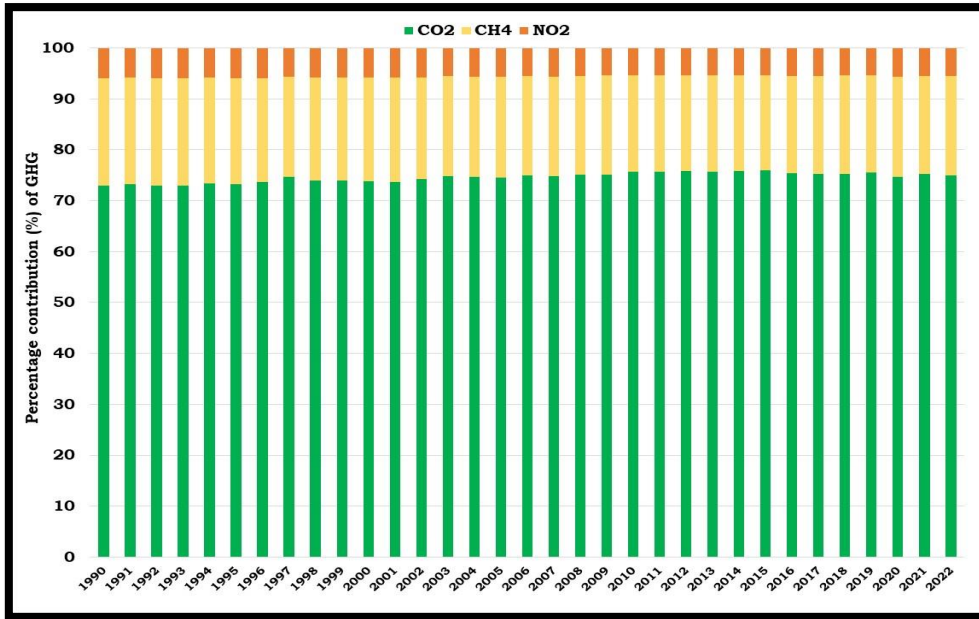


**Fig.2. Percentage contribution of global greenhouse gases emissions**

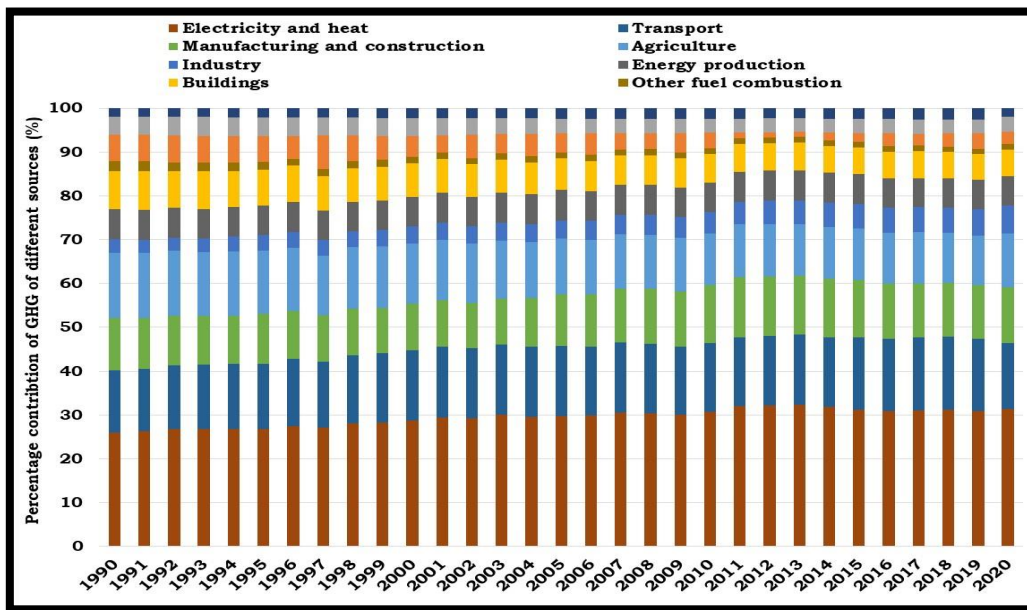


**Fig.3. Percentage contribution of different sources to Global GHG emission**

Emblematic of India's electricity transition is its national target of achieving 500GW of non-fossil electricity capacity by 2030 and its global commitment to achieve net-zero by 2070. However, a focus on energy capacity and emissions only captures a part of India's transition story. Apart from a shift from fossil-based to clean power generation, India is experiencing multiple simultaneous transitions, such as: a shift from public to private control over energy infrastructure; growing per capita energy demand; expanding domestic power markets; and transitions in coupled sectors such as transport and industry. Therefore, solar power, wind power, clean and green nuclear energy, biopower and hydrogen fuel are the contenders of future energy need of the country. However, reliable and low-cost nuclear power has multiple advantages over other energy sources like constant base load power, concentrated, small land

foot print, climate compatible, non-dependent on weather, higher capacity factor, etc.. Like global trend, nuclear energy is very much part of the energy mix and considered sincerely to enhance the national contribution to reduce emission of greenhouse gases. Similarly, India has a national policy to enhance installed nuclear capacity to 100 GWe by 2047 from current less than 10 GWe [4].

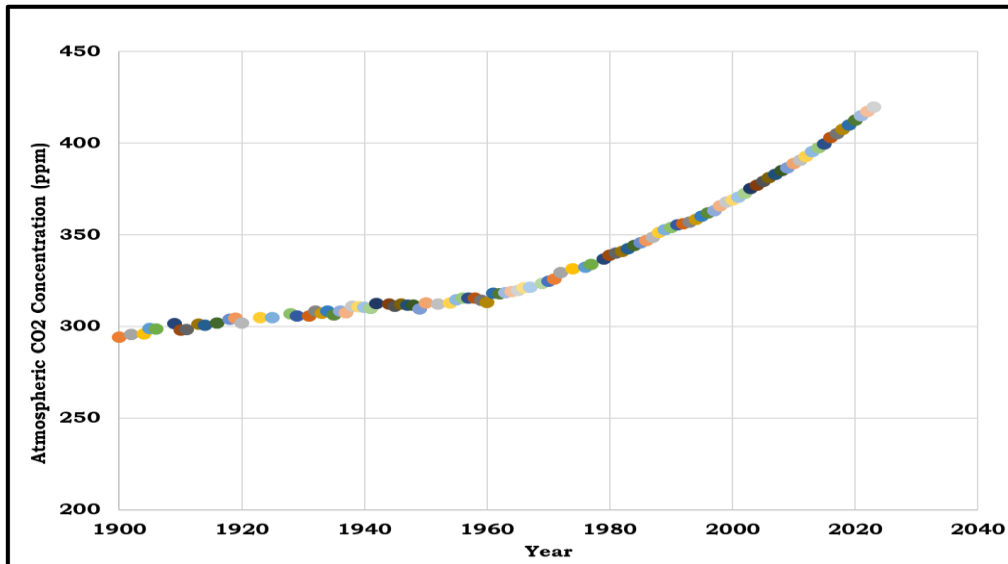


**Fig.4. Global atmospheric average CO<sub>2</sub> concentration (ppm) in last century**

#### References:

1. IPCC, 2018: Global Warming of 1.5°C. An IPCC Special Report on the impacts of global warming of 1.5°C above pre-industrial levels and related global greenhouse gas emission pathways, in the context of strengthening the global response to the threat of climate change, sustainable development, and efforts to eradicate poverty [Masson-Delmotte, V., P. Zhai, H.-O. Pörtner, D. Roberts, J. Skea, P.R. Shukla, A. Pirani, W. Moufouma-Okia, C. Péan, R. Pidcock, S. Connors, J.B.R. Matthews, Y. Chen, X. Zhou, M.I. Gomis, E. Lonnoy, T. Maycock, M. Tignor, and T. Waterfield (eds.)].
2. Open sources data - [www.ourindata.org](http://www.ourindata.org) accessed on Oct. 3, 2024
3. IPCC, 2023: Summary for Policymakers, In: Climate Change 2023: Synthesis Report. Contribution of Working Groups 1, II and III to the sixth Assessment Report of the Intergovernmental Panel on Climate Change {Core Writing Team, H. Lee and J. Rometo (eds.)}. IPCC, Geneva, Switzerland, pp.1-34, doi:10.59327/IPCC/AR6-9789291691467.001.
4. NITI Aayog, India Energy Security Scenarios (IESS), 2024, Version 3.0, Government of India, 2023.

# Band Gap Engineering and Frequency Dispersive Dielectric Properties of Rare Earth ( $\text{Sm}^{3+}$ ) Modified $\text{Ba}_{0.8}\text{Sr}_{0.2}\text{TiO}_3$ Ceramics for Potential Use as an Optoelectronic Materials

Jyotirekha Mallick and Manoranjan Kar\*

*Department of Physics, Indian Institute of Technology Patna, Bihta, Bihar-801106, India*

*Volume 1, Issue 5, October 2024*

*Received: 30 July, 2024; Accepted: 29 October, 2024*

*DOI: <https://doi.org/10.63015/5C-2434.1.5>*

*\*Correspondence Author Email: [mano@iitp.ac.in](mailto:mano@iitp.ac.in)*

**Abstract:** Lead free perovskite materials have the capability to be used in various multifunctional applications. In this regard, dielectric and light absorption properties of Sm modified  $\text{Ba}_{0.8-x}\text{Sm}_x\text{Sr}_{0.2}\text{TiO}_3$  have been explored. The dielectric constant has been estimated to be 2788 for  $\text{Ba}_{0.77}\text{Sm}_{0.03}\text{Sr}_{0.2}\text{TiO}_3$ . The optical band gap of all prepared samples has been evaluated by employing Tauc plot method and observed that the band gap varies 3.13-2.97 eV with the increase in Sm concentration. In brief, the present study reports the physical properties of  $\text{Ba}_{0.8-x}\text{Sm}_x\text{Sr}_{0.2}\text{TiO}_3$  ceramics which open window for possible use of it as lead-free optoelectronic material.

**Keywords:** Perovskite materials, Dielectric constant, Optoelectronic, Band gap

**1. Introduction:** Recently, the importance of the lead-free perovskite materials in the electronic industries has gained significant attention because of their rapid development in various technologies such as sensor, light emitting diode, dielectric capacitors as well as commitment to environment protection [1,2]. These materials can also enhance/change their physical properties when expose to light and considered as a potential candidate to be used in photovoltaic devices. So researchers are very much interested to understand the light matter interaction and investigate its various applications such as photodetector, photovoltaic devices, etc. [3-5]. Among all lead-free perovskite materials, Barium titanate ( $\text{BaTiO}_3$ ) has earned so much attention of researchers due to its excellent dielectric, ferroelectric, piezoelectric properties.  $\text{BaTiO}_3$  belongs to  $\text{ABO}_3$  type structure, with  $\text{Ba}^{2+}$  and  $\text{Ti}^{4+}$  are placed at the A and B-site, respectively, within the octahedral coordination of oxygen atoms, hence possesses unique ferroelectric properties [6]. Most importantly it also exhibits significant optical

properties and become suitable to be utilized in different electro-optical system. Optoelectronic devices play an important role to produce various materials for advanced electronic equipment. For example, rare earth ions have an empty and entangled 4f electron structure which has capability to enhance various physical properties. Previously, Tihtih. M et. al. reported that rare earth modified BTO system can improve the materials optical properties and expand its potentiality in different technological applications [7]. Also, by the addition of lower ionic radii element, such as  $\text{Sr}^{2+}$  at A site of BTO system stabilizes the perovskite structure and noticeably enhance the dielectric constant [8]. Hence,  $\text{Ba}_{0.8}\text{Sr}_{0.2}\text{TiO}_3$  (BSTO) is the one of the most important member of the  $\text{BaTiO}_3$  family which has achieved a lot of attention from the researchers due to its high dielectric constant with diffuse phase transition behaviour [8]. With the increase in  $\text{Sr}^{2+}$  in  $\text{BaTiO}_3$  the relaxor behaviour of BSTO increases and it exhibits better relaxor ferroelectric when the concentration of  $\text{Sr}^{2+}$  is 20% as compared to

other compositions [8]. That's why BSTO has been chosen to be substitute rare earth element at Ba site. The introduction of rare earth elements ( $\text{Re}^{3+}$ ) at the Ba site of BSTO can significantly enhanced the physical properties of the modified BSTO by inducing structural deformation of octahedra as well as modifies the lattice symmetry [9]. Basically, the ionic radius of the rare earth element (trivalent element) varies between 0.8 and 1.13 Å which are suitable to be placed at the  $\text{Ba}^{2+}$  site of the  $\text{ABO}_3$  structure. So it is the most crucial work to choose the perfect rare earth element which can produce better dielectric constant with low dielectric loss as well as induced low optical band gap of modified BTO system [10]. It has been observed that the dielectric constant, transition temperature and electrical resistance can be controlled strongly by the proper addition of donor impurity ions at the A site of BTO [11]. Thakur and their group observed that by the substitution of  $\text{Sm}^{3+}$  at the  $\text{Ba}^{2+}$  site can enhance the dielectric constant at room temperature [12]. The microstructure and dielectric properties of rare earth (Sm, Ho, Yb), modified  $\text{BaTiO}_3$  has been investigated by Jo et. al. and they concluded that the unit cell volume of rare earth doped BTO plays an important role in the regulation of Curie temperature [13]. In this context the  $\text{Sm}^{3+}$  substituted  $\text{Ba}_{0.8-x}\text{Sm}_x\text{Sr}_{0.2}\text{TiO}_3$  were prepared and their crystal structure, temperature dependent dielectric and electrocaloric properties were reported by the present authors [14]. However, the frequency dependent dielectric constant is important to explore for the technological application. As well as these materials are very promising for the optoelectronic application as their optical band gap is around 3 eV. Hence, in this article the frequency dependent dielectric constant and band gap engineering by Sm substitution in BSTO have been explored. The present article will guide the researcher for further modification of band gap of BTO for its technological applications.

**2. Experimental details:** Polycrystalline ceramics  $\text{Ba}_{0.8-x}\text{Sm}_x\text{Sr}_{0.2}\text{TiO}_3$  ( $x = 0.01 \leq x \leq 0.05$ ) were prepared by employing the

conventional high temperature solid-state reaction method. Previously, the sample preparation method, characterization, temperature dependent dielectric, ferroelectric and electrocaloric effect properties are reported elaborately in the author's previous publication [14]. For the present study, the N4L impedance analyser has been used to measure the room temperature complex impedance spectroscopy within the frequency range 1Hz-1MHz. The UV visible Shimadzu UV-2600 spectrophotometer (Japan) has been employed to record the diffuse reflectance spectra for exploring the optical properties of all the prepared samples.

### 3. Results and discussion

**3.1 Crystal structure and structural properties:** The XRD patterns of Polycrystalline ceramics  $\text{Ba}_{0.8-x}\text{Sm}_x\text{Sr}_{0.2}\text{TiO}_3$  ( $x = 0.01, 0.02, 0.03, 0.04$  and  $0.05$ ) as previously reported confirm that all the sample have good crystallinity without any impurity [14]. All samples are belonging to tetragonal symmetry with  $P4mm$  space group. Also all sintered pellets are exhibited a dense and compact surface morphology which is an important factor in the improvement of different physical properties. The temperature dependent dielectric properties, ferroelectric and electrocaloric properties are reported as discussed in the introduction [14]. However, in this article, the frequency dependent dielectric constant and optical band gap properties are discussed.

### 3.2. Dielectric Properties

**3.2.1. Dielectric constant:** Room temperature dielectric constant as function of frequency of  $\text{Ba}_{0.8-x}\text{Sm}_x\text{Sr}_{0.2}\text{TiO}_3$  ( $x = 0.01, 0.02, 0.03, 0.04,$  and  $0.05$ ) are represented in the Figure 1(a). Basically, the dielectric constant of a ceramic involves different types of polarization such as ionic, dipolar, electronic, and interfacial. Depending upon the relaxation time, their

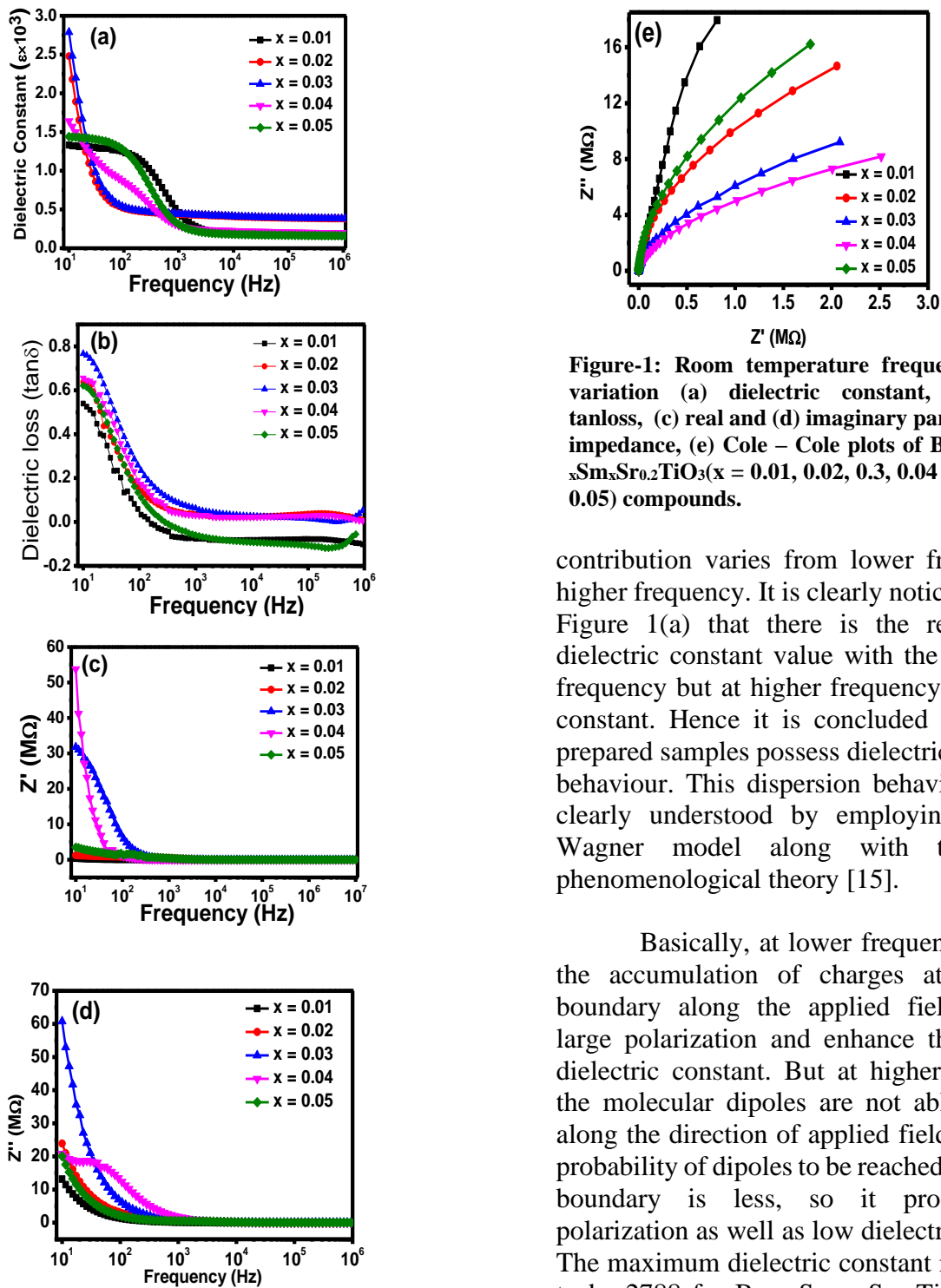


**Figure-1: Room temperature frequency variation (a) dielectric constant, (b) tanloss, (c) real and (d) imaginary part of impedance, (e) Cole – Cole plots of Ba<sub>0.8-x</sub>Sm<sub>x</sub>Sr<sub>0.2</sub>TiO<sub>3</sub> (x = 0.01, 0.02, 0.3, 0.04 and 0.05) compounds.**

contribution varies from lower frequency to higher frequency. It is clearly noticed from the Figure 1(a) that there is the reduction of dielectric constant value with the increase in frequency but at higher frequency it becomes constant. Hence it is concluded that all the prepared samples possess dielectric dispersion behaviour. This dispersion behaviour can be clearly understood by employing Maxwell Wagner model along with the Koops phenomenological theory [15].

Basically, at lower frequency, there is the accumulation of charges at the grain boundary along the applied field, produce large polarization and enhance the value of dielectric constant. But at higher frequency, the molecular dipoles are not able to orient along the direction of applied field, hence the probability of dipoles to be reached at the grain boundary is less, so it produces low polarization as well as low dielectric constant. The maximum dielectric constant is estimated to be 2788 for Ba<sub>0.77</sub>Sm<sub>0.03</sub>Sr<sub>0.2</sub>TiO<sub>3</sub> ceramic. Also, this dielectric constant value increases with the Sm<sup>3+</sup> concentration up to x = 0.03, after that it diminishes. The c/a ratio i.e. tetragonality is mainly responsible for this behaviour. With the increase in Sm<sup>3+</sup> concentration the tetragonality behaviour of the sample increases up to x = 0.03 which enhances spontaneous polarization as well as

the dielectric constant value increases [14]. But when the concentration value is more than 0.03, there might be production of oxygen vacancies because of the replacement of  $\text{Sm}^{3+}$  at  $\text{Ba}^{2+}$  site. These oxygen vacancies can oppose the orientation of dipoles and inhibits the increase of dielectric constant, when the concentration of  $\text{Sm}^{3+}$  is more than  $x = 0.03$ .

**3.2.2. Dielectric loss:** Dielectric loss as a function of frequency of all the prepared samples is shown in Figure 1(b). It decreases with increase in frequency and at higher frequency range, dielectric loss become constant, which can also be understood by Maxwell Wagner model [14]. The Maxwell Wagner model describes that a dielectric material made up of a semiconducting grain enclosed by highly insulating grain boundary. At low frequency, insulating grain boundaries are active, so accumulation of charge carriers increases. Hence more energy is required to transport the charge carriers through the grain boundary and produce high dielectric loss. But at high frequency, semiconducting grains are more active so charge carriers can easily pass through the grain without loss of more energy and produce low dielectric loss. Hence, this characterization indicates the lossless behaviour of the prepared sample and depict that these samples have the capability to be used in the devices which are operated at high frequency.

### 3.2.3. Complex Impedance spectroscopy:

The real ( $Z'$ ) and imaginary ( $Z''$ ) part of ac impedance as a function of frequency for all the prepared samples  $\text{Ba}_{0.8-x}\text{Sm}_x\text{Sr}_{0.2}\text{TiO}_3$  ( $0.01 \leq x \leq 0.05$ ) are represented in Figures 1(c) and 1(d). Figure 1(c) confirmed that Real ( $Z'$ ) part of impedance decreases with the increase in frequency and become frequency independent at higher frequency. At low frequency, all types of polarizations are contributed towards total impedance hence the value of  $Z'$  is high. The imaginary ( $Z''$ ) part of ac impedance is also exhibit similar types of behaviour. The dielectric properties of ceramic materials over a broad range of frequency can be understood properly by Complex

Impedance Spectroscopy (CIS) technique. Figure 1(e) represents the Cole-Cole plot of all the samples. The total impedance is the contribution of grain, grain boundary, and electrodes. Figure 1(e) represents a semicircle arc bend towards the X axis, which confirm that the contribution of grain is dominated over the grain boundary and electrodes.

**3.3. Optical Properties:** The optical properties of  $\text{Ba}_{0.8-x}\text{Sm}_x\text{Sr}_{0.2}\text{TiO}_3$  ( $x = 0.01, 0.02, 0.03, 0.04, \text{ and } 0.05$ ) have been discussed by using UV visible spectrometer in the range of (200 – 1000) nm as represented in the Figure 2.

The optical band gap energy ( $E_g$ ) has been estimated by employing the Kubelka and Munk function. The KM function [ $F(R_\infty)$ ] is [15]:

$$F(R_\infty) = \frac{(1-R_\infty)^2}{2R_\infty} = \frac{\alpha}{s} \quad (1)$$

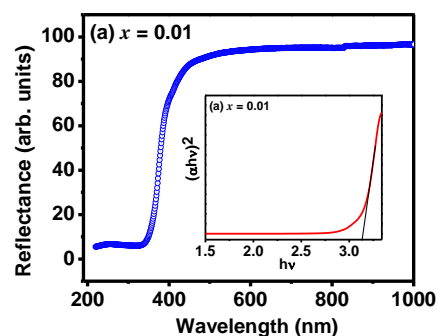
Where,  $\alpha$ ,  $R_\infty$ , and  $s$  denote absorbance coefficient, the reflectance of the ceramics, and scattering coefficient, respectively.

So, the KM function is influence by the absorption spectrum. The absorption coefficient ( $\alpha$ ) as a function of energy can be represented as [15];

$$\alpha \propto \left[ \frac{(h\nu - E_g)^n}{h\nu} \right] \quad (2)$$

The Tauc's method has been used to calculate the optical band gap of prepared ceramics,

$$\alpha h\nu = A(h\nu - E_g)^n \quad (3)$$





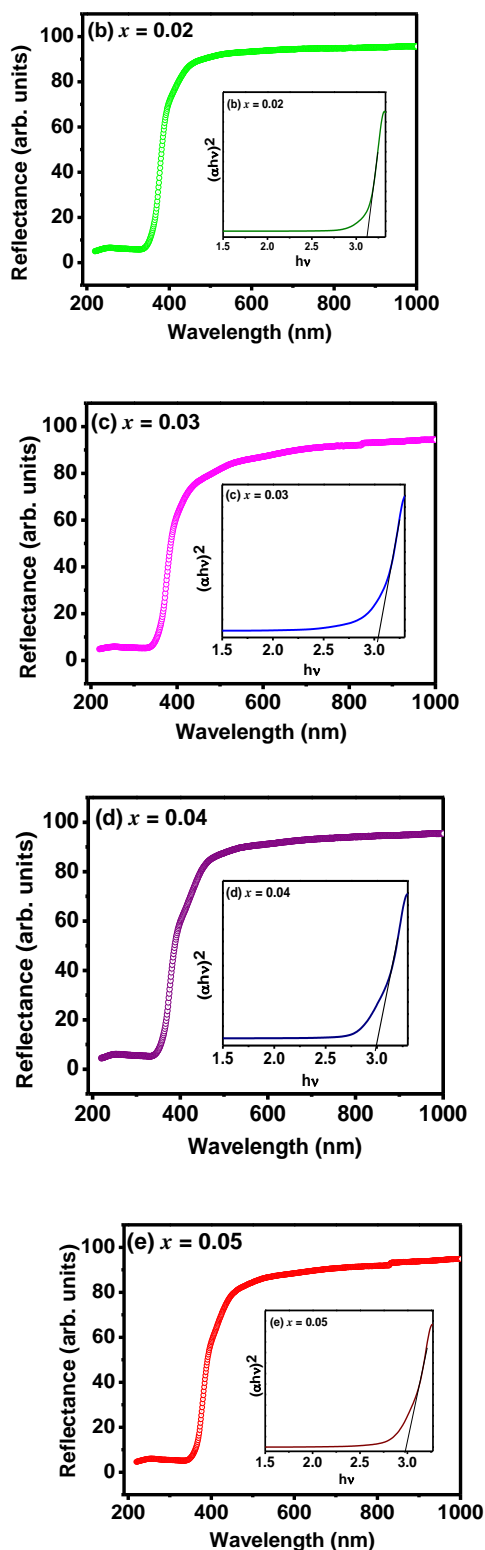


Figure 2: UV visible diffuse reflectance spectra and Tauc plots (inset in the Figure) of  $\text{Ba}_{0.8-x}\text{Sm}_x\text{Sr}_{0.2}\text{TiO}_3$  for (a)  $x = 0.01$ , (b)  $x = 0.02$ , (c)  $x = 0.03$ , (d)  $x = 0.04$ , and (e)  $x = 0.05$ .

Here,  $A$ ,  $h\nu$ ,  $E_g$ ,  $n$  and  $\alpha$  represent a constant, photon energy, optical band gap, a

constant related to different types of electronic transition and absorbance, respectively. The value of  $n$  is different for different types of transition such as  $n = 1/2$ ,  $2$ ,  $3/2$ , and  $3$  for direct allowed transition, indirect allowed transition, directly forbidden, and indirect forbidden, respectively.

Here,  $\text{Ba}_{0.8-x}\text{Sm}_x\text{Sr}_{0.2}\text{TiO}_3$  is considered as direct band gap. Hence,  $(\alpha h\nu)^2$  vs.  $h\nu$  have been plotted and shown in the Figure 2 (inset figure). The optical band gap has been estimated by extrapolating the tangent of the curves that intersects the  $h\nu$ -axis directly and gives the optical band gap of the samples. The obtained band gaps are 3.13, 3.12, 3.03, 2.99 and 2.97 eV for  $x = 0.01$ , 0.02, 0.03, 0.04, and 0.05, respectively. One can noticed that the optical energy gap decreases with the  $\text{Sm}^{3+}$  concentration, this is due to the structural disorder induced in the lattice because of the formation of A-site vacancies and distortions in the octahedral clusters ( $\text{TiO}_6$ ). This A-site vacancy creates shallow defects in the band gap of BSTO and decreases its value. So with increase in  $\text{Sm}^{3+}$  concentration, the A-site vacancies increase as well as increases the shallow defects and distortion in  $\text{TiO}_6$  octahedron [16]. Hence optical band gap decreases with further increase in  $\text{Sm}^{3+}$  concentration. Overall, the formation of shallow defects is the reason behind the optical characteristics of  $\text{Ba}_{0.8-x}\text{Sr}_{0.2}\text{Sm}_x\text{TiO}_3$ .

**4. Conclusion:** Incorporation of  $\text{Sm}^{3+}$  plays an important role in the reduction of dielectric constant in BSTO. The highest dielectric constant value is found to 2788 for  $\text{Ba}_{0.77}\text{Sm}_{0.03}\text{Sr}_{0.2}\text{TiO}_3$ . The estimated optical band gap of  $\text{Sm}^{3+}$  modified BSTO is varies between (3.13-2.97) eV. This is basically because of the new electronic levels in the BSTO band gap due to the  $\text{Sm}^{3+}$  addition to its lattice site. These electronic levels modify the conduction band and make a continuous band by lowering the band gap. Overall, the above discussion indicates that the  $\text{Sm}^{3+}$  substituted BSTO has the potential to be used in different applications mainly in optoelectronic devices.

## Acknowledgements

The authors acknowledge the support from the UGC-DAE CSR project (Project No. CRS/2021-22/03/595).

## References

- [1] J.F. Li, K. Wang, F.Y. Zhu, L.Q. Cheng, F.Z. Yao, (K,Na)NbO<sub>3</sub>-Based lead-free piezoceramics: fundamental aspects, processing technologies, and remaining challenges, *J. Am. Ceram. Soc.* **96** (2013) 3677–3696.
- [2] J. Wu, D. Xiao, J. Zhu, Potassium–sodium niobate lead-free piezoelectric materials: past, present, and future of phase boundaries, *Chemi. Rev.* **115** (2015) 2559–2595.
- [3] Feteira, D. C. Sinclair, I. M. Reaney, Y. Somiya, and M. T. Lanagan BaTiO<sub>3</sub>-based ceramics for tunable microwave applications *J. Am. Ceram. Soc.* **87**, 1082–7(2004).
- [4] B. Wang, Z. Huang, P. Tang, S. Luo, Y. Liu, J. Li, X. Qi, One-pot synthesized Bi<sub>2</sub>Te<sub>3</sub>/ graphene for a self-powered photoelectrochemical-type photodetector, *Nanotechnology* **31** 115201(2020).
- [5] J. Zhang, S. Jiao, D. Wang, S. Ni, S. Gao, J. Wang, Solar-blind ultraviolet photodetection of an  $\alpha$ -Ga<sub>2</sub>O<sub>3</sub> nanorod array based on photoelectrochemical selfpowered detectors with a simple, newly-designed structure, *J. Mater. Chem. C.* **7** 6867–6871(2019).
- [6] K.M. Sangwan, N. Ahlawat, R. Kundu, S. Rani, S. Rani, N. Ahlawat, S. Murugavel, Improved dielectric and ferroelectric properties of Mn doped barium zirconium titanate (BZT) ceramics for energy storage applications, *J. Phys. Chem. Solid.* **117** (2018) 158–166.
- [7] M. Tihtih, J.E.F. Ibrahim, M.A. Basyooni, R. En-Nadir, I. Hussainova, I. Kocserha, Functionality and activity of sol-gel-prepared Co and Fe co-doped lead-free BTO for thermo-optical applications, *ACS Omega* **8** (2023) 5003–5016.
- [8] Mallick, J., Manglam, M. K., Pradhan, L. K., Panda, S. K., & Kar, M. (2022). Electrocaloric effect and temperature dependent scaling behaviour of dynamic ferroelectric hysteresis studies on modified BTO. *Journal of Physics and Chemistry of Solids*, **169**, 110844.
- [9] J.Q. Qi, B.B. Liu, H.Y. Tian, H. Zou, Z.X. Yue, L.T. Li, Dielectric properties of barium zirconate titanate (BZT) ceramics tailored by different donors for high voltage applications, *Solid State Sci.* **14** (2012) 1520–1524.
- [10] E.H. Yahakoub, A. Bendahhou, K. Chourti, F. Chaou, I. Jalafi, S. El Barkany, Z. Bahari, M. Abou-salama, Structural, electrical, and dielectric study of the influence of 3.4% lanthanide (Ln<sup>3+</sup> = Sm<sup>3+</sup> and La<sup>3+</sup>) insertion in the A-site of perovskite Ba<sub>0.95</sub>Ln<sub>0.034</sub>Ti<sub>0.99</sub>Zr<sub>0.01</sub>O<sub>3</sub>, *RSC Adv.* **12** (2022) 33124–33141
- [11] S. Garcia, R. Font, J. Portelles, R.J. Quinones, J. Heiras, J.M. Siqueiros, “Effect of Nb Doping on (Sr,Ba)TiO<sub>3</sub> (BST) Ceramic Samples, *J. Electroceram.*” **6**, 101 (2001).
- [12] O.P. Thakur and C. Prakash, Dielectric Properties of Samarium Substituted Barium Strontium Titanate, *Phase Transitions*, **76**, 567-574 (2003).
- [13] S. K. Jo, J. S. Park, and Y. H. Han, “Effects of multi-doping of rare-earth oxides on the microstructure and dielectric properties of BaTiO<sub>3</sub>,” *Jour. of Alloys and Comps.* **501**, 259–264 (2010).
- [14] Mallick, J., Shukla, A., Panda, S. K., Manglam, M. K., Biswal, S. K., Pradhan, L. K., & Kar, M. (2023). Enhanced ferroelectricity and electrocaloric effect of Sm modified BSTO with temperature stability near room temperature. *Journal of Applied Physics*, **133**(6).
- [15] Mallick, J., Shukla, A., Panda, S. K., Biswal, S. K., Rout, S. N., Yadav, M. K., & Kar, M. (2024). Crystal symmetry transition and its influence on optical, dielectric, and ferroelectric properties in (1-x) Na<sub>0.5</sub>Bi<sub>0.5</sub>TiO<sub>3</sub>-xSrTiO<sub>3</sub> system. *Journal of Alloys and Compounds*, **978**, 173403.
- [16] Ganguly, M.; Rout, S.K.; Woo, W.S.; Ahn, C.W.; Kim, I.W.; *Phys. B Condens. Matter* **2013**, **411**, 26–34.

# Geometry Dependent Microwave Absorption Properties in Carbonaceous Materials over X-Band Frequencies (8.2-12.4 GHz) for Stealth Applications

Lokesh Saini<sup>1</sup>, Priyambada Sahoo<sup>2</sup>, Raj Kumar Jani<sup>1</sup>, Ambesh Dixit<sup>\*2</sup>

<sup>1</sup>Stealth Technologies Division, Defence Laboratory, Defence Research & Development Organisation (DRDO), Ratanada, Jodhpur, 342011, India

<sup>2</sup>Advanced Materials and Devices (A-Mad) Laboratory, Department of Physics, Indian Institute of Technology Jodhpur, Karwar, Jodhpur, 342037, India

Volume 1, Issue 5, October 2024

Received: 6 September, 2024; Accepted: 16 October, 2024

DOI: <https://doi.org/10.63015/5C-2438.1.5>

\*Correspondence Author- [ambesh@iitj.ac.in](mailto:ambesh@iitj.ac.in)

**Abstract:** Carbonaceous materials of two different types, viz. spherical nano carbon black (NCB) powder (Brunauer-Emmett-Teller (BET) surface area  $\sim 1400$  m<sup>2</sup>/g) and multiwalled carbon nanotube (MWCNT) (BET surface area  $\sim 75$  m<sup>2</sup>/g), have been impregnated in room temperature vulcanized (RTV) silicon rubber matrix to study the effect of geometries of filler particles on microwave absorption characteristics, over X-band frequencies (8.2 -12.4 GHz). The rubber-based composites are prepared by dispersion of NCB and MWCNT fillers in the liquid rubber with loading fractions ranging from 0.3-0.9 wt% and 1.1-1.7 wt%, respectively. The dielectric loss tangent ( $\tan\delta_\epsilon$ ) profiles were evaluated for the filler-loaded rubber composites at different concentrations. The calculated Reflection loss (RL) profiles suggest that NCB-based rubber provides maximum RL value,  $(RL)_{\max} \sim -20$  dB (99.00 % absorption), at a lower filler concentration of 0.5 wt%, as compared to MWCNT. However, the MWCNT-based rubber composite shows enhanced  $(RL)_{\min}$  values of  $\sim -29$  dB ( $\sim 99.99\%$  absorption) due to multiple scattering phenomena. The identified NCB and MWCNT-based rubber-based MW absorbers have potential stealth applications for military aerial vehicles.

**Keywords:** Stealth, DC conductivity, rubber composites, loss tangent, reflection loss

**1. Introduction:** With the escalating progress in Microwave (MW)/Radar technology during the last few decades, serious concerns are also emerging in society, viz., the unkind effect of MW radiation on human health, detection of fighter aircraft by enemy Radars during wartime operations, communicational interferences/clutters among MW instrumentations, etc., [1]–[3]. Therefore, the development of Microwave Absorbing Materials (MAMs) and their products in the forms of sheets/coatings/structures having desired properties picked up the interest of scientific community to suit the requirements. The electromagnetic parameters of these materials, viz. complex permittivity ( $\epsilon^* = \epsilon' - j\epsilon''$ ), complex permeability ( $\mu^* = \mu' - j\mu''$ ), and conductivity ( $\sigma$ ) play a critical role in microwave absorption, which decide the type of absorption (magnetic/dielectric) and MW

frequency band coverage [4]. Among the other MW frequency bands, X-band (8.2-12.4 GHz) has been widely used in the defence sector for the detection, tracking, and surveillance of objects requiring airborne objects' protection for their survivability [5].

Different types of materials, viz. metal flakes [6], ferrites [7], [8], carbonyl iron [9], ferroelectrics [10], core-shell materials [11], [12], etc., have been explored by researchers due to their wide frequency range of MW absorption as well as superior reflection loss values. However, higher loading fractions of filler material in host matrices are reported to achieve the optimum MW absorption in composites made of these MAMs. The implication of higher filler loading in the matrix translates into high density, weight penalty, and lower mechanical strength of MW absorbing composites. Therefore, carbonaceous materials

are being explored to fabricate lightweight & low-cost MW absorbers with thermal, mechanical, chemical, and environmental stability.[13]

Various carbonaceous materials, viz. graphene [14], carbon black [15], carbon nanotubes (CNTs) [16], graphite [17], carbon nanofibers (CNFs) [18], etc., have been used in resin [19], rubber [20], [21] and ceramic [22] matrices for their microwave absorption studies over the broad frequency range of 2-18 GHz. It is evident that carbonaceous materials, which are being used as MAMs, possess low density (range 1.6-2.3 g/cm<sup>3</sup>) and high surface-to-volume ratio, which make them unsuitable for dispersion in resin/rubber matrix at higher filler loading, resulting in the formation of lumps, uneven distribution/segregation of filler powders, voids/crack in coating/sheets, etc. The inadequate dispersion of carbonaceous filler also resulted in inferior MW absorption properties. Therefore, selecting functional carbonaceous fillers and dispersing host matrix should be judicious to achieve the desired MW absorption properties at lower filler loading. The imaginary permittivity ( $\epsilon_r''$ ) of the MW absorber represents the loss characteristics against incident MW signals, which is directly dependent on its DC conductivity ( $\sigma_{dc}$ ) [23]. Hence, to achieve the desired conductivity of the composite absorber at a lower filler fraction, the conductive network of filler should be formed in an insulating host matrix, which eventually depends on the dispersion of filler particles in the matrix.

Resins/liquid rubbers are found to be better host matrix as compared to solid rubbers to attain the lower percolation threshold due to the attainment of strong crosslinking in rubbers during vulcanization, which prevents connection of long-range ordering of conducting filler in the host matrix [24]. Further, the filler particle shape, size, and surface area also determine the dispersion characteristics in resin matrices. In the present work, we have attempted to study the effect of particle shape, size, surface area, and aspect ratio on electromagnetic (EM) parameters and microwave absorption characteristics of the resin-filler composite. For the study, two

different filler materials, viz. nano carbon black (NCB) powder with high surface area and multiwalled carbon nanotubes (MWCNT) with high aspect ratio, were dispersed in room temperature vulcanized (RTV) liquid silicon rubber in different filler fractions. Electromagnetic parameters of rubber composites were evaluated using a Vector Network Analyzer (VNA) over the X-band MW frequency range (8.4-12.4 GHz).

## 2. Experimental Details

### 2.1. Fabrication of Filler-Loaded Rubber Composite:

Commercially available nanocarbon black and multiwalled carbon nanotubes were used as functional materials for MW absorption. Details of materials are given in Table 1. Two components of RTV silicone rubber (liquid rubber 95 wt%: catalyst 5 wt%) were used as a host matrix for the dispersion of carbonaceous filler materials. Initially, 95g of silicone rubber and 10 ml of solvent (o-Xylene) were mixed with the required filler powder and stirred for 30 minutes at 1200 RPM for its uniform dispersion in rubber. After thorough mixing, 5g of catalyst was added to the rubber-filler compound and stirred again for homogenization. The admixed compound was transferred uniformly into a die of size 100 mm × 100mm × 3mm and pressed into a hydraulic press at 01 Ton pressure to avoid any voids/pores in the composite structure. The rubber composite was removed from the die after 4 hours and kept in ambient for 24 hours for proper curing. The schematic for filler-loaded silicone rubber composite sheet fabrication is shown in Fig. 1. Further, a series of silicon rubber sheets were prepared by impregnating Nano Carbon Black (NCB) and multiwalled Carbon Nanotubes (CNT) as per the details provided in Table 2.

The filler-loaded silicon rubber sheets were cut in 22.86 × 10.16 mm (L × W) size for measurement through VNA over X-band frequencies (8.2 – 12.4 GHz).

Table 1: Details of Functional Materials

Sl. No.	Type of Material	Particle size (nm)	Particle Morphology	BET Surface area (m <sup>2</sup> /g)	Source of Availability
1.	Nano Carbon Black (NCB) (Ketjenblack EC-600JD)	~5-10	Spherical	1400	AkzoNobel Functional Chemicals, USA
2.	Multiwalled Carbon Nano Tubes (MWCNT)	~5-10 (diameter)	Tubular Aspect ratio ~ 2000	75	Commercialized, Sigma Aldrich

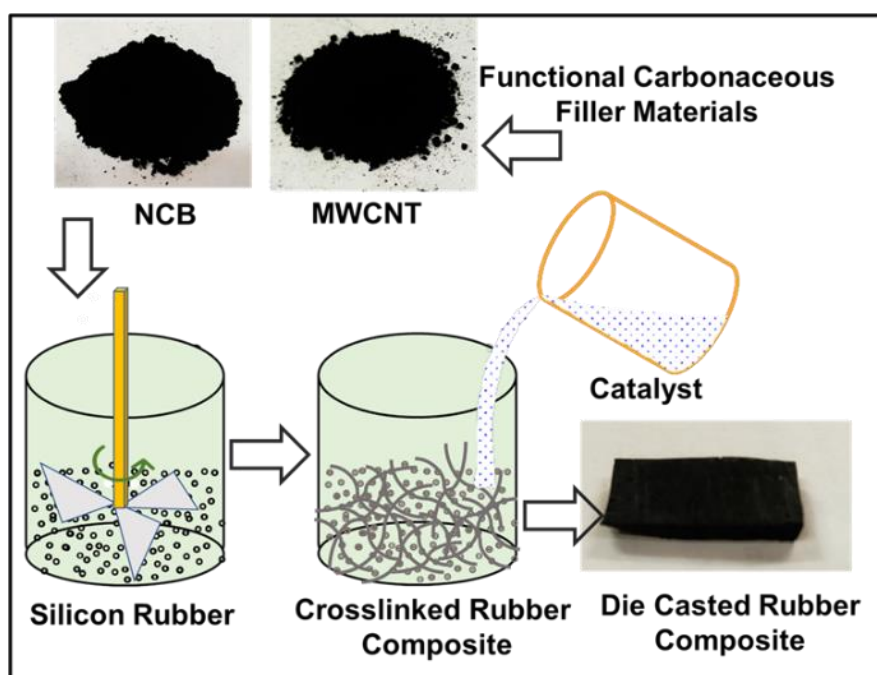


Figure 1. Schematic representation of fabrication of carbonaceous filler loaded silicon rubber composite sheet.

## 2.2. Characterization of Filler Materials and Rubber Composites:

The crystal structure of NCB and CNT powders was investigated using an X-ray diffraction (XRD) system (Model: X'Pert Pro; Make: Philips) over the  $2\theta$  range of  $20^\circ$ - $80^\circ$  with incident radiation of  $\text{Cu K}\alpha$  ( $\lambda = 1.540 \text{ \AA}$ ). The morphology of both the powder samples was estimated using a Scanning Electron Microscope (SEM) (Model EVO5; Make:

Oxford) for the filler powder samples. DC Conductivity of all the rubber composite samples was measured using a four-probe conductivity measurement set-up. EM parameters viz. complex permittivity and permeability of NCB/MWCNT loaded rubber composites sheets were estimated using a two-port waveguide transmission line technique with the help of Vector Network Analyzer (VNA) (Model: Keysight PNA;

Make: Keysight Technologies) over the frequency range 8.2-12.4 GHz. The reflection ( $S_{11}$ ) and transmission ( $S_{22}$ ) scattering parameters were measured through VNA,

which were used in the estimation of complex permittivity ( $\epsilon_r^*$ ) and complex permeability ( $\mu_r^*$ ) using Nicolson-Ross-Weir (NRW) Algorithms [25].

**Table 2: Details of Fabrication of Filler Loaded Silicon Rubber Sheet**

Type of Material	Silicon resin (g)	Catalyst	Filler Amount (g)	Loading Fraction	Sample Nomenclature
Nano Carbon Black (NCB)	95	05	0.3	0.3 wt%	NCB0.3
	95	05	0.5	0.5 wt%	NCB0.5
	95	05	0.7	0.7 wt%	NCB0.7
	95	05	0.9	0.9 wt%	NCB0.9
Multiwalled Carbon Nanotubes (MWCNT)	95	05	1.1	1.1 wt%	CNT1.1
	95	05	1.3	1.3 wt%	CNT1.3
	95	05	1.5	1.5 wt%	CNT1.5
	95	05	1.7	1.7 wt%	CNT1.7

**3. Results and Discussion**

**3.1. X-ray Diffraction Studies:** The XRD pattern of nano carbon black (NCB) is shown in Fig. 2(a), which confirms the presence of hexagonal graphitic carbon peaks with (002) and (100) crystal planes in NCB [26]. The Fig. 2(b) shows the XRD pattern of MWCNT powder, where the intense characteristic

graphite peak (002) at  $\sim 26^\circ$  corresponds to tubular carbon atoms, and other peaks correspond to graphitized carbon peaks of (100) and (004) planes, respectively [27]. The XRD spectra of NCB and MWCNT powders confirm the phase purity materials, exhibiting no diffraction peak for other carbon allotropes.

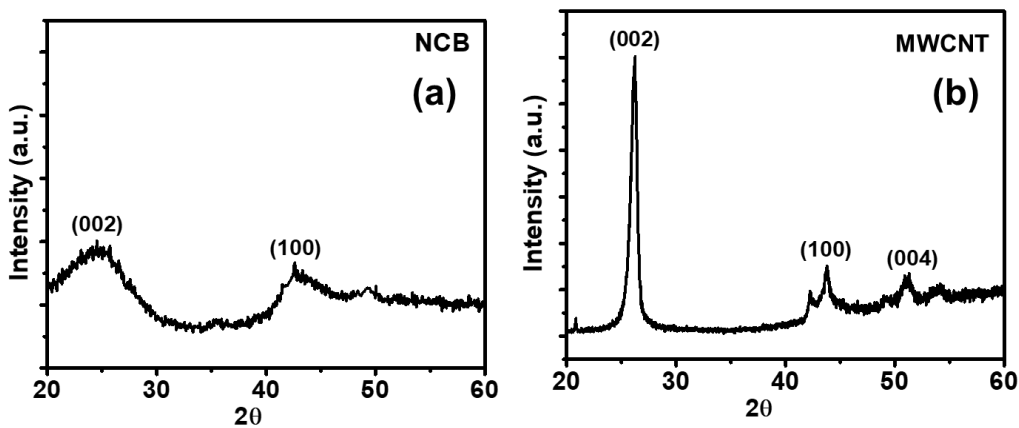
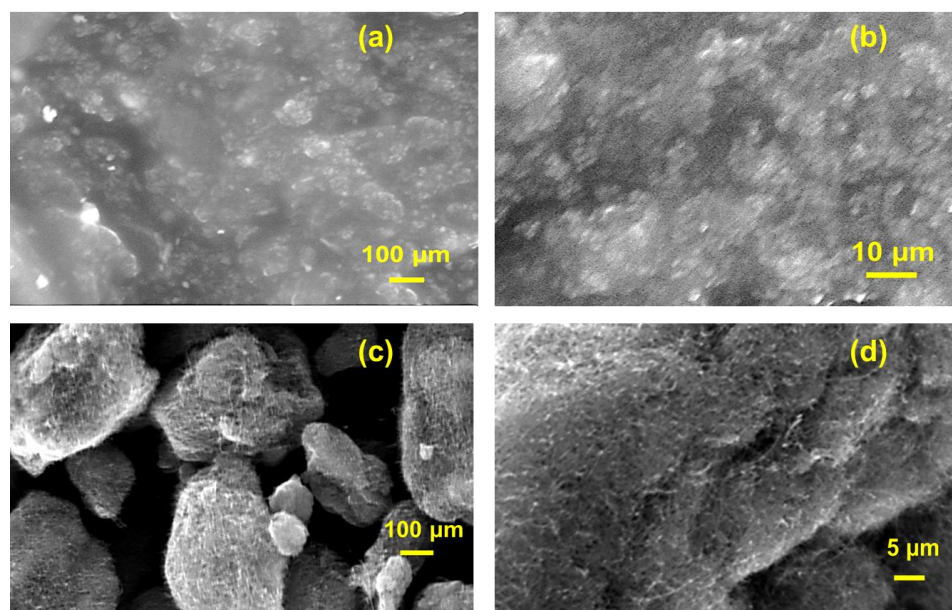


Figure 2. XRD spectra of (a) Nano carbon black (NCB) and (b) Multiwalled CNTs

**3.2. Morphological Studies:** Figure 3(a)-(b) show SEM micrographs of nanocarbon black powder (NCB) in different magnifications, which confirms the nearly spherical

morphology. The SEM micrographs of MWCNT powder shown in Figure 3(c)-(d) confirm the fiber statures of the material.



**Figure 3.** (a)-(b) SEM micrograph of NCB filler powder, (c)-(d) SEM micrograph of multiwalled CNT filler powder

**3.3. DC Conductivity Studies:** The DC conductivity ( $\sigma$ ) values of NCB-rubber composites with filler loading in the 0.3-0.9 wt% range are shown in Fig. 4 (a). Initially, at lower NCB loading in NCB0.3 (0.3 wt%) & NCB0.5 (0.5 wt%) rubber composites, the  $\sigma$  values are found  $\sim 1.25 \times 10^{-5}$  S/cm and  $6.75 \times 10^{-5}$  S/cm. With a further increase in NCB content to 0.7 wt% (NCB0.7), the values of  $\sigma$  increased to  $\sim 9.18 \times 10^{-3}$  S/cm. However, with a further increase in NCB concentration to 0.9 wt% in the NCB0.9 composite sample, the  $\sigma$  increases drastically up to 0.17 S/cm due to forming a conducting network of nano carbon particles in silicon rubber composite [23]. Similarly, the MWCNT-loaded rubber composites CNT1.1 (1.1 wt%) & CNT1.3 (1.3 wt%) have  $\sigma$  values  $1.95 \times 10^{-4}$  S/cm and  $5.86 \times 10^{-5}$  S/cm, respectively. The 1.5 wt%

MWCNT loaded sample (CNT1.5) exhibit  $\sigma \sim 1.06 \times 10^{-5}$  S/cm. The increment of MWCNT filler powder up to 1.7 wt% in the composite, the  $\sigma$  value was increased abruptly up to 0.23 S/cm because of the formation of the conduction network. It is interesting to note that NCB-based rubber composite attains the DC conductivity value 0.17 S/cm at lower filler loading of 0.9 wt%, where the almost similar  $\sigma$  value in MWCNT-based rubber composite (0.23 S/cm) could be achieved at 1.7 wt% loading of filler powder. The main reason for this finding is attributed to the very high surface area of NCB powder ( $1400 \text{ m}^2/\text{g}$ ) as compared to MWCNT ( $75 \text{ m}^2/\text{g}$ ), which facilitates the formation of a conduction network in nanocarbon powder at a lower loading fraction as compared to MWCNT.

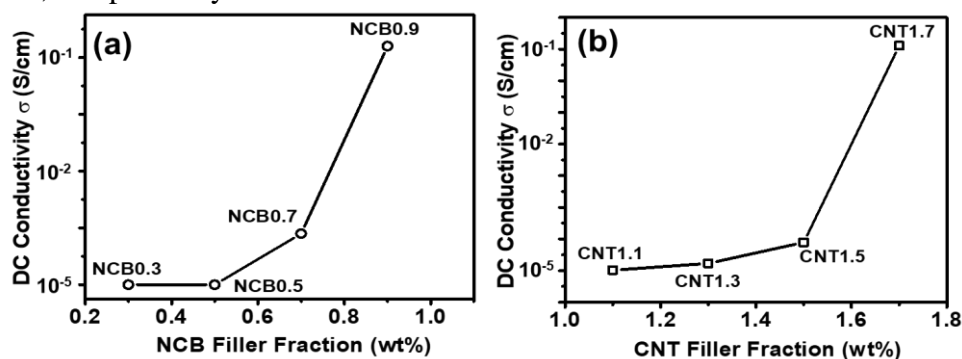


**Figure 4.** (a) Variation of DC conductivity with NCB filler loading in Si rubber (b) Variation of DC conductivity with MWCNT filler loading in Si rubber

**3.4. Evaluation of EM Parameters:** The EM parameters viz. real ( $\epsilon_r'$ ) & imaginary ( $\epsilon_r''$ ) relative permittivity for NCB and MWCNT loaded rubber composites are shown in Fig. 5(a)-(d). The  $\epsilon_r'$  values for 0.3 wt% NCB loaded composites NCB0.3 are almost constant  $\sim 6.5$  over 8.2-12.4 GHz frequency range. The  $\epsilon_r'$  values of NCB-based composites increase with enhancement in filler loading  $\sim 11.5 \pm 1$  (NCB0.5),  $\sim 12.5 \pm 1$  (NCB0.7) &  $\sim 14 \pm 2$  (NCB0.9)] due to an increase in the effective concentration of conductive nano carbon filler in the insulating rubber matrix (Fig. 5a). These plots have dispersive nature with frequency variation. The real permittivity in such composites, in which conductive fillers (NCB & MWCNT) are dispersed in an insulating rubber matrix, is governed by Maxwell-Wagner type interfacial polarization. With the increase in the filler loading, the contribution of interfacial polarization also increases, which may be saturated beyond a threshold [15]. This effect may be more prominent beyond the frequency range of 10 GHz, as observed in Fig 5(a). Therefore, the  $\epsilon_r'$  values for NCB0.7 &

NCB0.9 are found to be almost similar. The imaginary permittivity ( $\epsilon_r''$ ) value of NCB/rubber composites, which is attributed to conduction losses, increases with increasing nanocarbon concentration due to an increase in DC conductivity ( $\sigma$ ) governed by equation  $\epsilon_r'' = \sigma / 2\pi f \epsilon_0$ , where  $f$  is the frequency (GHz), and  $\epsilon_0$  is free space permittivity ( $8.85 \times 10^{-12}$  F/m) [28]. The imaginary permittivity ( $\epsilon_r''$ ) values for NCB0.3, NCB0.5, NCB0.7 & NCB0.9 are observed  $\sim 1.6$ ,  $\sim 5.3$ ,  $\sim 7.8 \pm 0.2$ , and  $13 \pm 1$ , respectively. Similarly, for MWCNT filler-loaded rubber composites CNT1.1-CNT1.7 (1.1 wt% to 1.7 wt%), the  $\epsilon_r'$  values increase from  $\sim 15.4 \pm 0.9$  (CNT1.1) to  $\sim 21 \pm 3$  (CNT1.7) over 8.2-12.4 GHz frequency range, as shown in Fig. 5(c). The imaginary permittivity values of MWCNT-loaded rubber specimens also show an increasing trend with filler loading, viz.  $\sim 5 \pm 1$  (CNT1.1),  $8 \pm 1$  (CNT1.3),  $11 \pm 1$  (CNT1.5) and  $14 \pm 2$  (CNT1.7) as depicted in Fig. 5(d).

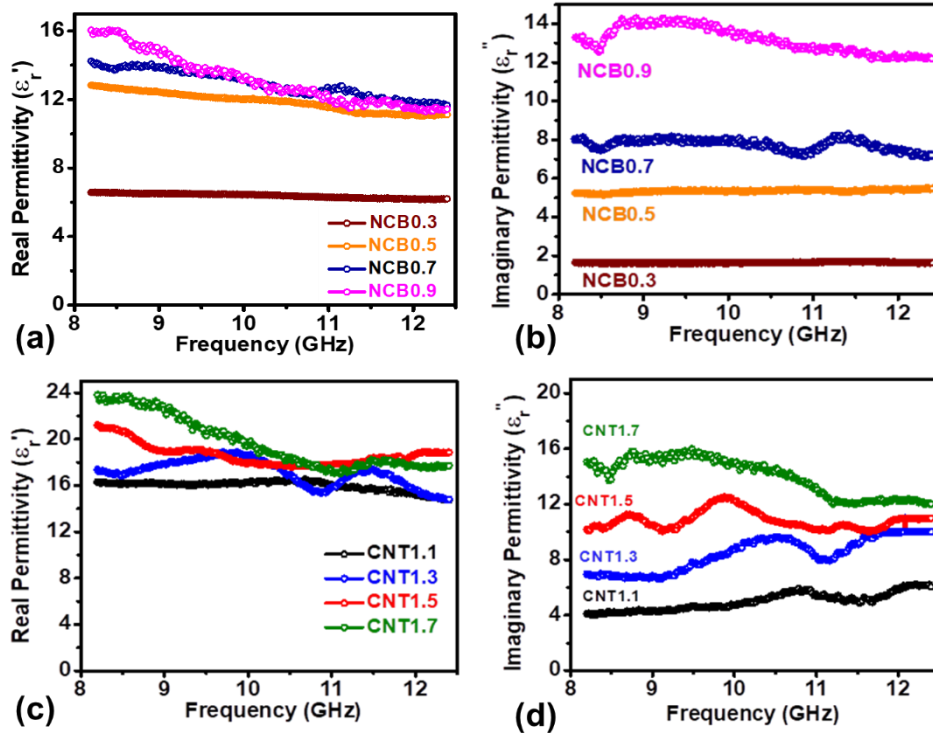


Figure 5. (a)-(b) Variation of relative real permittivity ( $\epsilon_r'$ ) & imaginary permittivity ( $\epsilon_r''$ ) values for NCB filler loaded rubber composites (c)-(d) Variation of relative imaginary permittivity ( $\epsilon_r''$ ) values for MWCNT filler loaded rubber composites



The dielectric loss tangent  $\tan\delta_e$  values, which are the ratio of  $\epsilon_r''$  and  $\epsilon_r'$  ( $\tan\delta_e = \epsilon_r'' / \epsilon_r'$ ) for NCB & MWCNT based rubber composites are plotted in Fig. 6(a)-(b). The  $\tan\delta_e$  values for both the materials systems increase with the loading fraction of functional filler due to the enhancement of conduction loss in the rubber matrix. The NCB0.3, NCB0.5, NCB0.7 &

NCB0.9 samples have corresponding  $\tan\delta_e$  values  $\sim 0.25$ ,  $\sim 0.45 \pm 0.05$ ,  $\sim 0.55 \pm 0.05$  and  $\sim 0.95 \pm 0.05$ , respectively. Whereas,  $\tan\delta_e$  values for CNT1.1, CNT1.3, CNT1.5 & CNT1.9 samples are observed  $\sim 0.35 \pm 0.1$ ,  $\sim 4.5 \pm 0.15$ ,  $\sim 5.5 \pm 0.1$  and  $\sim 7 \pm 0.1$ , respectively.

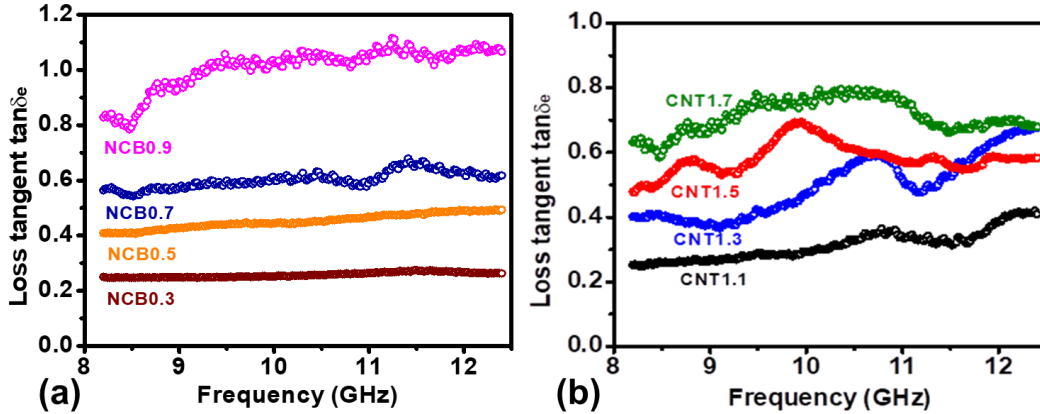


Figure 6. (a) Dielectric loss tangent ( $\tan\delta_e$ ) plots for NCB loaded rubber composites (b) Dielectric loss tangent ( $\tan\delta_e$ ) plots for MWCNT loaded rubber composites

### 3.5. Estimation of Reflection Loss (RL):

The reflection loss (RL) value, which is represented in decibels (dB), is the quantitative estimation of the MW absorption capability of any stealth product. The RL values can be calculated by Equation 1 [29].

$$RL \text{ (dB)} = 20 \log_{10} \left| \frac{\sqrt{\frac{\mu_r^*}{\epsilon_r^*}} \tanh\left(\frac{j 2\pi d}{\lambda} \sqrt{\mu_r^* \epsilon_r^*}\right) - 1}{\sqrt{\frac{\mu_r^*}{\epsilon_r^*}} \tanh\left(\frac{j 2\pi d}{\lambda} \sqrt{\mu_r^* \epsilon_r^*}\right) + 1} \right| \quad (1)$$

Where  $\epsilon_r^*$  is complex permittivity,  $\mu_r^*$  is complex permeability,  $d$  is absorber thickness, and  $\lambda$  is wavelength. Generally, the targeted RL value for any absorber used for stealth application is considered as minimum -10 dB or more (negative sign represents MW loss characteristics), which quantifies to 90% or more MW absorption capabilities. The matching thickness ( $d_m$ ) where the RL values are found maximum is given by  $d_m = \frac{c}{4f \sqrt{|\mu_r^*| |\epsilon_r^*|}}$ , provides the critical design

thickness for the fabrication of any stealth product. The RL plots for NCB-based absorbers NCB0.3-NCB0.9 are shown in Fig. 7(a)-(d). The NCB0.3 rubber composite has  $d_m$  value of 3.0 mm with a maximum RL( $RL_{max}$ )

value of  $\sim -13$  dB at 10.3 GHz, shown in Fig.7(a). The RL profiles shift towards the lower frequency side with increasing absorber thickness, substantiating its reciprocal dependence. The NCB0.5 absorber shows improved RL performance as compared to NCB0.3, where ( $RL_{max}$ ) value is  $\sim -20$  dB at 9.8 GHz, at a reduced matching thickness of 2.2 mm, contributed by enhanced dielectric loss properties (Fig. 7(b)). Further, the absorption bandwidth for  $RL \geq 10$  dB is  $\sim 3.3$  GHz over the entire X-band frequencies. With further increase in NCB content to 0.7 wt% in NCB0.7 absorber, the ( $RL_{max}$ ) value decreases to  $\sim -18$  dB at 10.2 GHz, having optimum thickness of 2.0 mm, however the absorption bandwidth is still found  $\sim 3.3$  GHz (Fig. 7c). Interestingly, with still increase in NCB content to 0.9 wt% (NCB0.9), the ( $RL_{max}$ ) value decreases to  $\sim -6$  dB with almost constant values throughout the frequency range of 8.2-12.4 GHz, as shown in Fig. 7(d). The loss tangent  $\tan\delta_e$  values of this composite are maximum  $\sim 0.95 \pm 0.05$  compared to other specimens; however, the RL values are still found inferior due to the onset of impedance mismatch of incident MW signals at the high conducting surface of the absorber [30].

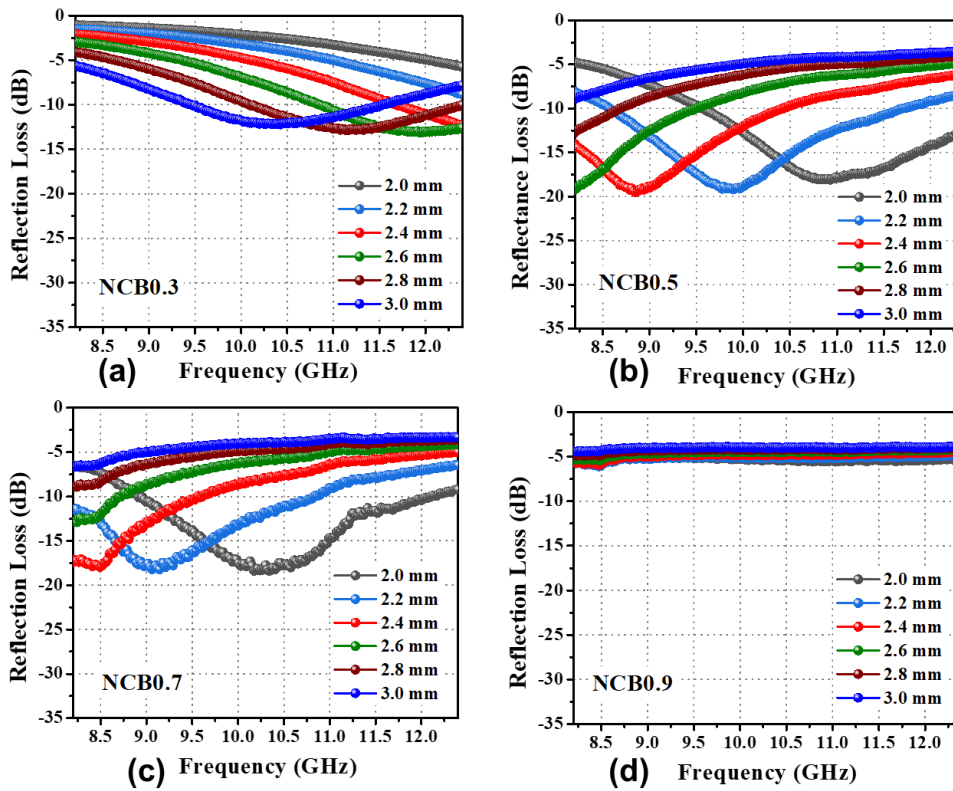


**Figure 7. Frequency vs Reflection Loss (RL) plots for (a) NCB0.3 (b) NCB0.5 (c) NCB0.7 (d) NCB0.9**

Figure 8 shows RL plots of MWCNT filler-based rubber absorbers with different loading ranges of 1.1-1.9 wt%. CNT1.1 sample has  $RL_{max}$  value  $\sim -18$  dB at 8.5 GHz, having a matching thickness of 2.0 mm. The  $RL_{max}$  value of the CNT1.3 absorber significantly improved to  $\sim -29$  dB at  $\sim 9.5$  GHz with the same matching thickness of 2.0mm. The effective absorption bandwidth of this composition is at  $\sim 3$  GHz at a thickness of 1.8 mm. The higher  $RL_{max}$  values in MWCNT-based rubber composite may be triggered by a high aspect ratio, which helps in multiple scattering of EM signals and enhances MW absorption. In the MWCNT-filled composites, the impedance mismatch was observed beyond the filler content of 1.3 wt%, which results in a lower  $RL_{max}$  value of  $\sim -10$  dB in both CNT1.5

& CNT1.7 absorbers. Table 3 compares reported CB and MWCNT composite materials used for microwave absorption. Hence, these studies confirm that both high dielectric loss and impedance matching criteria should be met to achieve the optimum reflection loss values in MW absorbers. Further, the nanocarbon-based absorbers attain the desired MW absorption capabilities at lower filler loading than MWCNT-based composites due to the large surface area and proper dispersion attributed to spherical morphology. However, both the NCB and MWCNT-based rubber composites at optimized composition and thickness, viz. NCB0.5 and CNT1.3 are promising materials for stealth applications.

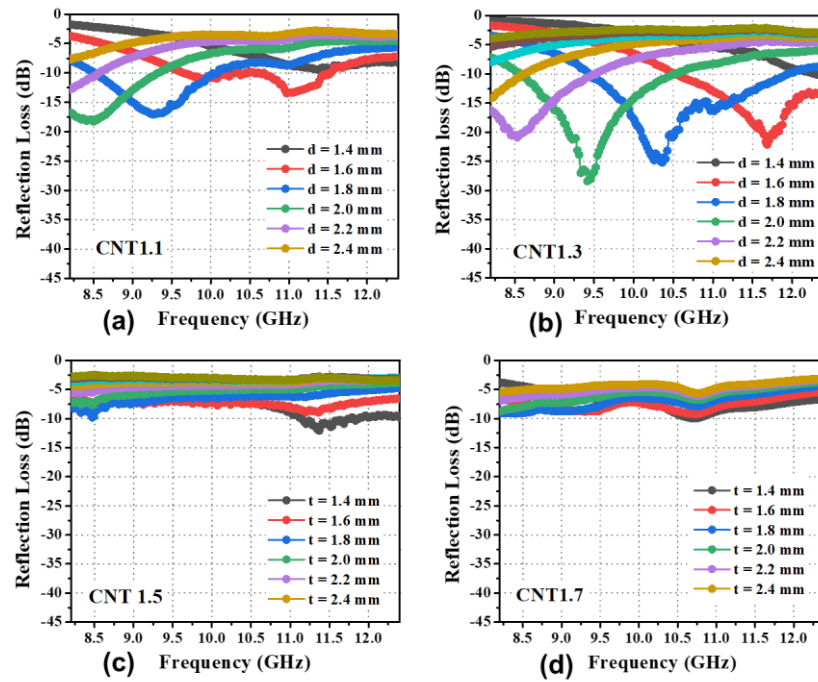


Figure 8. Frequency vs Reflection Loss (RL) plots for (a) CNT1.1 (b) CNT1.3 (c) CNT1.5 (d) CNT1.7

Table 3. The pristine carbonaceous (Carbon Black/Multiwalled CNT) and composite materials for MW absorption applications, borrowed from Ref [3].

Materials	Synthesis Route	Matrix	t (mm)	R <sub>L</sub> (dB)	Frequency (GHz)	Bandwidth (GHz)	Ref.
CB	Commercial	Silicon Rubber	2.7 (X-band)	~ -21 (X-band)	~ 10.0 (X-band)	4 (X-band)	[23]
			1.9 (Ku-band)	~ -25 (Ku-band)	~ 14 (Ku-band)	6 (Ku-band)	
CB	Commercial	polypropylene	2.8 (X-band)	-62.6 (X-band)	10.64 (X-band)	4.56 (X-band)	[31]
			1.9 (Ku-band)	-39.15 (Ku-band)	15.08 (Ku-band)	5.63 (Ku-band)	
CB & tetrapod like ZnO whiskers (T-ZnO)	Commercial	Epoxy Resin	3.0	-19.31	10.4	4.56	[32]
CB/SiC	Commercial	Epoxy Resin	2.0	~ -41	~ 9	6	[22]

CB/quartz glass fiber (SiO <sub>2</sub> )	Commercial	Polyimide Resin	1.6	-46.18	16.07	3.95	[33]
MWCNT	Commercial	Epoxy Resin	8	-29	11.5	3	[34]
MWCNT/CdS	chemical co-precipitation	Wax	1.5	-45	~15	-	[35]
Nano Carbon Black (NCB)	Commercialized, AkzoNobel Functional Chemicals, USA	Silicon Rubber	2.2	-20	9.8	3.3	This Work
MWCNT	Commercialized, Sigma Aldrich	Silicon Rubber	2.0	-29	9.5	3	This Work

**4. Conclusion:** Commercially available spherical-shaped Nano Carbon Black (NCB) (Particle size: 5-10 nm; BET surface area: 1400 m<sup>2</sup>/g) and Multiwalled Carbon Nanotubes (MWCNT) (Diameter: 5-10 nm; BET surface area: 75m<sup>2</sup>/g; aspect ratio: 2000) were selected to study the effect of geometries of functional fillers on the MW absorption performance of rubber-based composites. XRD spectra confirm the phase purity of commercial carbonaceous fillers without the signature of any other carbon allotropes. SEM micrographs suggested nearly spherical and fiber structures of NCB and MWCNT filler powders. NCB and MWCNT-based rubber composites were synthesized by dispersing these filler powders in liquid silicon resin in the range of 0.3-0.9 wt% and 1.1-1.7 wt%, respectively. Further, DC conductivity ( $\sigma$ ) measurement suggests that NCB filler-based rubber composites possess high values of  $\sigma \sim 0.17$  S/cm even at the lower filler concentration of 0.5 wt%, as compared to MWCNT filler, which obtains  $\sigma \sim 0.23$  S/cm at 1.1 wt% loading attributed to higher surface area. The EM parameters of both NCB and MWCNT-loaded rubber composites were evaluated over the frequency range of 8.2-12.4 GHz, and dielectric loss tangent  $\tan\delta_e$  values increased with increasing filler loading. The

calculated RL profiles suggest that 0.5 wt% NCB rubber composite (NCB0.5) shows optimized maximum RL values  $\sim -20$  dB at the matching thickness of 2.2 mm due to complimentary participation of both dielectric loss and impedance matching. Further, the MWCNT-based composite with 1.1 wt% filler loading (CNT1.1) shows improved optimized RL values  $\sim -29$  dB at the matching thickness of 2.0mm due to dielectric loss, impedance matching, and multiple reflections in the absorber medium. Both these absorbers have potential applications for the stealth treatment of airborne platforms.

#### Acknowledgement:

The authors thank Mr. R. V. Hara Prasad, Director of the Defence Laboratory, for his constant guidance and support for the present work. The authors are also thankful to Dr. R Nagarajan, Technology Director, Stealth Technology Division, and Dr. M. K. Patra, Defence Laboratory, for their fruitful suggestions during the work.

#### Conflict of Interest:

Authors declare No conflicts of interest.

## References

- [1] D. G. Xu, J. S. Liu, S. Luo, and P. Li, "Development Status and Trend of Stealth Technology of Tactical Missiles," *J. Phys. Conf. Ser.*, 2460, **2023**, 012064
- [2] H. Ahmad *et al.*, "Stealth technology: Methods and composite materials—A review," *Polym. Compos.*, 40, **2019**, 4457–4472
- [3] P. Sahoo, L. Saini, and A. Dixit, "Microwave-absorbing materials for stealth application: a holistic overview," *Oxford Open Mater. Sci.*, 3, **2023**, itac012
- [4] L. Cui, X. Han, F. Wang, H. Zhao, and Y. Du, "A review on recent advances in carbon-based dielectric system for microwave absorption," *J. Mater. Sci.*, 56, **2021**, 10782–10811
- [5] B. Zohuri, *Radar Energy Warfare and the Challenges of Stealth Technology*. Cham: Springer International Publishing, Book, **2020**.
- [6] C. Zhang, J. Jiang, S. Bie, L. Zhang, L. Miao, and X. Xu, "Electromagnetic and microwave absorption properties of surface modified Fe-Si-Al flakes with nylon," *J. Alloys Compd.*, 527, **2012**, 71–75
- [7] S. M. Abbas, R. Chatterjee, A. K. Dixit, A. V. R. Kumar, and T. C. Goel, "Electromagnetic and microwave absorption properties of (Co<sup>2+</sup>-Si<sup>4+</sup>) substituted barium hexaferrites and its polymer composite," *J. Appl. Phys.*, 101, **2007**, 074105
- [8] L. Saini, M. K. Patra, R. K. Jani, G. K. Gupta, A. Dixit, and S. R. Vadera, "Tunable twin matching frequency (fm1 /fm2) behavior of Ni<sub>1-x</sub>Zn<sub>x</sub>Fe<sub>2</sub>O<sub>4</sub> /NBR composites over 2-12.4 GHz: A strategic material system for stealth applications," *Sci. Rep.*, 7, **2017**, 1–12
- [9] K. S. Sista, S. Dwarapudi, D. Kumar, G. R. Sinha, and A. P. Moon, "Carbonyl iron powders as absorption material for microwave interference shielding: A review," *J. Alloys Compd.*, 853, **2021**, 157251
- [10] L. Vovchenko, O. Lozitsky, L. Matzui, V. Oliynyk, V. Zagorodnii, and M. Skoryk, "Electromagnetic shielding properties of epoxy composites with hybrid filler nanocarbon/BaTiO<sub>3</sub>," *Mater. Chem. Phys.*, 240, **2020**, 122234
- [11] L. Wang *et al.*, "Synthesis and microwave absorption enhancement of graphene@Fe<sub>3</sub>O<sub>4</sub>@SiO<sub>2</sub>@NiO nanosheet hierarchical structures," *Nanoscale*, 6, **2014**, 3157–3164
- [12] X. Zhao *et al.*, "Excellent microwave absorption property of Graphene-coated Fe nanocomposites," *Sci. Rep.*, 3, **2013**, 3421
- [13] F. Ruiz-Perez, S. M. López-Estrada, R. V. Tolentino-Hernández, and F. Caballero-Briones, "Carbon-based radar absorbing materials: A critical review," *J. Sci. Adv. Mater. Devices*, 7, **2022**, 100454
- [14] F. Meng *et al.*, "Graphene-based microwave absorbing composites: A review and prospective," *Compos. Part B Eng.*, 137, **2018**, 260–277
- [15] S. K. Kwon, J. M. Ahn, G. H. Kim, C. H. Chun, J. S. Hwang, and J. H. Lee, "Microwave absorbing properties of carbon black/silicone rubber blend," *Polym. Eng. Sci.*, 42, **2002**, 2165–2171
- [16] X. Chen, H. Liu, D. Hu, H. Liu, and W. Ma, "Recent advances in carbon nanotubes-based microwave absorbing composites," *Ceram. Int.*, 47, **2021**, 23749–23761
- [17] D. J. Gogoi, "Microwave absorber based on encapsulated expanded graphite-silicone composite as meta-‘atom’ for X-band application," *J. Electromagn. Waves Appl.*, 34, **2020**, 1444–1459
- [18] H. Breiss, A. El Assal, R. Benzerga, C. Méjean, and A. Sharaiha, "Long Carbon Fibers for Microwave Absorption: Effect of Fiber Length on Absorption Frequency Band," *Micromachines*, 11, **2020**, 1081
- [19] X. Lv, S. Yang, J. Jin, L. Zhang, G. Li, and J. Jiang, "Preparation and Electromagnetic Properties of Carbon Nanofiber/Epoxy Composites," *J. Macromol. Sci. Part B*, 49, **2010**, 355–365
- [20] S. Vinayasree *et al.*, "Flexible microwave absorbers based on barium hexaferrite, carbon black, and nitrile rubber for 2-12GHz applications," *J. Appl. Phys.*, 116, **2014**, 024902
- [21] J. H. Kaiser, "Microwave evaluation of the conductive filler particles of carbon black-rubber composites," *Appl. Phys. A Solids Surfaces*, 56, **1993**, 299–302
- [22] X. Liu, Z. Zhang, and Y. Wu,

- “Absorption properties of carbon black/silicon carbide microwave absorbers,” *Compos. Part B Eng.*, 42, 2011, 326–329
- [23] R. K. Jani, L. Saini, and S. R. Vadera, “Size dependent percolation threshold and microwave absorption properties in nano carbon black/silicon rubber composites,” *J. Appl. Phys.*, 131, **2022**, 044101
- [24] R. K. Jani, L. Saini, and S. R. Vadera, “Rheological Dependence on Dielectric and Microwave Absorption Properties of Carbon Black/Rubber Nanocomposites Over 6–18 GHz,” *J. Electron. Mater.*, 53, **2024**, 3187–3198
- [25] A. M. Nicolson and G. F. Ross, “Measurement of the Intrinsic Properties Of Materials by Time-Domain Techniques,” *IEEE Trans. Instrum. Meas.*, 19, 1970, 377–382
- [26] R. Ramaraghavulu, V. K. Rao, K. C. Devarayapalli, K. Yoo, P. C. Nagajyothi, and J. Shim, “Green synthesized AgNPs decorated on Ketjen black for enhanced catalytic dye degradation,” *Res. Chem. Intermed.*, 47, **2021**, 637–648
- [27] R. Atchudan, A. Pandurangan, and J. Joo, “Effects of nanofillers on the thermo-mechanical properties and chemical resistivity of epoxy nanocomposites,” *J. Nanosci. Nanotechnol.*, 15, **2015**, 4255–4267.
- [28] L. Wang *et al.*, “Recent progress of microwave absorption microspheres by magnetic-dielectric synergy,” *Nanoscale*, 13, **2021**, 2136–2156.
- [29] F. Qin and C. Brosseau, “A review and analysis of microwave absorption in polymer composites filled with carbonaceous particles,” *J. Appl. Phys.*, 111, **2012**, 061301.
- [30] L. Saini *et al.*, “Impedance engineered microwave absorption properties of Fe-Ni/C core-shell enabled rubber composites for X-band stealth applications,” *J. Alloys Compd.*, 869, **2021**, 159360.
- [31] L. Lei, Z. Yao, J. Zhou, B. Wei, and H. Fan, “3D printing of carbon black/polypropylene composites with excellent microwave absorption performance,” *Compos. Sci. Technol.*, 200, **2020**, 108479.
- [32] H. Qin, Q. Liao, G. Zhang, Y. Huang, and Y. Zhang, “Microwave absorption properties of carbon black and tetrapod-like ZnO whiskers composites,” *Appl. Surf. Sci.*, 286, **2013**, 7–11.
- [33] J. Dong *et al.*, “Dielectric and microwave absorption properties of CB doped SiO<sub>2</sub>/PI double-layer composites,” *Ceram. Int.*, 44, **2018**, 14007–14012.
- [34] M. K. Naidu, K. Ramji, B. V. S. R. N. Santhosi, T. Shami, H. B. Baskey, and B. Satyanarayana, “Enhanced Microwave Absorption of Quartic Layered Epoxy-Mwcnt Composite for Radar Applications,” *Adv. Compos. Lett.*, 26, **2017**, 096369351702600.
- [35] X. X. Wang, M. M. Lu, W. Q. Cao, B. Wen, and M. S. Cao, “Fabrication, microstructure and microwave absorption of multi-walled carbon nanotube decorated with CdS nanocrystal,” *Mater. Lett.*, 125, **2014**, 107–110.

## **Special Theme**

# **Nuclear Energy for Sustainable Development and Environmental Management**

# Decentralized Clean Energy for Rural India: The Role of Small Modular Reactors

Anirudh Chandra\* and D K Aswal

Health, Safety and Environment Group, Bhabha Atomic Research Centre, Mumbai 400085, India

*Volume 1, Issue 5, October 2024*

*Received: 31 August, 2024; Accepted: 20 October, 2024*

*DOI: <https://doi.org/10.63015/7N-2437.1.5>*

*\*Corresponding author contact: [anirudhc@barc.gov.in](mailto:anirudhc@barc.gov.in)*

**Abstract:** India's rapid development and expanding population have intensified the need for sustainable energy solutions. This is particularly significant in addressing the growing disparity in energy access between urban and rural communities. As the country shifts from traditional fossil-fuel-based power generation to cleaner technologies, nuclear energy is poised to play an increasingly vital role. Small Modular Reactors (SMRs) represent a promising option to meet these energy demands in a decentralized and environmentally friendly manner, especially in rural regions. In this perspective article, we explore the technological, economic, social, and environmental advantages of deploying SMRs in rural India. SMRs offer the potential for faster and cheaper build, as well as stable and reliable power, which is essential for driving economic growth in underdeveloped areas. However, several challenges need to be addressed, including regulatory and legislative hurdles that could impede the integration of SMRs into the existing energy mix. This article also suggests solutions such as leveraging India's existing reactor technology expertise, utilizing the mature supply chain framework, co-locating SMRs with renewable energy sources, and advocating for necessary regulatory and legislative reforms. These would help SMRs serve as a crucial bridge in facilitating a smoother transition from fossil fuel plants to clean energy technologies, particularly in underserved rural communities.

**Keywords:** Small modular reactor, nuclear energy, India, rural, electrification, decentralisation

**1. Introduction:** India's rapid economic rise and growing population are driving an urgent demand for sustainable and reliable energy solutions. This requires a delicate balancing of energy security and a reduction in the national carbon footprint [1], which is further complicated by the growing divide in energy access between urban and rural areas [2].

Coal-based power generation has been a reliable energy source but is a major contributor to pollution and greenhouse gas emissions [3]. Its centralized nature, heavily dependent on inefficient transmission and distribution networks [4], also leads to inequitable energy access between urban and rural areas [5]. The need of the hour are innovative, clean, and green technologies that can revolutionize energy generation and

distribution. Here, nuclear energy has a crucial role to play.

In the transition from fossil fuels to cleaner energy sources, nuclear energy is a vital resource due to its high energy density, low emissions, and consistent power supply. From 1954 till date, India has developed and operated a robust and mature nuclear energy programme which contributes roughly 1.8% to installed national power capacity and nearly 3% to total electricity produced in the country [6]. With 20 operational nuclear power plants, several more under construction and in various stages of development [7], India is committed to significantly expanding its nuclear energy sector.

But the current and proposed fleets of nuclear power plants in India are large-scale centralized entities, located remotely. Which



means that they are susceptible to the same problems of transmission and distribution as their fossil-fuel counterparts. Also, such large power projects are not cheap and demand a significant capital investment. This is not a problem specific to India. Around the world, nuclear power plants have been shown to be quite expensive investments [8].

However, recent advancements in nuclear technology have opened new possibilities for more flexible and decentralized power generation. As a solution to the capital cost and centralization problem of nuclear power plants, Small Modular Reactors (SMRs) are garnering great attention. SMRs are not a new concept [9], but interest in these advanced nuclear reactor technologies has risen in recent history, especially following certain geopolitical events and a drive to quickly and cheaply provide stable, clean power to communities in the interest of meeting climate goals.

SMRs represent a significant advancement over traditional large nuclear reactors in terms of size, safety, and flexibility. They are smaller, safer, and more adaptable, making them ideal for deployment in remote areas and enabling scalable growth as demand increases. With these advantages in mind, the Indian Government recently proposed its interest in pursuing SMRs [10].

In this perspective article, we discuss the multifaceted advantages of deploying SMRs, specifically in rural India, focusing on their technological, economic, social, and environmental benefits. The insights and information presented here will be valuable for technocrats seeking to understand the broader applications and implications of SMRs, as well as for private companies considering investment opportunities in SMRs within India.

**2. A brief glance at SMR technologies around the world:** SMRs are compact nuclear reactors that range in size from under 10 MWe to 300 MWe [11], capable of producing 7.2 million kWh of electricity per day [12]. In contrast, large nuclear power plants generate over 1,000 MWe, producing 24 million kWh

daily. SMRs can utilize various coolants, such as light water, liquid metal, or molten salt, depending on the technology. While "SMR" is the general term, those using non-light water technology are often referred to as advanced modular reactors (AMRs) and **Error! Reference source not found.** illustrates the distribution of prevailing SMR/AMR design types based on the coolant of choice. Generally, all SMRs generate heat through nuclear fission, which can be used directly or for electricity generation.

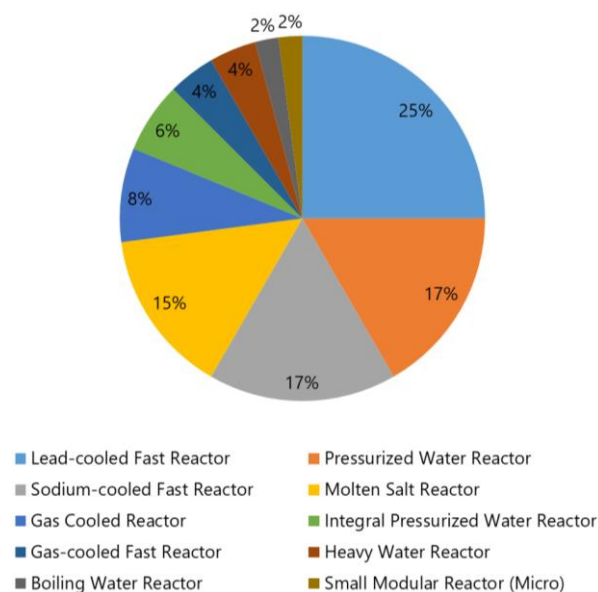


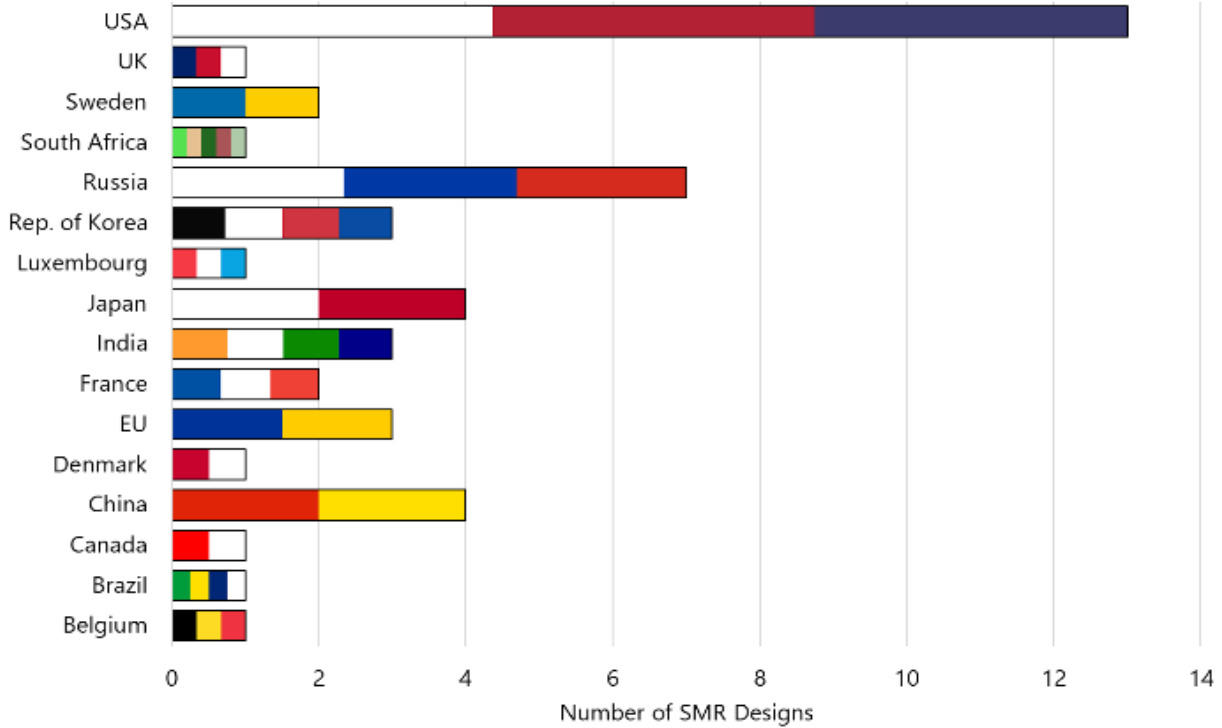
**Figure 1. Illustrating the popularity of reactor type among SMR designs around the world. Among the current designs, the Lead-cooled Fast Reactor (LFR) is the most popular choice, followed by Pressurized Water Reactor (PWR) and Sodium-cooled Fast Reactor**

Among the leaders in SMR designs are USA and Russia, who contribute to the bulk of current SMR designs, followed closely by China and Japan (**Error! Reference source not found.**). But, though there are large number of designs in existence, only a hand-full are under regulatory review and/or have been licensed, with only two designs under construction (see *Table 1*) – the High Temperature Gas Cooled Reactor with Pebble Bed Module (HTR-PM) in China and the light water based KLT-40S in Russia [13].

According to the IAEA dashboard [13], the Indian IPHWR-220 is classified as an SMR

and is stated as the only SMR in operation. This represents an effort by the Indian reactor community to modify the mature 220 MWe pressurized heavy water reactor (PHWR) design to enable modularity, factory-fabrication and fast construction times. In line with these efforts, the Indian Government recently put financial thrust into bringing these

modified 220 MWe PHWRs as ‘Bharat Small Reactors (BSR)’, the Indian Government is looking to leverage the modification of an already mature and indigenous reactor technology [15] to bring in new private investors to kickstart the SMR run in the country.



designs to fruition [14]. By terming these

**Table 1: Design status of various SMR types [13](refer Error! Reference source not found. for expansion of a cronyms)**

	BWR	GCR	GFR	HWR	iPWR	LFR	MSR	PWR	SFR	SMR micro
Conceptual Design	1	1	1			6	3	2	2	1
Construction		1						1		
Detailed Design							1	1	1	
In Operation				1						
Licensed					1					
On Hold		1								
Under Design		1	1	1	1	6	3	4	5	
Under Regulatory Review					1					

**Figure 2. Countries with the largest number of SMR designs [13]**

**3. Innovative Features of SMRs:** It is important to understand what makes SMRs unique and more importantly, useful in the present global scenario of climate change.

The uniqueness of SMRs lies in their compact size and faster construction. Their small power capacity allows for easier integration into smaller grids, better compatibility with renewable energy sources, and more flexible power management. Additionally, the reduced size means less contained radioactivity, leading to lower radiological risks in the event of an accident. Unlike traditional reactors, SMRs are often designed with an integral configuration, which means that various components are incorporated within a single, compact unit. This approach results in a lightweight and transportable reactor, significantly reducing the size of the nuclear island—the core area where the reactor and associated equipment are housed.

In some SMR designs, the primary coolant pumps, which are usually required to circulate the coolant through the reactor, are eliminated. For example, in the integral PWR design, primary circuit components are placed within the reactor pressure vessel, eliminating the need for primary circuit pipework [16]. Instead, these reactors rely on natural circulation of the coolant, driven by gravity and thermal gradients [16, 17]. This reduction in mechanical complexity not only simplifies the reactor design but also frees up space for other critical equipment. In other designs, pumps are mounted either horizontally or vertically on the reactor vessel [18], or even internally at the bottom of the vessel, further enhancing the compactness. Additionally, the use of once-through helical coil steam generators, which have a large heat transfer area within a compact geometry, contributes to the overall efficiency and space-saving design [19]. This simplification makes SMRs easier to operate and less prone to operational disturbances, which enhances their overall reliability and safety.

Safety is a paramount concern in nuclear reactor design, and SMRs have several

innovations in this area. One of the key safety features of SMRs is the use of passive safety systems. These systems operate based on natural laws, such as gravity and natural circulation, rather than relying on external power sources or active mechanical components [20]. For instance, in the event of an accident, passive systems can remove decay heat, provide emergency core cooling, and manage containment heat without the need for external intervention [21]. This reduces the likelihood of core damage, thereby significantly enhancing the safety of the reactor. Moreover, some SMR designs incorporate in-vessel control rod drive mechanisms [22], which prevent accidents such as rod ejection—a scenario that could otherwise lead to severe safety issues. Additionally, by eliminating the potential for large and medium breaks in critical reactor components like hot/cold legs, pressurizer surge lines, and primary pump suction/discharge lines [21], SMRs further minimize the risk of catastrophic failures.

The reliability of SMRs is another area where they excel [23]. The simplified and robust design of these reactors inherently contributes to their reliability. By minimizing the number of active components required for operation and maintenance, SMRs reduce the likelihood of mechanical failures. This is complemented using advanced instrumentation and control systems, which feature extensive automation to ensure smooth and consistent reactor operation. Furthermore, the incorporation of advanced diagnostic and prognostic methods allows for early detection of potential issues, enhancing the overall reliability of the system. Highly skilled and trained operators are also a key factor in maintaining the high reliability of SMRs.

Finally, SMRs are poised to be economically competitive, particularly in markets that differ from those traditionally served by large-scale nuclear power plants [24]. They offer an attractive option for developing countries with smaller electrical grids and limited financial resources. The economic advantages of SMRs are a function of several

factors, including the economy of mass production of prefabricated modules, a simplified and standardized design, and shorter construction times. Additionally, SMRs have lower operation and maintenance costs, and their modular nature allows for incremental capacity increases. These reactors can also be used for cogeneration and non-electric applications, further enhancing their economic appeal.

**4. Socio-Economic Impact of Deploying SMRs in Rural India:** Based on the several advantageous features of SMRs, we discuss one specific area of application that would have significant impact – electrification of rural India (see **Error! Reference source not f**

providing a consistent and reliable power source. This would not only light up homes but also enable the operation of schools, hospitals, and small industries, enabling economic growth and improving the quality of life.

Since SMRs can be deployed closer to the point of consumption, they reduce the need for extensive transmission infrastructure, which is often costly and inefficient. In rural areas, where the distance between energy generation sources and consumers can be vast, transmission losses are a significant issue [26]. By generating power locally with SMRs, these losses can be minimized, making electricity more affordable and reliable for rural populations. This

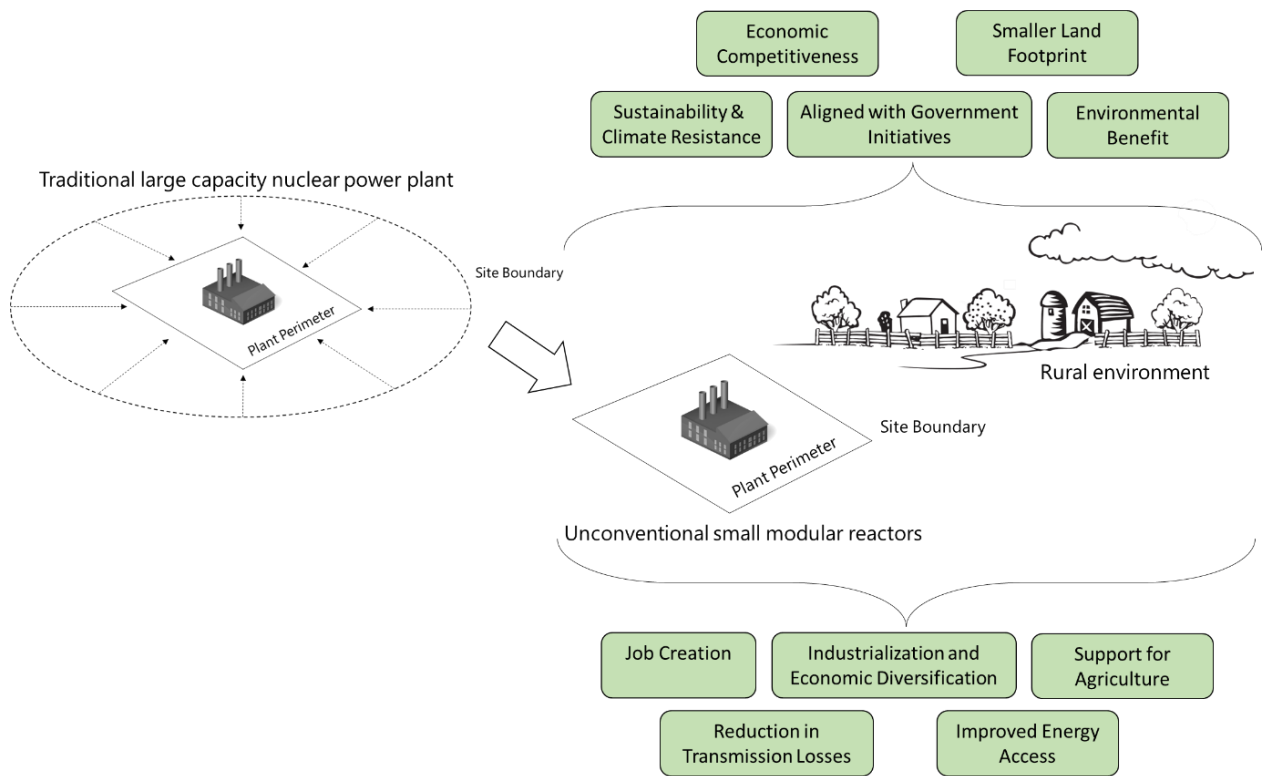


**Figure 3. Illustrating the several benefits of deploying small modular reactors (SMRs) in rural environments**

ound.). One of the most direct economic impacts of deploying SMRs in rural India would be improved energy access. Many rural areas in India still suffer from unreliable or non-existent electricity supply [25], which hampers economic development. SMRs, with their modular and scalable nature, can be deployed in remote and off-grid locations,

decentralized approach also makes the energy system more resilient to disruptions. Agriculture being the backbone of rural India's economy, often suffers from unreliable electricity supply, affecting irrigation, storage, and processing of agricultural products. And over the years, demand for electricity by the agricultural sector has only risen [27]. SMRs could

provide a stable and continuous power supply, enabling the use of electric pumps for irrigation, cold storage facilities for perishable products, and processing units. This would increase agricultural productivity, reduce post-harvest losses, and enhance the incomes of farmers.

The availability of reliable and affordable electricity is also crucial for industrialization. SMRs can support the establishment of micro, small and medium-sized enterprises (MSMEs) in rural areas, which in turn can create jobs, promote entrepreneurship, and stimulate local economies. Industries such as agro-processing and textile manufacturing could thrive with access to consistent power. The growth of these industries would lead to a more diversified rural economy, reducing dependency on agriculture and creating new avenues for income generation.

The deployment of SMRs could stimulate local economies through job creation. The construction, operation, and maintenance of SMR facilities would require a skilled workforce [28], leading to the creation of new jobs in rural areas. Additionally, the need for supporting infrastructure, such as roads, communication networks, and housing for workers, would further boost local economies. The presence of a stable power supply could also attract businesses and industries to rural areas, further enhancing economic opportunities.

The economic competitiveness of SMRs lies in their modular construction, which allows for economies of scale and shorter construction times compared to traditional large reactors [24]. This means that the initial capital investment required for SMRs can be lower, making them a financially viable option for rural electrification. Additionally, the lower operation and maintenance costs of SMRs, coupled with their ability to be mass-produced, could result in cost savings that could be passed on to consumers in the form of lower electricity tariffs. This would make electricity more affordable for rural populations, increasing their disposable income and enabling further economic activity.

The deployment of SMRs also allows for alignment with several government initiatives aimed at promoting rural development and sustainability. For example, SMRs could support the Indian government's goals under the Pradhan Mantri Sahaj Bijli Har Ghar Yojana (Saubhagya) scheme [29], which aims to provide universal household electrification. Additionally, SMRs could contribute to the Smart Cities Mission [30] by powering smart rural hubs that integrate energy, water, and waste management systems. By supporting these initiatives, SMRs could attract government funding and policy support, further enhancing their economic impact in rural India.

### **5. Environmental Considerations and Benefits for Rural India:**

One of the most significant environmental benefits of SMRs is their ability to generate electricity with minimal greenhouse gas (GHG) emissions. Unlike fossil fuel-based power plants, which are major contributors to climate change, SMRs produce energy through nuclear fission, which does not emit carbon dioxide during operation. For rural India, many communities rely on biomass or diesel generators for energy. Air pollution is often exacerbated by the burning of biomass for cooking and heating [31], as well as by diesel-powered irrigation pumps and generators [32]. SMRs can provide a reliable and clean source of electricity that reduces the need for these polluting practices. Access to clean electricity could lead to a shift from biomass to electric stoves and heaters, which would improve indoor air quality and reduce respiratory diseases that are common in rural areas [33]. Furthermore, the availability of electricity from SMRs could power electric vehicles and machinery, further cutting down on local air pollutants.

Traditional large-scale power plants require vast amounts of water for cooling, which can strain local water resources, especially in rural areas where water is already scarce. SMRs are designed to be more efficient in their use of water [34], and some designs

even utilize air-cooling systems that further reduce water usage. By deploying SMRs in rural areas, the pressure on local water resources can be alleviated, preserving these resources for agricultural use and daily consumption.

SMRs also have a much smaller physical footprint compared to traditional nuclear power plants [11] (see **Error! Reference source not found.**), making them suitable for deployment in rural areas with limited available land. Their compact size means they can be sited in locations that minimize disruption to local ecosystems and agricultural land. This is particularly important in rural India, where land is a critical resource for farming and biodiversity. The smaller land requirement of SMRs ensures that valuable agricultural land is preserved, and local ecosystems remain intact. Additionally, since SMRs can be deployed as decentralized power sources, they reduce the need for extensive transmission networks and minimize the

environmental impact associated with energy infrastructure development.

Overall, by providing access to reliable and clean electricity, SMRs can promote more sustainable agricultural practices in rural India. For example, SMRs can power energy-efficient irrigation systems, reducing the environmental impact of water extraction from rivers and groundwater sources. Additionally, electricity from SMRs can support the development of cold storage facilities, which reduce food wastage and enhance the sustainability of the agricultural supply chain. By enabling these practices, SMRs contribute to more sustainable rural economies and reduce the environmental footprint of agriculture.

The deployment of SMRs can also contribute to climate resilience in these areas by providing a stable and reliable source of electricity that is not dependent on weather conditions. Rural areas in India are often more vulnerable to the impacts of climate change,

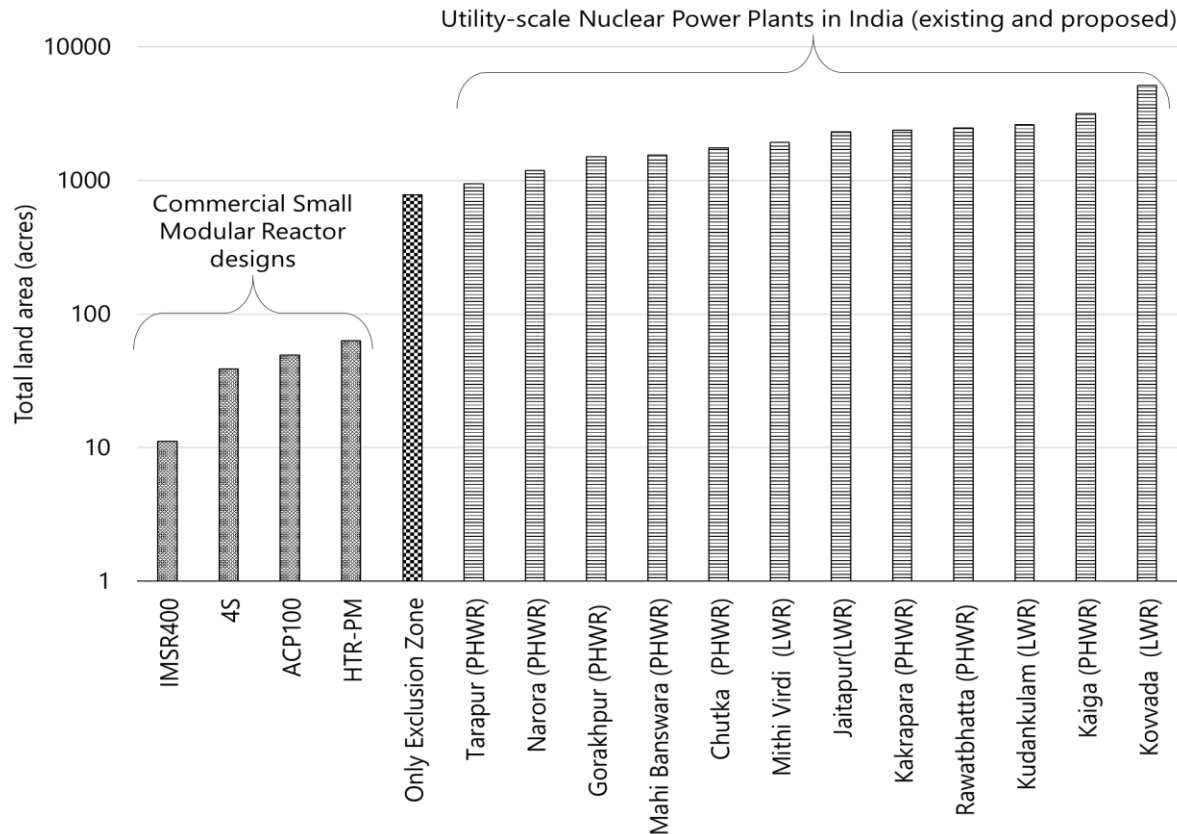


Figure 4: Comparing the total land area required by certain international SMR designs and existing large capacity nuclear power plants in India

such as extreme weather events, droughts, and changing rainfall patterns. Consistent power supply from SMRs can help rural communities better adapt to climate variability, ensuring that essential services, such as water supply and communication, remain operational during extreme events. By enhancing climate resilience, SMRs support the long-term sustainability of rural communities.

**6. Challenges in Deploying SMRs:** While SMRs exhibit several benefits for rural India, their development and deployment pose certain institutional, economic and regulatory challenges. India's nuclear regulatory framework is primarily designed for large-scale nuclear reactors. Adapting this framework to accommodate the unique characteristics of SMRs is a significant challenge. SMRs often have different safety profiles, operational modes, and deployment scenarios compared to traditional reactors, which may require a new set of regulations or the modification of existing ones [35]. The process of developing, approving, and implementing these regulations can be time-consuming, potentially delaying SMR projects [36]. Additionally, the decentralized and modular nature of SMRs, which may be deployed in multiple small units, could complicate the regulatory process, especially in rural areas with limited regulatory oversight.

1) The initial capital investment required for SMR development and deployment can be substantial [24], even though SMRs are generally less expensive than large reactors. Securing financing for these projects in rural India, where the return on investment might be uncertain, poses a significant challenge. Investors may be hesitant due to the perceived risks associated with nuclear energy, regulatory uncertainties, and the long payback periods typical of nuclear projects [37]. Furthermore, the economic viability of SMRs in rural areas depends on factors such as local electricity demand, the availability of skilled labour, and infrastructure costs. In regions with limited industrial activity and low population

density, generating sufficient revenue to justify the investment in SMRs can be challenging.

2) Deploying SMRs in rural India requires significant infrastructure development. This includes transportation networks capable of handling the heavy and complex components of SMRs, as well as the construction of facilities for assembly, operation, and maintenance. In many rural areas, existing infrastructure may be inadequate, necessitating substantial investments in roads, bridges, and other logistics systems. Additionally, SMRs require reliable grid connections to distribute the electricity they generate. In remote regions, where grid infrastructure may be underdeveloped or non-existent, creating the necessary connections could be costly and logistically challenging.

3) Nuclear energy has historically faced public scepticism and opposition, often due to concerns about safety, nuclear waste, and environmental impact [38]. In rural India, where awareness of nuclear technology may be lower, gaining public acceptance for SMRs could be difficult. Local communities might resist the deployment of SMRs due to fears of accidents or radiation exposure, particularly in regions that have limited experience with nuclear facilities. Building trust and ensuring public support will require comprehensive community engagement, education, and transparent communication about the safety and benefits of SMRs.

4) Operating and maintaining SMRs requires a skilled workforce with expertise in nuclear engineering, safety, and operations [28]. However, in rural India, the availability of such skilled professionals may be limited. Training and retaining qualified personnel in remote areas can be challenging, particularly if these regions lack educational and vocational training institutions focused on nuclear technology. The need to develop local expertise could delay SMR projects and increase operational costs, as specialized training programs and recruitment efforts would be necessary to build a capable workforce.

5) The successful deployment of SMRs in rural India depends on the availability of a robust supply chain capable of producing, transporting, and assembling the modular components. However, the nuclear manufacturing industry in India is still developing, and there may be gaps in the domestic supply chain that need to be addressed. For example, the production of specific materials, components, or advanced technologies required for SMRs might be limited or non-existent in India, leading to dependence on imports, which could increase costs and lead to delays. Furthermore, establishing manufacturing facilities in rural areas may be challenging due to logistical constraints and the lack of supporting industries.

6) While SMRs are designed to have a smaller footprint than traditional reactors, deploying them in rural areas still raises environmental and land use challenges. Site selection must consider the potential impact on local ecosystems, water resources, and agricultural land. In rural India, where land is often a critical resource for farming and biodiversity, finding suitable sites that meet safety and environmental requirements without disrupting local communities or natural habitats can be difficult.

7) The integration of SMRs into India's energy market poses its own set of challenges, particularly in rural areas where energy demand may be inconsistent or growing slowly. SMRs are designed to be economically competitive, but their success depends on stable and predictable demand for electricity. In rural areas with lower energy consumption or seasonal variations in demand, ensuring consistent utilization of SMRs can be challenging. Moreover, the pricing of electricity generated by SMRs needs to be competitive with other sources of energy, including renewables like solar, which is becoming increasingly cost-effective in India [39]. Balancing the cost-effectiveness of SMRs with the need to provide affordable energy to rural communities is a complex challenge.

8) With SMRs, long-term sustainability and the management of nuclear waste remain critical concerns. Rural areas may lack the infrastructure required for the safe handling, storage, and disposal of nuclear waste, which could become a significant issue over time. Ensuring that the waste produced by SMRs is managed in an environmentally sound and socially acceptable manner is crucial, particularly in regions where there may be limited regulatory oversight or public understanding of nuclear waste issues. Developing a comprehensive waste management strategy that addresses the specific needs of rural areas is essential for the long-term success of SMRs.

**7. Strategic Solutions and Recommendations:** As a way around these challenges, we offer some technological, economic, regulatory, environmental, social and policy-level solutions.

#### **Technological**

- 1) Promote the use of standardized designs for SMRs, which can streamline manufacturing and reduce costs.
- 2) Invest in the development of a robust domestic supply chain for SMR components. Encourage local manufacturing of key components through subsidies, tax breaks, or preferential procurement policies. This can reduce dependence on imports and ensure timely delivery of essential parts.
- 3) Implement pilot SMR projects, especially by private vendors, in selected rural areas to demonstrate their safety, reliability, and economic viability. Successful pilot projects can serve as benchmarks, helping to refine regulations and build confidence among stakeholders.
- 4) Develop hybrid energy systems that combine SMRs with renewable energy sources like solar, wind, and biomass. This can optimize energy production and provide a stable power supply,



particularly during periods of low renewable energy generation. It also enhances reliability and resilience while reducing transmission losses.

- 5) Implement advanced grid management technologies to integrate SMRs with rural microgrids, ensuring stability and efficient load management.

### **Economic**

- 6) Explore innovative financing models, such as crowd-funded investment, green bonds, or international funding from climate and energy transition funds, to support SMR deployment in rural areas.
- 7) The government can offer guarantees to mitigate financial risks for first-time investors, particularly in rural projects where returns may be uncertain. This can include power purchase agreements (PPAs) with assured offtake by state utilities or local governments.
- 8) Encourage public-private partnerships to share the financial burden of SMR projects. The government can provide subsidies, tax incentives, or low-interest loans to attract private investment in SMRs, particularly for rural electrification.

### **Regulatory**

- 9) The Indian nuclear regulatory body, the Atomic Energy Regulatory Board (AERB), could develop a specialized regulatory framework for SMRs. This framework should account for the unique safety features, modular construction, and deployment scenarios of SMRs.

### **Environmental**

- 10) Conduct thorough environmental impact assessments (EIAs) and land use studies to identify optimal sites for SMR deployment in rural areas.

### **Social**

- 11) Launch public education campaigns in rural areas to raise awareness about the benefits and safety of nuclear energy, specifically SMRs. These campaigns should address common concerns and misconceptions, using simple language and relatable examples to build trust and acceptance.
- 12) Establish vocational training centres in rural areas to develop a local workforce skilled in nuclear technology or its supply chain, specifically tailored to the needs of SMRs.
- 13) Provide incentives for skilled professionals to work in rural areas, such as housing allowances, educational benefits for their children, or career advancement opportunities. This can help attract and retain the necessary talent for operating and maintaining SMRs in remote locations.
- 14) Establish community benefit programs that provide direct advantages to rural communities hosting SMRs. This could include revenue-sharing schemes, infrastructure improvements, or community development projects funded by SMR operators.

### **Policy**

- 15) The Indian government should provide clear and consistent policy direction supporting SMR deployment, particularly in rural areas. This includes setting targets for rural electrification using SMRs, offering incentives, and ensuring alignment with broader energy and climate policies.
- 16) Maintain transparency in communicating the safety measures, environmental impact, and long-term benefits of SMRs to the local population. Open communication channels between project developers, regulators, and communities can help build trust.
- 17) Develop comprehensive infrastructure plans that integrate SMR deployment with other rural development

initiatives. This can include the simultaneous development of roads, grid connections, and water supply systems, reducing overall costs and ensuring that SMRs are part of a broader rural development strategy.

**8. Conclusion:** In conclusion, the deployment of SMRs in rural India offers a promising solution to the country's growing energy demands, particularly as it seeks to bridge the gap between urban and rural energy access. SMRs provide an opportunity for sustainable, reliable, and decentralized power generation that can significantly boost rural economies by supporting agriculture, industrialization, and overall quality of life. Though the path to widespread SMR adoption is fraught with challenges, including adapting India's regulatory framework, securing financing, developing infrastructure, and gaining public acceptance, these challenges can be addressed by a multi-faceted approach. India's existing nuclear expertise needs to be leveraged, public-private partnerships need to be fostered, and SMR deployment must align with national energy and climate goals. By implementing targeted technological, economic, and policy-driven strategies, India can overcome the above barriers and unlock the full potential of SMRs for rural electrification.

**Conflict of Interest:** Authors declare no conflict of interest.

#### References:

- [1] N. Mehrotra and C. Kalia, "How India can balance growth and sustainability in its net zero journey," Ernst & Young, 1 August 2023. [Online]. Available: [https://www.ey.com/en\\_in/insights/climate-change-sustainability-services/how-india-can-balance-growth-and-sustainability-in-its-net-zero-journey](https://www.ey.com/en_in/insights/climate-change-sustainability-services/how-india-can-balance-growth-and-sustainability-in-its-net-zero-journey). [Accessed 26 August 2024].
- [2] A. S. Alam, R. Banerjee, A. Singh and N. L. Mishra, "Access to electricity improves across states, urban-rural divide remains: NFHS-5," Down to Earth, 4 Jan 2021. [Online]. Available: <https://www.power-technology.com/>. [Accessed 19 August 2024].
- [3] IEA, "Greenhouse Gas Emissions from Energy Data Explorer," IEA, 2 August 2024. [Online]. Available: <https://www.iea.org/data-and-statistics/data-tools/greenhouse-gas-emissions-from-energy-data-explorer>. [Accessed 25 August 2024].
- [4] G. Kapoor, "Power Distribution Challenges in India: Overcoming the Obstacles," Power Distribution, 28 June 2023. [Online]. Available: <https://powerdistribution.in/power-distribution-challenges-in-india/>. [Accessed 25 August 2024].
- [5] Business Today Desk, "Power crisis in India: These states facing electricity problems; full list," Business Today, 2 May 2022. [Online]. Available: <https://www.businesstoday.in/latest/story/power-crisis-in-india-these-states-facing-electricity-problems-full-list-332105-2022-05-02>. [Accessed 19 August 2024].
- [6] Ministry of Power, "National Power Portal," Government of India, [Online]. Available: <https://npp.gov.in/dashBoard/cp-map-dashboard>. [Accessed 19 August 2024].
- [7] IAEA, "Power Reactor Information System (PRIS) - India," IAEA, 28 August 2024. [Online]. Available: <https://pris.iaea.org/PRIS/CountryStatistics/CountryDetails.aspx?current=IN>. [Accessed 23 August 2024].
- [8] NEA, "Levelised Cost of Electricity Calculator," NEA, [Online]. Available: <https://www.oecd-neo.org/lcoe/>. [Accessed 26 August 2024].
- [9] J. Fabian, "Scratching the surface of SMR history: What's in a name?," Nuclear Newswire, 13 January 2024. [Online]. Available: <https://www.ans.org/news/article-5635/scratching-the-surface-of-smr-history-whats-in-a-name/>. [Accessed 26 August 2024].
- [10] Department of Atomic Energy, "Union Minister Dr Jitendra Singh says, India taking steps for development of Small

Modular Reactors (SMR), with up to 300 MW capacity to fulfill its commitment to Clean Energy transition,” Press Information Bureau, 27 November 2022. [Online]. Available:

<https://pib.gov.in/PressReleasePage.aspx?PRID=1879298>. [Accessed 19 August 2024].

[11] J. Liou, “What are Small Modular Reactors (SMRs)?,” IAEA, 13 September 2023. [Online]. Available:

<https://www.iaea.org/newscenter/news/what-are-small-modular-reactors-smrs>.

[Accessed 26 August 2024].

[12] European Commission, “Small Modular Reactors explained,” European Commission, [Online]. Available:

[https://energy.ec.europa.eu/topics/nuclear-energy/small-modular-reactors/small-modular-reactors-explained\\_en](https://energy.ec.europa.eu/topics/nuclear-energy/small-modular-reactors/small-modular-reactors-explained_en). [Accessed 20 August 2024].

[13] IAEA, “Advanced Reactors Information System (ARIS),” IAEA, [Online]. Available:

<https://aris.iaea.org/sites/overview.html>. [Accessed 18 August 2024].

[14] Team TOI, “Budget 2024: Big role for small reactors in India's N-power play,” Times of India, 24 July 2024. [Online]. Available:

<https://timesofindia.indiatimes.com/business/india-business/budget-2024-big-role-for-small-reactors-in-indias-n-power-play/articleshow/111973245.cms>. [Accessed 19 August 2024].

[15] A. Nair, “Bharat Small Reactors being readied, modification of 220 MW reactors under way, says Atomic Energy Commission's Grover,” Business Line, 17 August 2024. [Online]. Available:

[https://www.thehindubusinessline.com/economy/bharat-small-reactors-being-readied-modification-of-220-mw-reactors-under-way-says-atomic-energy-commissions-grover/article68535895.ece?utm\\_source=pocket\\_shared](https://www.thehindubusinessline.com/economy/bharat-small-reactors-being-readied-modification-of-220-mw-reactors-under-way-says-atomic-energy-commissions-grover/article68535895.ece?utm_source=pocket_shared). [Accessed 18 August 2024].

[16] E. M. A. Hussein, “Emerging small modular nuclear power reactors: A critical review,” *Physics Open*, vol. 5, p. 100038, 2020.

[17] M. K. Rowinski, T. J. White and J. Zhao, “Small and Medium sized Reactors (SMR): A review of technology,” *Renewable and Sustainable Energy Reviews*, vol. 44, pp. 643-656, 2015.

[18] Westinghouse, “Westinghouse Small Modular Reactor Development Overview,” Westinghouse Electric Company LLC, 2011.

[19] A. Sabir and J. JIang, “Comparing the dynamic response of U-tube and helical coil steam generators in small modular reactor flexible operation,” *Nuclear Engineering and Design*, vol. 388, p. 111610, 2022.

[20] J. I. Lee, “Review of Small Modular Reactors: Challenges in Safety and Economy to Success,” *Korean Journal of Chemical Engineering*, pp. 1-20, 2024.

[21] H. Hidayatullah, S. Susyadi and M. H. Subki, “Design and technology development for small modular reactors - Safety expectations, prospects and impediments of their deployment,” *Progress in Nuclear Energy*, vol. 79, no. 10.1016/j.pnucene.2014.11.010, pp. 127-135, 2015.

[22] I. G. Kim and I. C. Bang, “Hydraulic control rod drive mechanism concept for passive in-core cooling system (PINCs) in fully passive advanced nuclear power plant,” *Experimental Thermal and Fluid Science*, vol. 85, pp. 266-278, 2017.

[23] IAEA, “Quality and Reliability Aspects in Nuclear Power Reactor Fuel Engineering - Guidance and Best Practices to Improve Nuclear Fuel Reliability and Performance in Water Cooled Reactors, IAEA Nuclear Energy Series No. NF-G-2.1 (Rev. 1),” IAEA, Vienna, 2024.

[24] B. Mignacca and G. Locatelli, “Economics and finance of Small Modular Reactors: A systematic review and research agenda,” *Renewable and Sustainable Energy Reviews*, vol. 118, p. 109519, 2020.

[25] A. Jain, J. Urpelainen and L. Stevens, “Measuring Energy Access in India - Insights from applying a multi-tier framework in cooking energy and household electricity,” Practical Action Publishing, Warwickshire, 2016.

- [26] Electrical India, “Losses in Distribution & Transmission Lines,” Electrical India, 5 January 2018. [Online]. Available: <https://www.electricalindia.in/losses-in-distribution-transmission-lines/>. [Accessed 18 August 2024].
- [27] Press Trust of India, “Electricity use in agriculture sector jumps to 37.1 per cent since 2009-10,” The Economic Times, 25 January 2024. [Online]. Available: <https://economictimes.indiatimes.com/news/economy/agriculture/electricity-use-in-agriculture-sector-jumps-to-37-1-per-cent-since-2009-10/articleshow/107145796.cms?from=mdr>. [Accessed 14 August 2024].
- [28] J. M. Egieya, M. A. Amidu and M. Hachaichi, “Small modular reactors: An assessment of workforce requirements and operating costs,” *Progress in Nuclear Energy*, vol. 159, p. 104632, 2023.
- [29] Ministry of Power, “Saubhagya - Pradhan Mantri Sahaj Bijli Har Ghar Yojana,” Government of India, [Online]. Available: <https://powermin.gov.in/en/content/saubhagya>. [Accessed 18 August 2024].
- [30] Ministry of Housing and Urban Affairs, “About Smart Cities,” Government of India, [Online]. Available: <https://smartcities.gov.in/about-the-mission>. [Accessed 18 August 2024].
- [31] Press Trust of India, “41% in India still rely on biomass for cooking, emitting 340 million tonnes of CO<sub>2</sub> annually, says report,” The Economic Times, 29 January 2024. [Online]. Available: <https://economictimes.indiatimes.com/industry/renewables/41-in-india-still-rely-on-biomass-for-cooking-emitting-340-mn-tonnes-of-co2-annually-says-report/articleshow/107237963.cms?from=mdr>. [Accessed 19 August 2024].
- [32] GHG Platform India, “An Analysis of the Trends of GHG Emissions in India. 2007-2012,” GHG Platform India, 2016.
- [33] M. A. Faizan and R. Thakur, “Association Between Solid Cooking Fuels and Respiratory Disease Across Socio-Demographic Groups in India,” *Journal of Health & Pollution*, vol. 9, no. 23, p. 190911, 2019.
- [34] M. L. Wald, “Nuclear Reactors Don’t Need to Be So Thirsty,” The Breakthrough Institute, 17 October 2023. [Online]. Available: <https://thebreakthrough.org/blog/nuclear-reactors-dont-need-to-be-so-thirsty>. [Accessed 18 August 2024].
- [35] NITI Ayog, “A Report on the Role of Small Modular Reactors in the Energy Transition,” NITI Ayog, <https://www.niti.gov.in/whats-new/role-small-modular-reactors-energy-transition>, 2023.
- [36] R. Sam, T. Sainati, B. Hanson and R. Kay, “Licensing small modular reactors: A state-of-the-art review of the challenges and barriers,” *Progress in Nuclear Energy*, vol. 164, p. 104859, 2023.
- [37] OECD NEA, “The Financing of Nuclear Power Plants. NEA no. 6360,” OECD, Paris, 2009.
- [38] A. Khan, “Anti-Nuclear Movement in India: Protests in Kudankulam and Jaitapur,” *South Asia Research*, vol. 42, no. 1, pp. 7-20, 2021.
- [39] A. Koundal, “What explains the steepest dip in solar installation costs in India?,” *ET Energy World*, 4 September 2023. [Online]. Available: <https://energy.economictimes.indiatimes.com/news/renewable/what-explains-the-steepest-dip-in-solar-installation-costs-in-india/103329903>. [Accessed 22 August 2024]

# Uranium Mill Tailings Generation and Management Challenges

Pallavi Singhal\*, Sanjay. K. Jha

Health Physics Division, Bhabha Atomic Research Centre, Mumbai 400085, India  
Homi Bhabha National Institute, Anushakti Nagar, Mumbai 400094, India

Volume 1, Issue 5, October 2024

Received: 20 August, 2024; Accepted: 13 September, 2024

DOI: <https://doi.org/10.63015/7N-2436.1.5>

\*Corresponding Author Email: [psinghal@barc.gov.in](mailto:psinghal@barc.gov.in)

**Abstract:** Uranium mining has been ongoing for the past 200 years, yet managing uranium waste remains a significant challenge. This difficulty arises due to strict regulations imposed on uranium-related industries, driven by the assumed health risks associated with radiation. As a result, much of the waste generated by nuclear industries is currently stored. In India, uranium mining and milling waste is stored that require large tracts of land and continuous monitoring. Given the high value of land in India and the potential expansion of uranium mining to meet net-zero emission targets, an effective solution for managing uranium mill tailings is urgently needed. Meanwhile, India's construction sector is rapidly growing that require a huge quantity of materials. This paper reviewed the history of uranium mining and mill tailings generation and propose that the construction industry could effectively utilize these tailings. This approach not only addresses resource scarcity but also promotes environmental sustainability by conserving natural resources, reducing ecological imbalances, and advancing a circular economy.

**Keywords:** Uranium, Mining, tailings, Circular Economy, Construction Industry, NORMs.

**1. Introduction:** The mining industry plays a crucial role in the global economy, holding a key position in the resource supply chain. There is substantial evidence indicating that enhancing mining activities can significantly improve a country's socio-economic conditions. In India, the Atma-Nirbhar Bharat initiative emphasizes innovative and cost-effective strategies to boost domestic mineral production. While the mining and milling processes contribute greatly to development, they also generate large amounts of waste which is dependent on the mineral being extracted, location, ore grade, and composition. The rock to mineral ratio [1] is an important metric that defines the amount of waste generated by a mining industry and is a sum of all the waste (waste rock, tailings and slag) to the final metal produced. The RMR is different for different metals for ex. for gold it is in the range of  $10^5$ - $10^6$  while for Fe it is around 10. For Indian Uranium industry also RMR is  $10^5$ - $10^6$ .

Presently, energy generation is prime requirement for a self sustainable nation. Earlier, this requirement was fulfilled by the coal but with the known effect of the environmental pollution and green house gas emission by the coal burning, a lot of focus has been shifted towards the use of low carbon emission energy sources such as solar, wind, hydrothermal etc. Among the available resources, solar, wind and nuclear are found to be the best in terms of Indian scenario. Singhal et. al. [2,3] has carried out a detailed analysis on available energy sources in terms of their availability, scalability, raw material availability, waste generation, green house gas emission and cost. Based on these estimates and known facts it was concluded that out of all the energy sources available, nuclear energy is one of the great options because it is a low carbon emission, high density energy source that has capacity factor >90%. This suggests that nuclear energy is as reliable as coal energy in terms of energy generation and has very low carbon emissions like other

green technologies. The fuel for nuclear energy is uranium which is present naturally in low concentrations in soil, rock and water. Figure 1 depicts the global distribution of uranium in various rocks, industrial waste and sea water [4].

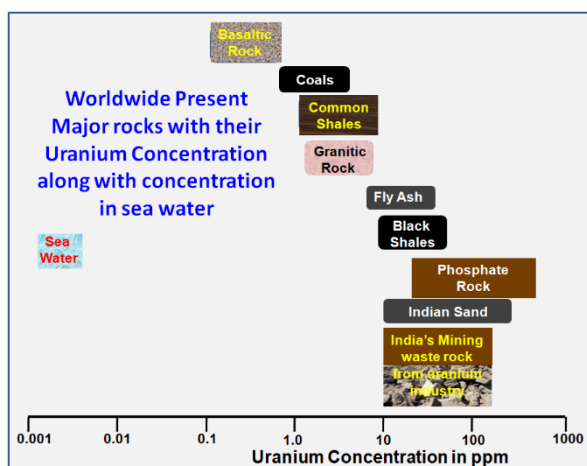


**Figure 1. Uranium concentration in various matrices such as different rocks, industrial waste and sea water.**

Uranium is present naturally both in the earth and in sea water. The terrestrial reserves are estimated to be ~5 million tons while sea water reserves account for ~4.5 billion tons. In spite of almost ~1000 times more amount of uranium in sea water; most of the uranium presently is extracted from terrestrial reserves. The reason being; extremely low concentrations of uranium in sea water ~3.3 ppb, presence of large concentration of other competing ions and biofouling [5]. These processes make the uranium extraction from sea water uneconomical. In the past decade the technologies have been progressed significantly and the cost to extract uranium from sea water has come down drastically but still it has not reached to its commercial viability yet. Once the uranium extraction from sea water becomes commercialized; the nuclear energy will be a renewable source of energy [6]. Sea water is almost an infinite source of uranium. The uranium mill tailings which are the byproduct from uranium mining can be largely ignored in case of uranium mining from sea water [5].

**2. The History of Uranium Mining:** The history of uranium mining date back >200

years ago wherein the uranium is extracted from its Pitchblende ore for different purposes. Uranium mill tailings are the waste generated from the processing of uranium ore [6]. Here a brief historical overview of uranium mining is given.

The Central European uranium deposits were the first industrially mined deposits in the world [7] (Milos, 2017). Initially uranium minerals were noticed in some silver ore deposits in 1565. Later uranium was discovered by Klaproth in 1789 [8]. After the discovery of uranium Klaproth used yellow uranium compound;  $U_3O_8$  in making colored glasses [9] and these colored glasses became very popular [10]. It is to be noted that the original production of uranium color glasses, also known as Vaseline glasses in 1853 was 84.6 kg which rose to 12,776 kg in 1886 [11]. This suggests the vast usage of these colored glasses [12]. These glasses were primarily used for decorative purpose but in some cases they were also used in some ultra-violet protective eye glasses. Other uses of uranium glass include use in photographic dark room window glasses and electric light bulbs. With time, the applications of uranium in other areas were also discovered. In Germany, uranium salts were used in dyeing textiles, papers and leather. Dentist in United States and England used uranium yellow for coloring artificial teeth. Uranium was also used to improve the elasticity and hardness of the steel. After ~100 years of use the radioactive properties of uranium were discovered by Henri Becquerel in 1896. Follow up research by Marie Curie had led to the invention of two other radioactive elements in uranium series namely, radium and polonium. Soon the interest on radium developed [13] and Vaseline glass industry saw a dip. Uranium mining is then being carried out for the production of radium which became a material of high demand. In 1911, Kelly first demonstrated therapeutic use of radium and was among the first to treat cervical cancer using radium [13]. Radium was used in luminescent paints, to decorate the dials of clocks and watches and in medical industry. It

was also being used in water, food, facial creams and toothpaste until its toxicity was reported and the famous case of radium girls came to the light [14]. By 1930, the radium use declined drastically.

United states, during the mid 1950s almost 750 uranium mines were in operation and 7 million tons of uranium ore has been identified till 1958. The US government was the sole purchaser of this produced uranium

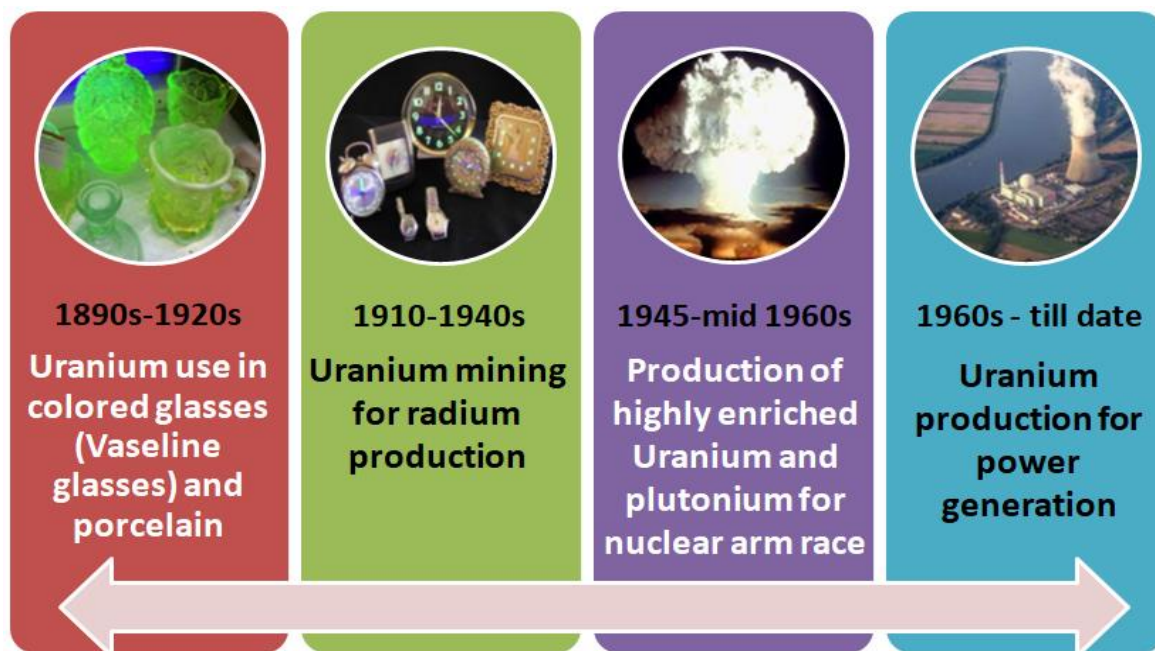


Figure 2. Use of uranium in industries at different time periods.

Otto Hahn and Fritz Strassmann in 1934 found that uranium can undergo fission and release a large amount of binding energy. This energy can be used to fulfill the power requirement and replace coal because it is an extremely dense and clean source of energy. It was also discovered that uranium can be converted to  $^{239}\text{Pu}$  which like  $^{235}\text{U}$  isotope is also fissile by thermal neutrons and a weapon grade material. On 2 December 1942, Enrico Fermi has made the world's first artificial nuclear reactor named Chicago Pile-1 (CP-1) which has shown the world that a controlled self sustained chain reaction is possible. With the start of World War - II, the efforts has been shifted from generating power from this extremely clear energy source to the production of nuclear weapons to become the world power. The Cold War between the Soviet Union and the United States resulted in massive uranium stockpiles and the creation of tens of thousands of nuclear weapons using enriched uranium and plutonium derived from uranium ores. After 1949, uranium ore became a highly strategic mineral resource. In

till 1971 to meet the requirement in the country [7].

After the World War - II, the construction of nuclear power plants for electricity generation started and United States in December 1951 made the first small scale nuclear reactor, EBR- 1 to produce electricity. The technology spread all over the world and uranium is now being used in the construction of nuclear power reactors. Figure 2 depict the importance of uranium mining in different industries and their dominance in a particular era.

**3. Uranium mining at different time periods:** Different countries have mined uranium based on the resources available and the requirement [15]. Figure 3 shows the uranium production from 1945 till 2010. It is clearly seen from Figure 3 that uranium production sees a fluctuating pattern over time and can be correlated well with the events and regulations came during that time. It can be seen that uranium production increases from 1945 till 1960 and then decreases. This is because two nuclear accidents occur in the

United States of America in 1961 and 1966. Then the uranium production again increases and peak around 1980 because of oil crises. The world has understood the need to explore

were discovery of mutation in fruit fly by Muller [18] in 1927 and linear no threshold model (LNT), Hiroshima Nagasaki bombing in 1945, US NAS recommendation to adapt

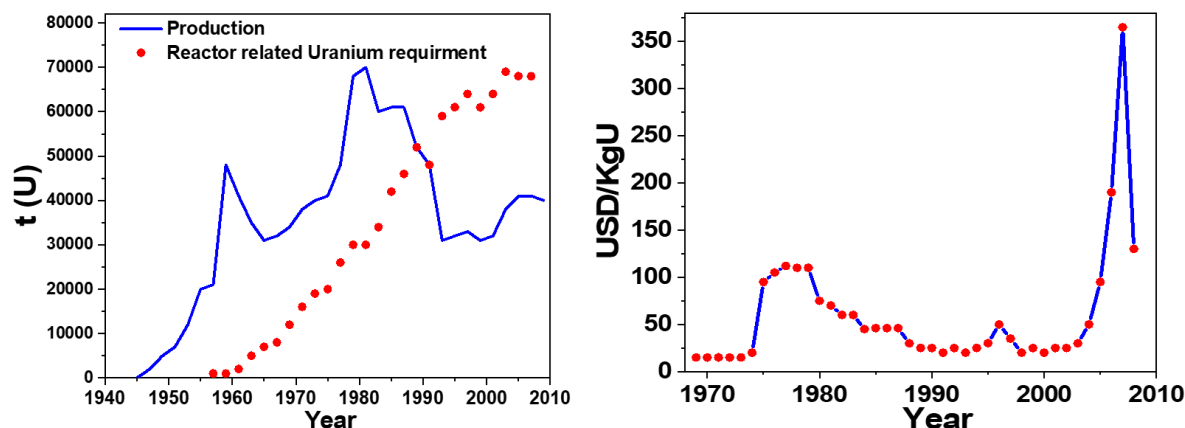


**Figure 3. Production, demand of reactor related uranium along with the cost over different time periods.**

other clean and independent sources of energy. Following this, the production suddenly decreased because of two major nuclear accident; three miles accident in United States on March 28, 1979 and Chernobyl, Soviet Union on April 26, 1986. However, the demand continued to climb. After this uranium production again increases from 2000 onwards. This shows that the activities related to uranium is strongly affected by the past effects and the policies formed so forth.

Apart from these nuclear accidents, uranium industry is badly suffered by the stringent regulations imposed on uranium related activities. This was largely because of the radiation induced effect such as cancer [16] and hereditary effects which were found at extremely high doses but still unproven at low doses. It is noteworthy that in 1928, the radiation exposure limit for the public was set at 1 Sv per year, which was reduced to 500 mSv per year in 1934. By 1966, the limits were further lowered to 50 mSv per year for workers and 1 mSv per year for the public. Currently, the accepted radiation dose limit is 20 mSv per year for workers and 1 mSv per year for the public [17]. The ratcheting down of dose limit can be correlated with several events and the studies published related to radiation risk. Some of the prominent events

LNT in 1956 and nuclear accident as mentioned above. This demonstrates the increasingly stringent regulations imposed on uranium-related industries.

Uranium mining results in generation of large amount of uranium tailings. The next section of this article will focus on the generation of these tailings.

#### **4. Uranium Mill Tailings generation:**

Terrestrial mining of uranium results in large amount of unutilized material generation called as uranium mill tailings. Tailings are the by-product of uranium mining and primarily the sandy process waste material that contains the radioactive decay products from the uranium chains (mainly the U-238 chain) along with the un-extracted uranium, heavy metals and all the associated liquids. After finding the uranium ore; mining is being carried out to extract this ore and depending upon the ore grade, its mineralogical properties and depth from surface; uranium extraction activities are being planned [19]. The processes involved in uranium mining and milling till the formation of yellow cake and the associated tailings are shown in Figure 3.

Worldwide, uranium mining and milling is



based primarily on hydrometallurgical operations such as leaching, solvent extraction, and precipitation. The first step in uranium extraction is uranium mining. Uranium ore can be present in underground depository or on the surface. A particular particle size is suitable for the maximum uranium leaching and therefore the ore is crushed and grind to achieve a desired particle size by suitable techniques. Uranium is leached from the ore either by acid leaching or alkaline leaching process depending on the ore mineralogy. If the ore is present on the surface in-situ leaching process is adopted for uranium extraction. Based on the exploration of different uranium reserves and with the advancement of technologies; the leaching method changes. In 1990, 55% of the uranium comes from underground mines (acid or alkaline leaching) but presently around 55% of the uranium is recovered from *in-situ* leaching process [15]. Here, a brief description about each process with their advantages will be discussed.

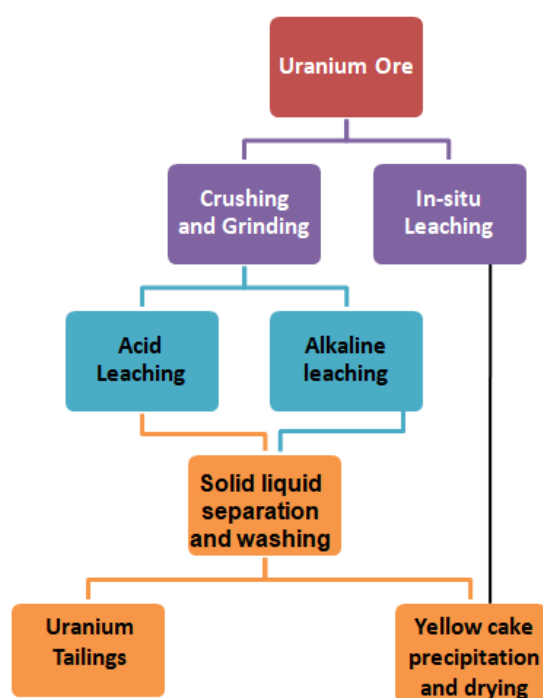
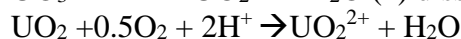
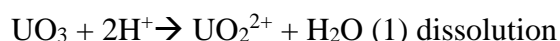


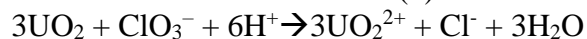
**Figure 4. Processes involved in uranium extraction from uranium ore.**

Acid leaching is one of the most common underground methods for uranium extraction from its ore [15]. Sulphuric acid is used for

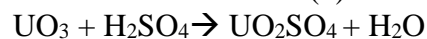
leaching. The amount of the acid consumption is controlled by the ore chemical properties and it may vary from 10 - 100 kg of H<sub>2</sub>SO<sub>4</sub> per tonne of ore. In certain cases, heating is used to reduce the leaching time and increase the efficiency of the process. Sometimes an oxidant such as manganese dioxide or sodium chlorate is also added to achieve satisfactory uranium extraction and convert all uranium into oxidized form that is readily soluble. By this process ~85-95% uranium recovery is reported<sup>5</sup>. The resulting leach solution is then separated from solid and after repeated washing solid goes to the tailing ponds while the leach solution goes for the further processing. The concentration of uranium in leach solution is normally 1- 2 g/litre along with the presence of other ions that is present in the ore. The selective uranium extraction is carried out by solvent extraction or ion exchange process wherein uranium is extracted selectively in organic phase by a suitable solvent or with an ion exchanger and then strip back into the water by contacting it with an inorganic salt solution, such as sodium chloride, ammonium sulphate or changing the pH conditions in ion exchange. Both the organic solvent and ion exchangers are repeatedly used in the process and after reaching the designated leaching efficiency the waste goes into the tailing ponds. The yellow-cake is precipitated from the strip solution, and the resulting solid is dried. The chemical reaction involved in the process are shown below [20]:



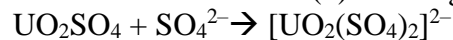
(2) oxidation



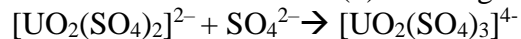
(3) oxidation



(4) leaching



(5) leaching

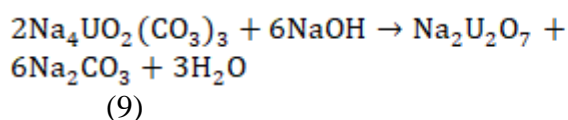
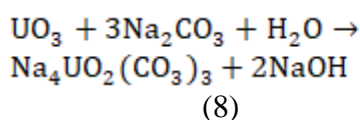
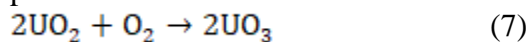


(6) leaching

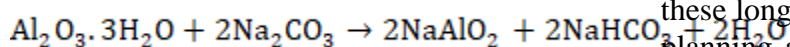
The concentration of uranium sulphate complex formed by reaction 4, 5, 6 depends on the concentration of sulphuric acid used

and uranium. The formed compound can be selectively extracted using an anion exchanger followed by elution and precipitation. All the other processed material goes to the tailing ponds and need proper management.

Alkaline leaching process for uranium production is adopted where the ore is rich in limestone and henceforth acid leaching is not favourable. Since uranium is known to form different complexes under different conditions, in this process soluble carbonate complexes of uranium are being formed to leach out the uranium. The most common alkaline leaching solutions are mixtures of sodium carbonate and sodium bicarbonate [19]. The chemical reactions involved in the process are:



#### Side reactions:



It can be seen that in alkaline leaching process,  $\text{Na}_2\text{SO}_4$  formation occur if pyrite is present. Because of this acid drainage may occur from the tailings and efforts are being taken to remove this sulphate. In *insitu* leaching process, the uranium is extracted from the host rock by chemical solutions followed by the recovery of uranium at the surface [21]. In this process a suitable leach solution is injected into the ore zone below the water table. The uranium is leached into the solution which is pumped to the surface for further processing. The technology was first used in 1962 at Ukraine for uranium extraction and has evolved a lot since then. In 1990s, *insitu* leaching process contributes 13-15% of world uranium production and now it contributes ~55%. The leaching can be

carried out either with acid ( $\text{H}_2\text{SO}_4$ ) or with the base ( $\text{Na}_2\text{CO}_3$ ) depending upon the ore composition. The chemical reaction involving these processes are same as mentioned above in acid and alkaline leaching process. Since the process does not involve any ore extraction, the generation of uranium mill tailings is least in this process.

#### 5. Challenges associated with Uranium Mill tailings management:

Uranium mill tailings, although primarily a material that is present naturally in the earth but its management involve huge cost and challenges [22, 23]. One of the primary challenges is radioactivity present in tailings [24]. Uranium mill tailings contain radioactive isotopes, primarily uranium and its decay products, such as thorium and radium. Although most of the uranium is extracted from the ore, still some uranium is present in these tailings along with the decay product. Many of the radioactive isotopes present in uranium tailings have long half-lives and they remain radioactive for extended periods. For example, uranium-238 has a half-life of about 4.5 billion years, while radium-226 has a half-life of approximately 1,600 years. Because of these long lived isotopes and stringent regulations kept; managing these long lived radioisotopes requires careful planning and monitoring. It is also postulated that uranium tailings if not adequately contained can contaminate soil, water, and air. As per many reports radioactive and heavy elements present in the tailings can leach into the surrounding environment, posing risks to ecosystem and human health [22]. The other challenges that lie in tailings management is erosion. Uranium tailings are often stored in surface impoundments or piles. These structures are susceptible to erosion, which can lead to the dispersion of contaminated particles into the surrounding environment through wind and water erosion. Proper containment and erosion control measures are essential to mitigate this risk. Therefore, it is essential to find a suitable solution for tailings management that can mitigate all these challenges and

environmental monitoring for a long period of time.

Because of the above challenges, tailings impoundments or ponds are constructed to ensure the containment and isolation of these tailings. These are engineered containment structures where tailings are deposited and stored. Some of the countries also explore the option of placing uranium mill tailings in underground repositories, where geological formations provide natural barriers against the release of radioactive materials. In certain situations, mined-out areas are backfilled with processed tailings, effectively returning the tailings to the underground workings of the mine. This approach aims to minimize surface storage and reduce the long-term environmental impact. Geotechnical engineering measures, such as compacting and stabilizing tailings, are employed to enhance the physical properties of the stored material. This helps reduce the potential for erosion, settling, and the generation of dust.

Addressing uranium mill tailings management requires a multi-faceted approach involving rigorous environmental monitoring, engineering controls, risk assessments, and stakeholder engagement. Effective management of uranium tailings is essential to minimize environmental impacts and protect public health in both active and legacy mining areas.

## **6. Worldwide scenario on management of tailings containing natural radioactivity:**

As mentioned above uranium can be extracted from ore via acid leaching, alkaline leaching or in-situ leaching process and depending on the process, the characteristics of uranium tailing changes. The utilization of these tailings in any form requires its thorough characterization including mineralogical, chemical and radiological constituents, their transport behavior and impact on the environment. Since the tailings have materials of potential interest, these baseline studies are necessary to see their potential in different industries [25]. In today's world efforts are

being put to follow the principal of circular economy which states "sharing, leasing, reusing, repairing, refurbishing and recycling existing materials and products as long as possible". Many industries have successfully fulfilled this approach by utilizing their waste in different industries for example ceramic, glass, building materials, agriculture and cement industries etc [26]. One of the major concerns with uranium mill tailings management is the low radioactivity content. Few industries such as thermal power plant which produce fly ash and fertilizer industry that produce phosphogypsum; both of these products is known to have radioactivity content but they are being utilized successfully in other industries [27]. Herein, we will mention some of these studies and show that similar strategies should be adopted for uranium mill tailings management also.

Coal remains one of the major primary source for power production not only in India but throughout the World. The burning of coal produces fly ash as a by product. The major constituent of fly ash are silica, alumina, calcium oxide and iron oxide; all the major elements used in various industries. Coal is known to contain radioactivity and the content may vary depending upon the geological origin and age of formation [27]. A significant portion of this radioactivity is passed to the fly ash also. A large amount of work has been carried out in India on utilization of fly ash in bricks, cement, fertilizer and polymer industry. Government of India has also issued various notification on fly ash utilization time to time and emphasized on increased utilization of fly ash and creating wealth from waste at the expense of natural reserves. It is important to mention that in 1996-97 there was a huge gap in fly ash generation and its utilization but with time and recently in past 7-8 years its utilization has increased exponentially suggesting the growth and demand in the sector. These efforts suggest the technological advancement, public acceptance in fly ash utilization. Some of the major industries for fly ash utilization are the cement, road and

highway construction, tiles and bricks and reclamation of low lying areas.

Since India is the most populous country in the world and land is a very precious community, Government of India has adopted various technologies to use industrial waste in construction materials [26]. Various standards have also been formulated in this direction [28-31]. Here it is important to mention that Indian uranium ore reserves are in low to very low category. Therefore the uranium concentration present in tailings is very low. The uranium mill tailings come under the category of Naturally Occurring Radioactive Materials (NORMs) [27]. Other industries such as oil, gas, coal, and phosphate also produce NORMs [27] and these residues have been successfully repurposed in construction sector. For instance, fly ash has been optimized for use as construction materials while maintaining radiological safety [32-34]. Kovler has demonstrated radiological concern in using industrial byproducts in construction [35]. He has also stressed that a paradigm shift is required in management of radioactive waste with justified dose limits [27]. In India, the Atomic Energy Regulatory Board (AERB) permits the use of NORM-containing waste in construction if radiation doses remain below 1 mSv/year, in line with natural background levels. In India, millions of tons of uranium mill tailings is present that needs proper management. Therefore, technologies should be developed to manage this waste.

**7. Conclusions:** Uranium being fuel for the nuclear energy, its production is predicted to increase as more and more reactors are being planned in the coming years which in turn will increase the tailings. Therefore, it is essential to develop technologies where these tailings can be used. So far the construction industry has been the major choice for the waste utilization; in line with the principle of circular economy it is postulated that uranium mill tailings can also be used as raw materials in construction industry since the basic composition of tailings and various construction materials matches.

**Acknowledgement:** We would like to acknowledge Dr. D. K. Aswal, Director HS&EG for his support and encouragement

**Statements and Declarations:** The authors declare that they have no known competing financial interests or personal relationship that could have appeared to influence the work reported in this paper.

#### References:

1. Nedal T. Nassar, Graham W. Lederer, Jamie L. Brainard, Abraham J. Padilla, and Joseph D. Lessard (2022). Rock-to-Metal Ratio: A Foundational Metric for Understanding Mine Wastes. *Environmental Science & Technology* 2022, 56, 10, 6710-6721.
2. P. Singhal, Sanjay Kumar Jha, Vandana Pulhani and D K Aswal. *Renewable Energy in India: Resource Availability, Waste Generation and Management*, January 2024. (DOI: 10.63015/1R-2408.1.1)
3. Pallavi Singhal, Anirudh Chandra Anirudh, Vandana Pulhani Dinesh Kumar Aswal. Use of renewable energy in global energy mix and the challenges associated with their large-scale deployment. *March 2024 Radiation Protection and Environment* 46(4):144-149.
4. Publications of the U.S. Geological Survey, 1997
5. F. Parker, Z. Zhang, L. Rao, J. Arnold. An overview and recent progress in the chemistry of uranium extraction from seawater. *Dalton Trans.*, 2018,47, 639-644.
6. Magnetic Nanoparticles for the Recovery of Uranium from Sea Water: Challenges Involved from Research to Development, P. Singhal, B. G. Vats, V. Pulhani, *Journal of Industrial and Engineering Chemistry*, 90, 25, 2020, 17-35.
7. Milos Rene, *History of Uranium Mining in Central Europe. Chapter 1: Uranium - Safety, Resources, Separation and Thermodynamic Calculation*, IntechOpen2018.

8. Klaproth M. H. Chemical investigation of uranium, some new metal material. *Chemische Annalen*. 1789;2, 387-403.
9. Strahan, D. Uranium in Glass, Glazes and Enamels: History, Identification and Handling. *Studies in Conservation* **2001**,46 (3), 181-195.
10. Kirchheimer F. Uranium and its History. Stuttgart: E Schweizerbart'scheVerlagsbuchhandlung; 1963. 380
11. Vysoky A. About uranium, uranium minerals and uranium yellow's. *Ziva*. 1860;8:25-30.
12. Schwanker RJ, Eigenstetter M, Laubinger R, Schmidt M. Uranium as colour in glass and glaze. *Physik in Unserer Zeit*. 2005;36:160-167.
13. Rentetzi, M., The U.S. Radium Industry: Industrial In-house Research and the Commercialization of Science. *Minerva* **2008**,46 (4), 437-462.
14. Radium Girls Richard B. Gunderman, Angela S. Gonda, *Radiology* 2015; 274, 314–318.
15. World Nuclear Association, T. N. F. R., OECD-NEA & IAEA, Uranium 2022: Resources, Production and Demand ('Red Book'). **2022**
16. Brugge and Goble, Public Health Then and Now, *American Journal of Public Health*, 2002, 92, 1410-1419.
17. The 2007 Recommendations of the International Commission on Radiological Protection. ICRP Publication 103. *Ann. ICRP* 37 (2-4). (2007)
18. H. J. Muller, Artificial Transmutation ofThe Gene,*Science* 66, 1927, 84-87.
19. Seidel, D. C., Extracting uranium from its ores. *IAEA Bulletin* **1981**,23 (2), 24-28.
20. *Manual of Acid in Situ Leach Uranium Mining Technology*. International Atomic Energy Agency: Vienna, 2001.
21. Graham Taylor, Vic Farrington, Peter Woods, Robert Ring and Robert Molloy, Review of Environmental Impacts of the Acid In-situ Leach Uranium Mining Process, CSIRO Land and Water Client Report, 2004.
22. Frank B. Friedman, Environmental Problems Relating to Uranium Mining and Milling, *Natural Resources Lawyer* , 1978, 11, 277.
23. S. Feenstra, D. W. Reades, J.A. Cherry, D.B. Chambers, G.G. Case, B.G. Ibbotson, *Uranium Tailings Sampling Manual*, Energy Mines and Resources Canada, 1985.
24. K.T. Thomas, *IAEA BULLETIN*, VOL. 23, No.2
25. S. Willscher, D. Mirgorodsky, L. Jablonski, D. Ollivier, D. Merten, G. Büchel, J. Wittig, P. Werner, Field Scale Phytoremediation Experiments on a Heavy Metal and Uranium Contaminated Site, and further Utilization of the Plant Residue, *Hydrometallurgy*, 131-132, 2013, 46–53.
26. R.L. Shreekant, M. Aruna, H. Vardhan, Utilization of mine waste in the construction industry - A critical review, *International Journal of Earth Sciences and Engineering*, 2016, 9(1), 182-195.
27. IAEA-TECDOC-1712. Management of NORM Residues. International atomic energy agency Vienna, 2013.
28. IRC: SP:121-2018, Guidelines For use of Iron, Steel and Copper Slag in Construction of Rural Roads. *INDIAN ROADS CONGRESS* New Delhi-110 022, November, 2018.
29. IRC: SP:132-2022, Guidelines on use of Industrial wastes for road embankment and subgrade construction., *The Indian Roads Congress*. New Delhi, 2022.
30. IRC: SP:98-2013, Guidelines for the use of waste plastic in hot bituminous mixes (dry process) in wearing courses, *Indian Roads Congress*, New Delhi, 2013.
31. IRC: SP-58:2001, Guidelines for use of fly ash in road embankments *Indian Roads Congress*, New Delhi, 2021
32. A. Bieliatynskiy, S. Yang, V. Pershakov, M. Shao, M. Ta, The use of fiber made from fly ash from power plants in China in road and airfield construction. *Construction and Building Materials* 2022, 323, 126537.

33. R. Mehra, S. Kaur, R. Prakash, Optimization of fly ash content in cement and assessment of radiological risk. *Indoor and Built Environment* 2020, 29 (2), 286-292.
34. J.Temuujin, E. Surenjav, C. H.Ruescher, J.Vahlbruch, Processing and uses of fly ash addressing radioactivity (critical review). *Chemosphere* 2019, 216, 866-882.
35. K. Kovler, Radiological constraints of using building materials and industrial by-products in construction. *Construction and Building Materials* 2009, 23 (1), 246-253.

# Spatial Distribution of Water Quality Parameters in a Mineralized Region of Rajasthan

V. K. Thakur<sup>1</sup>, P. Lenka<sup>1</sup>, Sumesh C. G.<sup>1</sup>, Gopal P. Verma<sup>1,2</sup>, Aditi C. Patra\*<sup>1,2</sup>

<sup>1</sup>Health Physics Division, BARC, Mumbai, 400085, India

<sup>2</sup>Homi Bhabha National Institute, Mumbai, 400094, India

Volume 1, Issue 5, October 2024

Received: 11 September, 2024; Accepted: 21 October, 2024

DOI: <https://doi.org/10.63015/7N-2441.1.5>

\*Correspondence Author: [aditic@barc.gov.in](mailto:aditic@barc.gov.in)

**Abstract:** Water quality parameters, anionic concentrations and uranium levels were measured in groundwater samples collected from Rohil, Sikar District, Rajasthan as a part of radiological baseline survey. This region hosts disseminated uranium deposits. The uranium concentration in water samples showed a mean value of  $107 \pm 141$   $\mu\text{g/L}$  and more than 40% samples crossed the AERB limit. The mean conductivity and TDS of samples were  $2221 \pm 1513$   $\mu\text{S/cm}$  and  $1583 \pm 1085$  ppm, respectively. The mean value of fluoride, chloride, nitrate and sulphate were  $2.4 \pm 1.4$  ppm,  $414 \pm 466$  ppm,  $33.70 \pm 37.2$  ppm and  $140 \pm 133$  ppm, respectively. Measured parameters in many samples were above the respective limits set by BIS, AERB and WHO. No particular trend was observed for any of the parameters with increasing distance from the proposed site and no correlation was evident in the measured parameters.

**Keywords:** Uranium mineralization, Groundwater, Water quality, Ionic composition

**1. Introduction:** Water is an important renewable resource when managed responsibly and used properly. Water is required for human beings, plants and animals. Water from bore wells, tube wells and hand pumps etc. are used for drinking purposes and irrigation of different crops in different seasons. Ground water flows through various types of soils and rocks, it carries diverse amounts of different compounds, minerals, substances, metals anions and cations. Uranium concentration is also found to vary along with other parameters [1].

Radiological baseline studies are required for environmental impact assessment during the pre-operational, operational and decommissioning stages of any nuclear facility. These studies are carried out for uranium mining facilities only after economically viable grades of uranium deposits are ascertained. The information collected during such studies serve as a prerequisite for regulatory compliance. The primary purpose of the mining operation is to extract uranium, which is used as a fuel in nuclear reactors to generate electricity. Proper

environmental safeguards and regulatory measures are practiced to mitigate any possible environmental impacts that may be caused due to the operation of such facilities [2].

This paper presents the water quality, anionic composition and uranium concentrations of ground water samples collected from the upcoming uranium mining complex at Rohil, Rajasthan. A low grade polymetallic (U, Cu, Mo, Ni and Co) vein type uranium deposit is located in Rohil, Sikar district, Rajasthan. As a part of preoperational radiological survey of the site, environmental groundwater samples were collected at pre-determined locations, for quantification of prevalent trace elements, cations, anions and radionuclides. Factors affecting uranium concentrations, like, water quality and ionic composition have also been presented on spatially resolved domains.

**2. Study area:** The upcoming Rohil uranium mineralized zone is located in the Sikar district of Rajasthan, India. Uraninite is the main uranium bearing mineral associated with pyrite, chalcopyrite, pyrrhotite and molybdenum in this deposit [3, 4]. Geologically, the area falls under Delhi Super

Group of rocks of Mid-Proterozoic Era of the North Delhi Fold Belt (NDFB). The deposit lies within the albitite zone and occurs within the metasediments. Stratigraphically, rock units exposed in the Rohil area have been grouped into the meso-Proterozoic Ajabgarh Group of the Delhi Super group. The main topographic feature of the area is an isolated N-S trending quartzite ridge with steep eastern and western slopes. The rocks have a general strike of NNE-SSW. Rocks exposed in this area are quartz-biotite schist and quartzite. Quartz-biotite schist underlies the quartzite. Intrusives in the meta-sedimentary rocks are younger pegmatite and quartz veins [3, 4].

**3. Material and methods:** A total of 31 groundwater samples (borewell) were collected from borewells around the study area and water quality parameters pH, conductivity, salinity and TDS were measured in-situ by Eutech PCS Testr35. The sampling locations for the current study are shown in the below map (Fig-1).

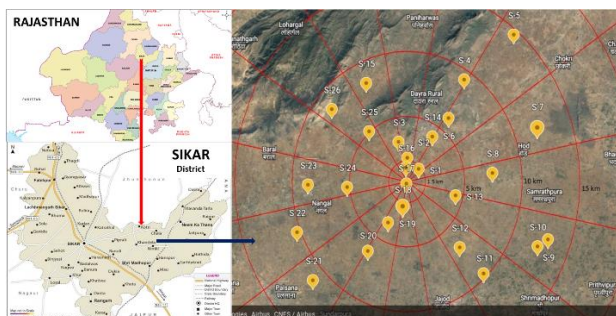


**Figure 1: Map showing sampling locations from the study area**

The samples were analysed for anions by Ion chromatographic (IC) system 850 professional (Metrohm make) using anion exchange column. The mobile phase was a mixture of millimolar solutions of sodium carbonate and sodium bi-carbonate. 100 mmol solution of H<sub>2</sub>SO<sub>4</sub> was used for regeneration of suppresser. The samples were diluted using Millipore ultra-purified water. IC system was calibrated with 0.5 ppm, 1.0 ppm and 5 ppm of mixed anion standards (Fluka). Calibration curve was obtained for each anion and routine instrument blank, standards and duplicate sample analyses were carried out for anions

like fluoride (F<sup>-</sup>), chloride (Cl<sup>-</sup>), bromide (Br<sup>-</sup>), nitrate (NO<sub>3</sub><sup>-</sup>) and sulphate (SO<sub>4</sub><sup>2-</sup>).

Water sample was filtered through 0.45 µm membrane filter prior to analysis. Uranium analysis was carried out using LED fluorimetry system following standard addition method. Standard addition method takes care of matrix effect, and other interferences. For QA/QC purposes all the measurements are carried out using micropipettes and analytical micro weighing balance. Further details of analysis and quantification of low levels of uranium can be found elsewhere [5].

The equipments used for analysis of parameters and the methods used for the same are given in table-1.

**Table 1: Equipments and standard methods adopted for sample analysis**

Sl no .	Paramet er	Instrume nt & Make	Method
1	pH, EC, TDS & Salinity	PCS Testr35 (Eutech)	pH: Potentiometry [6] EC,TDS, Salinity: Specific conductance [7]
2	F <sup>-</sup> , Cl <sup>-</sup> , NO <sub>3</sub> <sup>2-</sup> , SO <sub>4</sub> <sup>2-</sup>	850 Professional IC (Metrohm)	Ion Chromatogra phy [8]
3	Total Uranium	LED U Analyzer (Quantalse)	Fluorimetry [9]

**4. Results and discussion:** The uranium concentration in water samples varied from 0.21- 522 µg/L with a mean value of 107 ± 141 µg/L. The concentration of uranium in more than 40% of water samples crossed the limit (60 µg/L) set by AERB [10] and about



52% of samples crossed the limit (30 µg/L) set by WHO [11]. The conductivity of samples ranged from 202 – 7360 µS/cm, with mean of 2221 ± 1513 µS/cm. Range of TDS was found to be 144 - 5210 ppm with mean of 1583 ± 1085 ppm. The TDS and U concentration were observed to have somewhat similar spatial distribution patterns in the mineralised region.

The range of fluoride, chloride, nitrate and sulphate was found to be 0.17 - 8.1 ppm, 17.10 - 2108 ppm, 1.9– 149 ppm, 2.79 - 635 ppm, respectively. The mean value of fluoride was 2.4 ± 1.4 ppm with median of 2.41 ppm. The mean of chloride was 414 ± 466 ppm with median 259 ppm. The mean of nitrate and sulphate were 33.70 ± 37.2 ppm, 140 ±133 ppm with median of 20.8 ppm and 113 ppm, respectively. The BIS limits for anions in drinking water are: fluoride - 1.0 ppm; chloride - 250 ppm; nitrate - 45 ppm and sulphate - 200 ppm. Limit of TDS in drinking water as per BIS is 500 ppm, whereas in the absence of any other source it can be relaxed to 2000 ppm [12]. It can be observed from table 2 that some parameters exceed the drinking water limits. Water quality parameters of Sikar district in the present study are found to be in agreement with that of the study conducted by Central Ground Water Board, Jaipur for Sikar district in 2013 [13]. Similar reports have also been mentioned in several other studies and reports [14-16]. This may be due to the local geology and presence of widespread disseminated mineralization in this region. The local hydrogeology shows that water is contained in a hard rock aquifer and the predominant minerals are quartzite, schist, phyllite, gneiss and amphibole. The water is under overexploited category in this region as per CGWB reports [13, 14].

Duggal et al. 2016 and Khyalia et al. 2023 reported similar results in Sikar district [15, 16]. Several mineralised regions have also reported elevated uranium concentrations in groundwaters. In Gogi, Karnataka; Jaduguda, Singhbhum Thrust Belt; and Tumulapalle, Andhra Pradesh, uranium concentrations in groundwater ranges from 1.3 ppb - 267 ppb, 0.5 ppb - 28 ppb and 0.38 - 79.70 ppb [17-19].

In mineralized zone of Quebec, Canada, 1–845 ppb uranium concentration has been observed in groundwaters [20]. In Mangolia, Northwest Mongolia concentration of uranium upto 1000 ppb in lake waters close to highly U-mineralized areas has been observed.

**Table 2: Water quality and U in groundwaters**

Parameter	Range	Mean	Median	Limit
pH	6.8 - 9.8	7.75 ± 0.67	7.6	6.5-8.5 (BIS)
Conductivity µS/cm	202 - 7360	2221 ± 1513	1942	----
Salinity (ppm)	99 - 4050	1160 ± 843	1000	----
TDS (ppm)	144 - 5210	1583 ± 1085	1380	500 ppm (BIS)
Uranium (ppb)	0.21 - 522	107 ± 141	57.1	60 ppb (AER B)
Fluoride (ppm)	0.17 - 8.1	2.4 ± 1.4	2.41	1.0 ppm (BIS)
Chloride (ppm)	17.1 - 2108	414 ± 466	259	250 ppm (BIS)
Nitrate (ppm)	1.9 - 149	33.7 ± 37.2	20.8	45 ppm (BIS)
Sulphate (ppm)	2.79 - 635	140 ± 133	113	200 ppm (BIS)

Fig. 2 depicts the uranium concentration at the sampling locations of the study area. The reason for such high concentration observed in the studied area mainly can be attributed primarily to the mineralogical profile of the host rock in the region. From the distribution of uranium and TDS (Fig. 2) it can be observed that elevated levels of these parameters are limited to few locations.

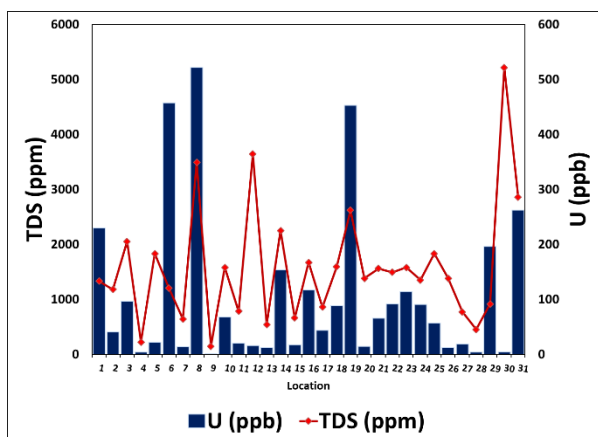


Figure 2: Distribution of total dissolved solids and U concentration in water samples

Table 3: Correlation of water quality parameters and U concentration

Parameter	pH	EC	TDS	Salinity	F <sup>-</sup>	Cl <sup>-</sup>	Br <sup>-</sup>	NO <sub>3</sub> <sup>-</sup>	SO <sub>4</sub> <sup>2-</sup>	U
pH	1.00									
EC	-0.36	1.00								
TDS	-0.36	1.00	1.00							
Salinity	-0.37	1.00	1.00	1.00						
F <sup>-</sup>	0.16	0.12	0.12	0.12	1.00					
Cl <sup>-</sup>	-0.37	0.93	0.93	0.94	0.25	1.00				
Br <sup>-</sup>	-0.09	0.15	0.15	0.14	-0.18	0.09	1.00			
NO <sub>3</sub> <sup>-</sup>	0.11	0.02	0.02	0.01	-0.10	-0.07	0.05	1.00		
SO <sub>4</sub> <sup>2-</sup>	-0.37	0.84	0.84	0.84	0.39	0.95	0.05	-0.18	1.00	
U (ppb)	-0.24	0.33	0.33	0.31	0.01	0.28	0.15	0.02	0.22	1.00

The Pearson correlation coefficient as shown in table 3 indicates that the electrical conductivity in these samples is governed mostly by the concentration of chloride and sulphate ions. The uranium concentrations are also seen to be influenced by none of the water quality parameters and anionic concentrations. It is observed that measured water quality parameters are not showing significant correlation with each other.

### 5. Conclusion

Water quality parameters, anionic concentrations and uranium levels were observed to lie beyond the limits of WHO, BIS and AERB in some water samples around the mineralised region of Rohil in Rajasthan. No particular trend was observed for any of the parameters with increasing distance from the proposed site and no significant correlation was evident between the anions and uranium concentrations. TDS was observed to be influenced by chloride and sulphate concentrations. The study is an important addition in generating baseline data and all

future environmental impact assessments for the region.

**Acknowledgements:** Authors are thankful to Director HS&EG, BARC and their colleagues for their kind support throughout the study.

**Conflict of Interest:** Authors declare no conflicts of interest.

### References

[1] A. Panghal, A. Kumar, S. Kumar, J. Singh, S. Sharma, P. Singh, R. Mehra, B. S. Bajwa, Radiation dose-dependent risk on individuals due to ingestion of uranium and radon concentration in drinking water samples of four districts of Haryana, India, *Radiation Effects and Defects in Solids*, 172 (5-6), 2017, 441-455.

[2] IAEA-TECDOC-1403, 2004, The long term stabilization of uranium mill tailings, Vienna, Austria.

[3] D. Rout, R. Krishnamurthi, D. K. Sinha. Mineralogy and Paragenesis of the Meso-Proterozoic Rohil Uranium Deposit, North Delhi Fold Belt, Rajasthan, India, *Ore Geology Reviews*, 2022, 105204.

[4] A. K. Padhi, M. K. Mukherjee, B. K. Tripathi, D. Pande, B. S. Bisht, B. C. Sarkar, Polymetallic Uranium Mineralisation in Rohil, Rajasthan, Western India: Insights from Mode of Occurrences, Structural Controls, Alteration Geochemistry and Exploration, *Minerals*, 13(4), 2023, 555.

[5] A. Chakrabarty, S. Mohapatra, R.M. Tripathi, V.D. Puranik and H. S. Kushwaha, Quality control of uranium concentration measurements, *Accreditation and Quality Assurance*, 15, 2010, 119-123.

[6] IS 6804: 1972, BIS, Specification for glass electrodes for direct reading pH meter.

[7] IS 3025(Part 14): 1984, BIS, Methods for sampling and test (physical and chemical) for water and waste water.

[8] IS 3025 (Part 75): 2022, BIS, Methods of sampling and test physical and chemical for water and waste water: Determination of dissolved anions by liquid chromatography of

ions – Determination of Bromide, Chloride, Fluoride, Nitrate, Nitrite, Phosphate and Sulphate.

[9] IS 14194 (Part 3/Sec 1): 2024, BIS, Radionuclides in environmental samples - Method of estimation: Part 3 Uranium: Sec 1 In water sample (Second Revision).

[10] AERB, Drinking water specifications in India, Department of Atomic Energy, Government of India, 2004.

[11] WHO, 2011. Guidelines for drinking water quality- 4<sup>th</sup> edition.

[12] IS 10500, 2012. Drinking water specification Indian Standard (Second Revision).

[13] CGWB, 2013, Groundwater scenario, Sikar district, Rajasthan. District groundwater brochure.

[14] CGWB, 2021, Groundwater Yearbook 2020-2021. Rajasthan.

[15] V.S. Duggal, A. Rani and V. Balaram. Assessment of age-dependent radiation dose due to intake of uranium and thorium in drinking water from Sikar district, Rajasthan, India. Radiation Protection Dosimetry, 2016, 1–5.

[16] B. Khyalia, N. Kumar, R. Beniwal, Shakuntala, A. Panghal, N. Kataria, P. Gautam and R. Dalal. Assessment of Age-Dependent Radiation Dose and Toxicological Risk of Uranium in Ground Water around Uranium Mines in Sikar, Rajasthan. Indian Journal of Pure & Applied Physics, 61, 2023, 874-885.

[17] R. Bhavya, K. Sivaraj and L. Elango. Assessing the Baseline Uranium in Groundwater around a Proposed Uraninite Mine and Identification of a Nearby New Reserve, Minerals, 2023, 13, 157.

[18] N. K. Sethy, R. M. Tripathi, V. N. Jha, S. K. Sahoo, A. K. Shukla. Assessment of Natural Uranium in the Ground Water around Jaduguda Uranium Mining Complex, India. Journal of Environmental Protection, 2011, 2, 1002-1007.

[19] B. K. Rana, M. R. Dhumale, P. Lenka, S. K. Sahoo, P. M. Ravi, R. M. Tripathi. A study of natural uranium content in groundwater around Tummalapalle uranium mining and processing facility, India. Journal of Radioanalytical and Nuclear Chemistry, 2016 307(2): 1499-1506.

[20] M.L.L. Zamora, J.M. Zielinski, G.B. Moodie, R.A.F. Falcomer, W.C. Hunt, K. Capello. Uranium in drinking water: renal effects of long-term ingestion by an aboriginal community. Arch. Environ. Occup. Health, 64 (4), 2009, pp. 228-241.

[21] O.L. Gaskova, V.P. Isupov, A.G. Vladimirov, S.L. Shvartsev, M. Kolpakova. Thermodynamic modeling of the behavior of Uranium and Arsenic in mineralized Shaazgai-Nuur Lake (Northwest Mongolia). Dokl. Earth Sc., 465, 2015, pp. 1159-1163.

# Modeling Cs-137 Migration in Groundwater due to Low Probability Event of Leaching from Near Surface Disposal Facility for Low Level Solid Radioactive Waste

Shelly Goel<sup>1\*</sup>, Manish Chopra<sup>2</sup>, R.B. Oza<sup>2</sup>

<sup>1</sup>Health Physics Division, Bhabha Atomic Research Centre, Mumbai 400 085, India.

<sup>2</sup>Radiation Safety Systems Division, Bhabha Atomic Research Centre, Mumbai 400 085, India.

Volume 1, Issue 5, October 2024

Received: 18 September, 2024; Accepted: 03 October, 2024

DOI: <https://doi.org/10.63015/7N-2440.1.5>

\*Corresponding Author Email: [shellygarg@barc.gov.in](mailto:shellygarg@barc.gov.in)

**Abstract:** In this paper, we present impact of Cesium-137 (Cs-137) disposal in a Near Surface Disposal Facility (NSDF) with respect to groundwater migration and its consumption for drinking. We employ the Multiple Area Source Model for simulating the fate of radionuclide in groundwater to evaluate its potential contamination due to extremely low probability event of leaching from the NSDF. The assessment conservatively assumes direct interaction between disposal trenches and the underlying aquifer neglecting the barrier provided by the unsaturated zone. Temporal profiles of concentration of Cs-137 at different down flow distances in groundwater are obtained over a period extending several years post-disposal. The results indicate that even under such a worst-case conservative scenario and for an annual disposal rate of 3 TBq/y for a period of 50y, the maximum Cs-137 concentration in groundwater remains significantly below the safe drinking water threshold of 10 Bq/L recommended by the World Health Organization. It is found that amount of Cs-137 generally disposed in NSDF is significantly lower than the allowable disposal limit corresponding to concentration defined for safe drinking water limit.

**Keywords:** Near surface disposal facility, Leaching, Groundwater contamination, Radionuclide transport, Multiple area source model.

**1. Introduction:** The operation and maintenance of nuclear facilities generate low level solid radioactive waste, which poses environmental and radiological hazards [1]. Among the radionuclides present in such waste, Cs-137 is of particular concern due to its long half-life of 30.1 years and its high fission yield of approximately 6.1% [2]. Low-level radioactive waste containing Cs-137 is typically disposed of in engineered structures such as stone-lined trenches, reinforced concrete trenches, and tile holes in Near Surface Disposal Facilities (NSDFs) [3]. Due to the low-level of radioactivity and employed engineered safety features in NSDFs, the probability of leaching of radioactivity from these facilities into groundwater due to ingress of water from precipitation etc. is negligible [4]. However, the impact assessment even of such a low probability event is required

according to the regulations applicable for such facilities, particularly given that the World Health Organization (WHO) recommends a maximum safe level of 10 Bq/l for Cs-137 in drinking water [5].

To ensure safety of the public, migration of Cs-137 in groundwater is modelled to ensure compliance with regulatory guidelines, both during the operational phase and post-closure phase of the disposal facilities. Groundwater modeling is a key tool in these assessments, enabling the prediction of radionuclide transport and dispersion within aquifers [6]. Analytical models offer exact solutions to simplified versions of the groundwater flow and solute transport equations [7]. On the other hand, numerical models such as MODFLOW and FEFLOW solve the more complex, multi-dimensional flow and transport equations

through numerical approximations [8]. While numerical models can account for more realistic scenarios, they require extensive input data and are computationally really intensive. That is why for regulatory assessments, despite their limitations related to simplifications, analytical models are valuable tools and a more practical alternative for predicting contaminant fate and evaluating their impact by employing conservatism in the simplified assumptions [9]. In this study, we employ the Multiple Area Source Model (MASOM), an analytical model developed by Sunny et al. (2006) [10], to model Cs-137 leaching from a typical NSDF and further migration in groundwater. Brief details of the model and the corresponding results are discussed in the following sections.

**2. Contaminant Transport Model:** Multiple Area Source Model (MASOM) is designed to simulate the dispersion and dilution processes of contaminants as they migrate through groundwater, taking into account the key physical and chemical processes involved. The release rate  $\psi(t)$  from the disposal facility into groundwater is mathematically expressed as [10]

$$\Psi(t) = \frac{QK_L}{K_L + \lambda} [1 - \exp(-(K_L + \lambda)t)] \quad (1)$$

where Q represents the disposal rate of the radionuclide (in Bq/s),  $K_L$  denotes the leach rate coefficient (in  $s^{-1}$ ),  $\lambda$  is the radioactive decay constant (in  $s^{-1}$ ) and t is the time (s). The leaching of radionuclides is affected by several factors including the structural integrity of the disposal modules, the radionuclide's distribution coefficient, and the rate at which water infiltrates through the disposal module. The leach rate coefficient  $K_L$  can be expressed as a function of the infiltration velocity, as described in the following formula.

$$K_L = \frac{v_L}{D\theta R_d} \quad (2)$$

where D represents the depth of the disposal module,  $\theta$  is the porosity of the aquifer and  $R_d$  is the retardation factor given by:

$$R_d = 1 + \frac{\rho K_d}{\theta} \quad (3)$$

where  $K_d$  is the distribution coefficient (ml/g) and  $\rho$  is the soil density (g/ml).

Eq. (2) provides the fundamental basis for estimating the rate at which radionuclides may enter groundwater systems from disposal facilities. The transport of radionuclides through groundwater is governed by several key processes including advection, molecular and turbulent diffusion, interaction with soil, radioactive decay, and chemical removal rates. For unidirectional flow primarily in the x-direction, and for homogeneous groundwater velocity and dispersion coefficients, these processes are translated into 3D mathematical equation known as advection dispersion equation as given below [10]:

$$\frac{\partial c}{\partial t} = \frac{D_x}{R_d} \frac{\partial^2 c}{\partial x^2} + \frac{D_y}{R_d} \frac{\partial^2 c}{\partial y^2} + \frac{D_z}{R_d} \frac{\partial^2 c}{\partial z^2} - \frac{u}{R_d} \frac{\partial c}{\partial x} - \lambda c \quad (4)$$

where  $D_x$ ,  $D_y$  and  $D_z$  are the dispersion coefficients along the x, y, and z axis respectively, u denotes the groundwater velocity along x-direction,  $\lambda$  is the decay constant, and C represents the concentration of radionuclides within the pore space (Bq/L).

Eq. (4) is solved under a set of assumptions for initial and boundary conditions viz. C is zero at initial time and at infinite distances from the source. Analytical solution for the concentration due to an instantaneous point source extended to account for an area source by integrating over the source dimensions is given as a convolution integral [10]:

$$C(x, y, T) = \int_0^T \psi(T - \tau) C_i(x, y, \tau) d\tau \quad (5)$$

Where T is the period of disposal operation,  $\tau$  is the running variable, and  $C_i$  is the radionuclide concentration in the groundwater due to instantaneous release of unit radioactivity [13]. Eq. (5) estimates the concentration profile up to the disposal period 'T'. The radionuclide concentration following the termination of the disposal operation can be assessed using the expression given below:

$$C(x, y, t) = \int_0^T \psi(T - \tau) C_i(x, y, T + \tau) d\tau + \psi(T) \int_0^t \exp[-\lambda_1(t - \tau)] C_i(x, y, \tau) d\tau \quad (6)$$

Where  $\lambda_1 = \lambda + K_L$  and  $t$  is the post disposal period with the origin at the termination time  $T$ . The first integral in Eq. 6 accounts for the radionuclide concentration in groundwater during the post- disposal reflecting the activity leached during the disposal period. The second integral represents the additional radioactivity in groundwater resulting from leaching that occurs after the termination of disposal. These integrals are evaluated using the Simpson’s 1/3 method.

**3. Parameters:** Site-specific hydrogeological parameters play a crucial role in determining the extent of radionuclide migration. For present work, we utilized the data for a typical NSDF site as reported by Shelly et al. [11] where they conducted field and laboratory studies in and around NSDF to determine the site specific hydrogeological parameters such as porosity, hydraulic conductivity, groundwater velocity, and the  $K_d$ . These hydrogeological data is used as input to simulate migration of Cs-137 in groundwater and the corresponding radiological impact through drinking water pathway. As the data had a range of values, the values selected for the deterministic estimation are based on the conservative assumptions to get the maximum potential radionuclide concentration in groundwater (Table 1). For modeling radionuclide leaching from disposal modules, the infiltration velocity for stone-lined trenches (SLT) was assumed to be equal to the design basis value generally used for uranium tailings ponds [12] i.e.  $1 \times 10^{-9}$  m/s,. Infiltration velocities for reinforced concrete trenches (RCCT) and tile holes (THs) were assumed to be one and two orders of magnitude lower, respectively considering their better integrity. We assumed a continuous disposal rate of 1 TBq/year of Cs-137 into each of the three modules over a 50-year period, resulting in a total inventory of 150 TBq, with 50 TBq allocated to each module.

**Table 1:** Parameters used in the modelling

Parameter	Value
$K_d$ of Cs-137 (ml/g)	116.7
$\theta$ of the waste matrix/aquifer	0.29
$\rho_b$ of the waste matrix/aquifer (g/cc)	1.6
$u$ (m/d)	3.22
Aquifer thickness (m)	2
Longitudinal dispersivity (m)	1
Transverse dispersivity (m)	1
Infiltration Velocity (SLT, m/s)	$1 \times 10^{-9}$
Infiltration Velocity (RCCT, m/s)	$1 \times 10^{-10}$
Infiltration Velocity (TH, m/s)	$1 \times 10^{-11}$

**4. Results and Discussion:** Modelling Cs-137 migration in groundwater from the NSDF incorporates several conservative assumptions to ensure the safety of the public. Although groundwater mapping indicates the flow direction towards the sea [11], for conservative estimation it is considered towards the population center. Figure 1 shows the temporal profiles of Cs-137 concentration at three distances along the centerline i.e. 500 m, 600 m and 1000 m. The maximum Cs-137 concentration in groundwater at 500 m is calculated to be  $1.62 \times 10^{-2}$  Bq/L, occurring 300 years after disposal (Table 2). At 600 and 1000 m, the concentrations are  $4.5 \times 10^{-3}$  Bq/L and  $2.72 \times 10^{-5}$  Bq/L, occurring 350 and 570 years after disposal respectively (Table 2, Figure 1). The concentration values estimated are significantly below the World Health Organization's (WHO) safe drinking water limit of 10 Bq/L for Cs-137 [5], demonstrating that the estimated concentrations are more than 600 times lower than the WHO recommendations. Based on the concentration at 500m distance and for concentration corresponding to WHO’s safe limit for drinking of 10 Bq/L, the allowable activity for Cs-137 disposal is estimated to be 1852 TBq/y which is orders of magnitude higher than the activity generally disposed of in NSDFs [13, 14].

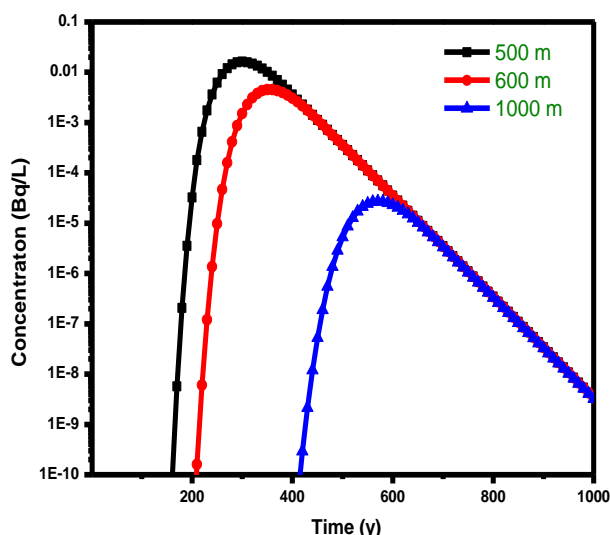


**Figure 1:** Concentration of Cs-137 in groundwater at three distances from NSDF

**Table 2:** Peak concentration of Cs-137 at different distances from NSDF and peaking time

Distance (m)	Peak conc. (Bq/L)	Time (years)
500	$1.62 \times 10^{-2}$	300
600	$4.5 \times 10^{-3}$	350
1000	$2.72 \times 10^{-5}$	570

**5. Conclusions:** Modeling of leaching of Cs-137 disposed at a typical NSDF and its migration with groundwater is carried out by utilizing site-specific hydrogeological data. Despite the conservative assumptions made in the modeling the radionuclide leaching and transport, the predicted Cs-137 concentrations at various distances from the disposal site remain well below the World Health Organization's safe drinking water limit of 10 Bq/L. Moreover, it is concluded that the activity of Cs-137 generally disposed of in the NSDFs is significantly lower than the allowable activity estimated corresponding to safe drinking water limit of WHO. These findings suggest that the risk of Cs-137 migration into groundwater from NSDF is minimal.

#### Acknowledgements:

The authors express their sincere gratitude to Dr. S.K. Jha, Head, Radiation Protection Section (Nuclear Fuels), Shri Probal

Chaudhury, Head, RSSD, and Dr. D.K. Aswal, Director, HS&E Group of Bhabha Atomic Research Centre (BARC), Mumbai, India, for their invaluable support. The authors also extend their gratefulness to Dr. P. Ashokkumar, Head, Health Safety Section (Radiological Laboratories), and Dr. Faby Sunny, formerly of BARC, Mumbai, India, for their encouragement, support, and guidance.

**Conflict of Interest:** Authors declare No conflicts of interest.

#### References

- [1] Folkers C., Gunter L.P., Radioactive releases from the nuclear power sector and implications for child health, *BMJ Paediatrics Open*, 6(1), 2021, e001326,
- [2] Kocherov N., Lanimer M. et al. Handbook of nuclear data for safeguards, Nuclear Data Section International Atomic Energy Agency, Vienna, Austria, 1997.
- [3] Ojovan M.I., Steinmetz H.J.. Approaches to Disposal of Nuclear Waste. *Energies* 2022, 15, 7804.
- [4] Subramanian M., Thirumurugan M. et al., Determination of distribution coefficient of uranium from physical and chemical properties of soil, *Chemosphere*, 2019, 125411.
- [5] WHO, Guidelines for Drinking Water Quality, fourth ed. (Geneva), 2011.
- [6] Lakshmanan E., Marimuthu T. Modeling of Radionuclide Transport in Groundwater, 2016.
- [7] Guyonnet, D., An analytical model for estimating impact of pollutant sources on groundwater, 2001.
- [8] Karmakar S., Tatomir A et al, Numerical Benchmark Studies on Flow and Solute Transport in Geological Reservoirs. *Water* 14, 2022, 1310.
- [9] Akter A., Ahmed S., Modeling of groundwater level changes in an urban area. *Sustain. Water Resour. Manag.*, 7, 2021.
- [10] Sunny F., Nair, R. N., Khan A. H., et al., Radiological Impact in Groundwater and Surface Water due to Open Cast Mining of Uranium, Andhra Pradesh, 2006, BARC/2006/I/003.
- [11] Garg S., Chopra M., Patra A.C., Sunny F. et al., Site-specific characterisation of

hydrogeological parameters for low-level solid radioactive waste disposal facility at Tarapur, India; *J. Earth Syst. Sci.*, 132:94, 2023.

[12] Lakshmanan E., Karthikeyan B., et al. Groundwater flow and radionuclide decay-chain transport modelling around a proposed uranium tailings pond in India. *Hydrogeol J* 20, 2012, 797–812.

[13] Seunghee L., Juyoul K., Post-closure safety assessment of near surface disposal facilities for disused sealed radioactive sources, *Nuclear Engineering and Design* 313, 2017, 425-436

[14] Canadian Nuclear Laboratories, "Near Surface Disposal Facility (NSDF)," [Online]. Available: <https://www.cnl.ca/environmental-stewardship/near-surface-disposal-facility-nsdf/>. [Accessed: Sep. 5, 2024].



# Radon and Gamma Radiation Dose to the Population Residing Near the Uranium Mill Tailings Disposal Site in Uranium Mineralized Zone at Jaduguda

Gopal P. Verma<sup>\*1,3</sup>, N. K. Sethy<sup>1</sup>, Aditi C. Patra<sup>1,3</sup>, V. N. Jha<sup>1</sup> and K. A. Dubey<sup>2,3</sup>

<sup>1</sup>Health Physics Division, Bhabha Atomic Research Centre, 400085, India

<sup>2</sup>Radiation Technology Development Division, Bhabha Atomic Research Centre, 400085, India

<sup>3</sup>Homi Bhabha National Institute, Mumbai 400094, India

Volume 1, Issue 5, October 2024

Received: 11 September, 2024; Accepted: 11 October, 2024

DOI: <https://doi.org/10.63015/7N-2439.1.5>

\*Corresponding author E-mail: [gpv@barc.gov.in](mailto:gpv@barc.gov.in)

**Abstract:** Members of the public residing in the villages situated near the uranium mill disposal site, such as those in the vicinity of uranium tailings ponds, may indeed be at risk of radiation exposure. Present study focuses to evaluate the radiological exposure condition for the resident of villages situated in nearby vicinity of the tailing disposal site in the uranium mineralized region of Jaduguda, Jharkhand, India. In this study, the dose from external gamma radiation and radon concentrations, both indoors and outdoors, is evaluated. The natural background radiation dose to the residents of villages located near the uranium mill tailings disposal site is estimated to be 2.99 mSv<sup>-1</sup>. Radon and its decay products contribute approximately 57.6% of the radiation dose to the villagers, while gamma radiation accounts for 42.4%. Residents of villages near the uranium tailings ponds receive a radiation dose is within the typical range of global natural background radiation dose of 1-10 mSv<sup>-1</sup> to the members of the public.

**Key words:** Tailings, Disposal Site, Radon, Gamma, Dose

**1. Introduction:** Natural radioactivity and radiation have always been a part of the environment since the inception of the earth [1]. The exposure to natural radiation includes cosmic, terrestrial, inhalation and ingestion through air, water and food materials etc. [2]. The average global radiation exposure from the natural background radiation sources is 2.4 mSv<sup>-1</sup> with a typical range of 1- 10 mSv<sup>-1</sup> [3 & 9]. Naturally occurring radioactive materials (NORMs) contribute a significant fraction to the natural background radiation exposure. The natural radiological condition may change drastically due to anthropogenic activities in the vicinity. There are some areas in India, Brazil, China & Iran where people are exposed to high level of natural background. However, anthropogenic activities like mining of

minerals have the potential to redistribute the minerals in the adjoining area and may enhance natural radioactivity if adequate safety measures are not implemented [4]. East Singhbhum district of Jharkhand state of India is well known for its widespread mineral deposits. Several copper and uranium mining activities are continuing since last five decades. In the case of uranium mines, the major radiological concern is airborne radon (<sup>222</sup>Rn) and its short-lived progeny (<sup>218</sup>Po, <sup>214</sup>Pb, <sup>214</sup>Bi and <sup>214</sup>Po). Unlike other sectors of the nuclear industry, uranium ore processing generates large volumes of low-specific-activity solid waste, commonly known as tailings. Due to the chemical and radioactive substances present in these tailings, their disposal requires special attention.

Consequently, tailings disposal systems must be carefully designed and situated in geologically stable locations to ensure long-term isolation from human populations. The composition of the tailings varies based on factors such as the type of leaching process used to extract uranium, the reagents involved, and the mineralogy of the ore. After uranium recovery in the processing plant, the majority of the processed material becomes tailings. These tailings are neutralized with lime to a pH of 10 to precipitate heavy metals, radionuclides, and toxins. The neutralized tailings are then separated into coarse and fine fractions using a hydrocyclone. The coarse fraction is used as backfill in mined-out areas, while the fine fraction is stored in a tailings pond (TP) for containment. The tailings pond is an engineered earthen dam designed to hold both solid and liquid waste. Solids settle at the bottom, while the clear liquid is directed through decantation wells to an effluent treatment plant (ETP) for the removal of chemical and radioactive pollutants. At Jaduguda, three tailings ponds have been in operation for over four decades, located in a valley surrounded by hills on three sides and an engineered embankment downstream. The radioactivity in the tailings pond primarily comes from long-lived radionuclides such as  $^{230}\text{Th}$ ,  $^{226}\text{Ra}$ ,  $^{210}\text{Pb}$ , and  $^{210}\text{Po}$  from the  $^{238}\text{U}$  series. Radon ( $^{222}\text{Rn}$ ) is produced by the decay of  $^{226}\text{Ra}$  in the tailings. The mill tailings pose potential environmental risks due to low-level radioactivity and the release of  $^{222}\text{Rn}$  gas. Radon, being an inert gas, does not significantly contribute to internal exposure. However, its short-lived progenies attach to dust particles, which are a major source of internal exposure in uranium mining sites. If proper safety measures are not implemented, the tailings pond could be a source of both external and internal radiation exposure for the nearby communities. The study assessed radon concentration and external gamma radiation around a tailings pond (TP) and nearby

villages. It used a portable radon detection system and an environmental radiation survey meter. The findings indicate that while tailings ponds have a localized impact on radon levels, their effect on the general environment is minimal due to their relatively small area compared to the large land area. Radiological assessment of areas in the close vicinity of mill tailings pond in Jaduguda is the subject matter of this paper.

**1.1. Study Area:** Jaduguda uranium deposit (Lat.  $22^{\circ} 39'$ , Long.  $86^{\circ} 22'$ ) in India is located in the center of Singhbhum Thrust Belt (STB) of Jharkhand State. The host rocks are autoclastic conglomerate (formed by crushing, fracturing and brecciation) and quartz-chlorite-apatite-tourmaline-magnetite schist in which uranium bearing fine grained uraninite minerals occur as disseminated grains and micro-veinlets [5]. The study area (Fig-1) is known for U mineralization in meta-sedimentary rocks [6]. The associated accessory minerals found along with uranium are the sulphide minerals of copper, nickel & molybdenum and magnetite. There are three uranium mill tailings pond at Jaduguda. One tailings pond is in operational where as other two are decommissioned. Some villages are situated very close to tailings pond. Assessment of radiological condition of these villages is essential in order to estimate the radiation exposure due to anthropogenic activity. Village Chatikocha and Tilaitand situated in the close proximity of U mill tailings pond were selected for the study. The assessment of radiological environment of these villages is the subject matter of this study.

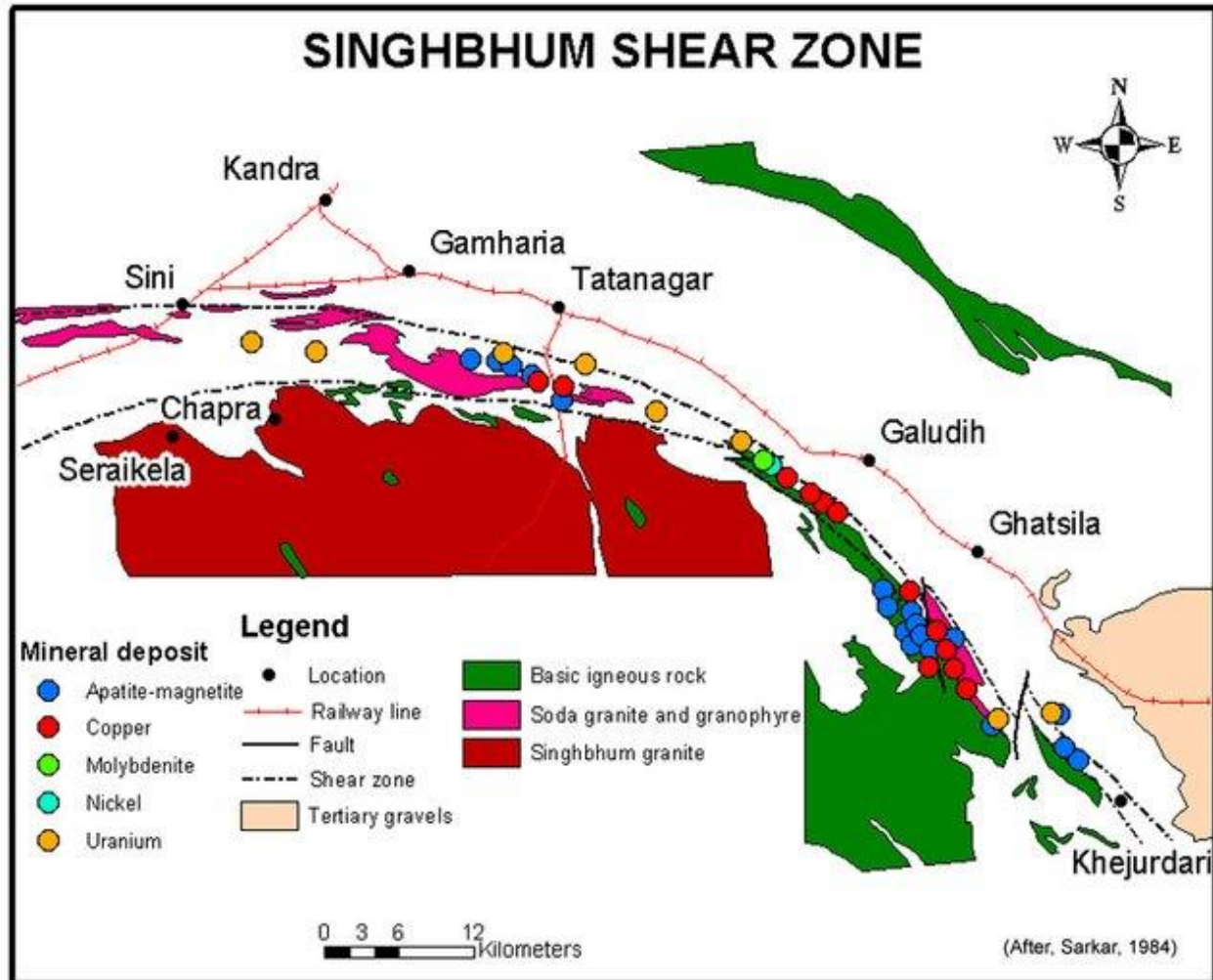


Figure 1. The Study Area Singhbhum Thrust Belt, Jharkhand

**1.2. The Uranium Tailings Pond:** Tailings Pond is an engineered impoundment system which is designed to hold the tailings for extended period of time. Tailings are discharged at elevated pH (> 9.5) to keep most of the radionuclide and heavy metals in precipitated state. Over the year the pH of the tailings pond may reduce by pyrite oxidation [7] in the presence of microbes creating a reduced pH condition favorable for migration of radionuclide. The reduced pH condition favors migration of radionuclide and chemical contaminates to adjoining ground water table to public domain. Reduction of pyrite also enhanced in presence of some micro-organisms and bacteria. Uranium mill

tailing contains bulk of radioactivity originally present in the ore as well as traces of residual uranium. Radionuclide which are alpha emitting and long radiological half-lives such as  $^{226}\text{Ra}$ ,  $^{230}\text{Th}$ ,  $^{210}\text{Po}$  etc. are present in the tailings.

**2. Material & methods:** External gamma radiation levels in the environment around the tailings pond are measured using pre-calibrated direct reading radiation survey meters (Nucleonix-UR705 & PLA-PRM-151S). The radiation survey meter is NaI(Tl) scintillation 1 in. x 1 in. plain detector with 1 in. PM tube and built in pre-amplifier, probe type PSP 101. The survey meter is used to measure low level radiation from  $1 \mu\text{Rh}^{-1}$  to 1

mRh<sup>-1</sup> with auto range selection. Atmospheric radon concentration was measured using Alpha-Guard (PQ 2000/MC 50) supplied by Genitron Instruments, Germany. One hour time integrated grab measurement technique was employed for estimation of radon and gamma dose rates at each location. The measurements were carried out at 1 m height above the surface at each location and periodically data were generated and recorded. The cylindrical ionization chamber of the Alpha Guard has an active volume of 0.56 L and its metallic interior has a potential of 750 V. Sensitivity of the system Alpha-Guard is 1 cpm at 20 Bqm<sup>-3</sup> and the background is less than 1 Bqm<sup>-3</sup>. Fast response, higher sensitivity and a wide dynamic range of linear over the interval 2 – 2 x 10<sup>6</sup> Bqm<sup>-3</sup> are the advantages of the Alpha Guard.

### 3. Radon & Gamma Radiation level in the Village situated near the Tailings Ponds:

The atmospheric out door radon concentration levels and external gamma radiation is measured in the villages situated near tailings ponds area and is presented in (Table-1) & (Fig.2 & Fig.3). The average concentration of outdoor radon was 26.26 Bqm<sup>-3</sup> which is slightly greater than the reported value of 18 Bqm<sup>-3</sup> [8] in the same study region and global average value of 10 Bqm<sup>-3</sup>. The slight elevated level of outdoor radon may be attributed to the close proximity of the two villages to the tailing ponds and natural mineralization. The resident of these villages is tribal and hence most of the houses are made from mud with vegetation forming the roof. Therefore, most of the dwellings in the villages are not properly closed and having natural ventilation. The reported value of average indoor radon level in the study region is 70 Bqm<sup>-3</sup> and is considered for internal dose estimation. The outdoor radon concentration varies from 19 - 31 Bqm<sup>-3</sup> with an average of 26.26 Bqm<sup>-3</sup> (Table-1). In general, occupancy factors suggested by UNSCEAR-2000 is used worldwide for dose

calculations [9]. But due to the different atmospheric condition and life style of the study area the indoor occupancy factor of 0.58 and outdoor of 0.29 was used for dose calculation. Annual effective dose due to exposure to radon and its short-lived progenies contribute maximum dose to the human population from natural sources of radiation. The outdoor radon exposure was calculated in terms of Working Level Month (WLM) year<sup>-1</sup> by using following equation.

$$\text{WLM year}^{-1} = [\text{Rn (Bqm}^{-3}) \times 0.58 \times 8760 \text{ hy}^{-1} \times 0.28] / [170 \times 3700 \text{ Bqm}^{-3}]$$

WLM per year was estimated from radon concentration is converted to effective dose using ICRP dose conversion factor [10]. Since terrestrial gamma radiation contribute a significant portion of the radiation exposure to the public the external gamma radiation. The indoor and outdoor radiation dose is evaluated to be 1.328 mSvy<sup>-1</sup> and 0.398 mSvy<sup>-1</sup> respectively (Table-3). The total dose due to radon and its progeny is slightly higher than the global and Indian average values. The gamma radiation (Fig.3) level was ranging from 60 to 200 nGyh<sup>-1</sup> with a mean value of 121 nGyh<sup>-1</sup>. The global outdoor radon concentration in different countries are provided in (Table-2). The average outdoor radon in the vicinity of the tailings pond areas in the present study is comparable with values observed in the USA [11] & Turkey [22] and lower than that of observed value in England [15]. The total annual external dose due to exposure to background gamma (Cosmic + Terrestrial) radiation is estimated to be 1.268 mSvy<sup>-1</sup> (Table-3). The total dose to the public residing in the villages near the tailings pond area due to exposure to radon and gamma radiation is estimated to be 2.99 mSvy<sup>-1</sup>. The estimated total annual dose to resident of the village situated nearby the tailing disposal site is within the typical range of global natural background radiation dose of 1-10 mSvy<sup>-1</sup> to the members of the public [9] and is not very significant.

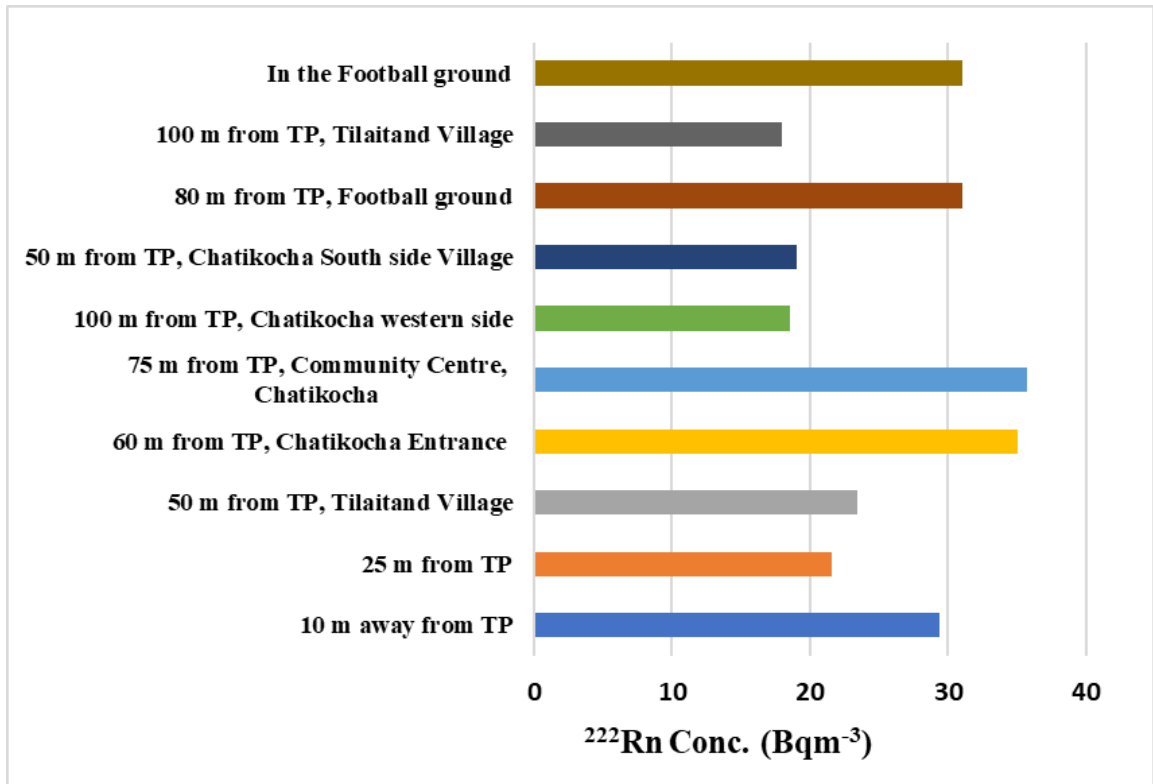


Figure 2. Outdoor  $^{222}\text{Rn}$  in the villages near the Tailing Pond (TP)

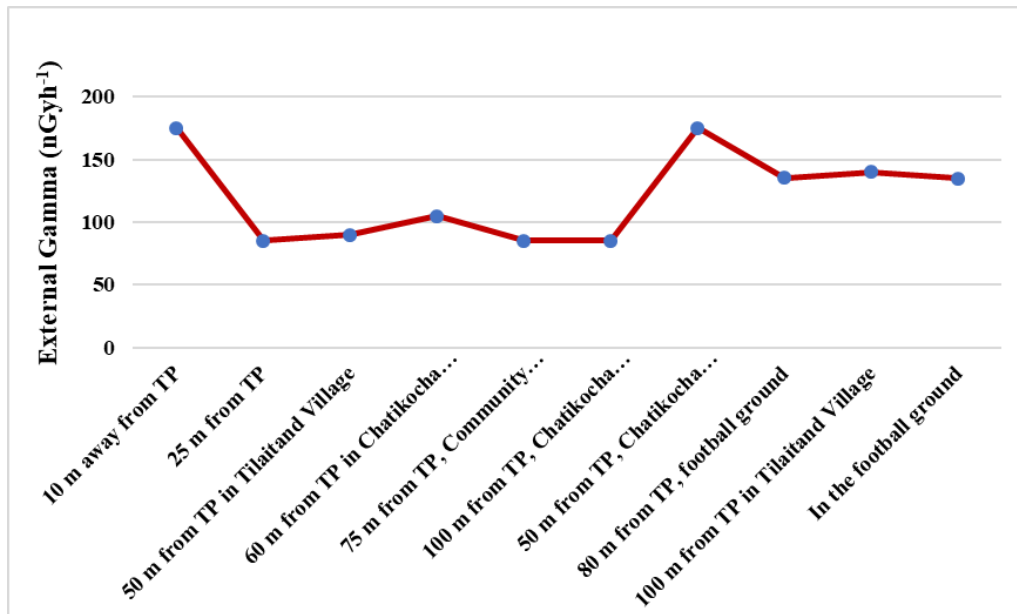


Figure 3. External gamma radiation near the Tailing Pond (TP) area

**Table-1. External gamma radiation & Outdoor  $^{226}\text{Rn}$  in the villages near the Tailing Pond (TP)**

Locations	$^{222}\text{Rn}$ Conc. ( $\text{Bqm}^{-3}$ )		External Gamma Level ( $\text{nGyh}^{-1}$ )	
	Range	Mean	Range	Mean
10 m away from TP	9.2-69.0	29.4	150 - 200	175
25 m from TP	7.4-91.0	21.6	60 - 110	85
50 m from TP, Tilaitand Village	5.5-34.5	23.4	60 -120	90
60 m from TP, Chatikocha Entrance	7.3-33.0	35.0	80 – 130	105
75 m from TP, Community Centre Chatikocha	35.0-36.0	35.7	60 – 110	85
100 m from TP, Chatikocha western side	7.1-40.1	18.5	60 - 110	85
50 m from TP, Chatikocha South side Village	6.0-42.0	19.0	150 - 200	175
80 m from TP, Football ground	22.0-36.0	31.0	120 - 150	135
100 m from TP, Tilaitand Village	5.0-33.0	18.0	130 – 150	140
In the Football ground	24.0-36.0	31.0	120 - 150	135
<b>Overall</b>	<b>5.5- 42.0</b>	<b>26.26</b>	<b>60-200</b>	<b>121</b>

1

**Table-2. Mean outdoor Radon in different countries**

Country	Rn ( $\text{Bqm}^{-3}$ )	Reference
USA, Iowa	29.0	Steck D. J. et al. [11]
USA, Minesota	19.0	Steck D. J. et al. [11]
Slovenia	19.0	Vaupotič J. et al. [12]
China	11.8	Wu Q. et al. [13]
Serbia	14.0	Žunic Z. S. et al. [14]
England	57.0	Wasikiewicz J. M. et al. [15]
Ireland	6.0	Gunning G.A. et al. [16]
Japan	6.1	Oikawa S. et al. [17]
Germany	9.0	Kümmel M. et al. [18]
Cyprus	5.6	Sarrou I. et al. [19]
East Asia	11.0	Zhuo W. et al. [20]
Syria	10.7	Shweikani R. et al. [21]
Turkey	34.0	Özen S. A. et al. [22]
<b>Present Study</b>	<b>26.26</b>	

**Table-3. Dose from external gamma radiation exposure and radon in the villages situated nearby to the tailing disposal site**

Sources	Components	Dose (mSvy <sup>-1</sup> )
External Gamma Radiation Exposure	Cosmic	0.315
	Terrestrial	0.953
Internal Exposure	Indoor radon	1.328
	Outdoor radon	0.398
	<b>Total Dose</b>	<b>2.99 mSvy<sup>-1</sup></b>

1

**4. Conclusions:** The annual natural background radiation dose to the inhabitant of villages in the vicinity of the uranium mill tailings pond estimated to be 2.99 mSvy<sup>-1</sup>. The estimated dose to the resident is within the typical range of global natural background radiation dose of 1-10 mSvy<sup>-1</sup> to the members of the public [9]. The contribution of radon and its progeny accounts close to 57.6% of the radiation dose to the villagers whereas gamma radiation contributes 42.4%. It can be concluded that the radiation doses received by people living in the village near the tailings pond are within the typical range of average worldwide exposure to natural radiation sources for the general public. Therefore, the radiological exposure for residents of villages located near the tailing disposal site is not significantly elevated.

**Acknowledgements:** Authors express their sincere thanks to Dr. D. K. Aswal, Director, Health Safety & Environment Group, BARC and Dr. S. K. Jha, Head, RPS(NF), HPD for their keen interest, constant encouragement and support during the study. Thanks are due to the UCIL management for extending the facilities and support to carry out the work. Co-operation received from other colleagues is duly acknowledged.

**References:**

- [1] ICRP-103, The 2007 Recommendations of the International Commission on Radiological Protection. Ann. ICRP. Publication: 103 (2007).
- [2] IAEA Technical Report Series No. 364, Handbook of parameter values for the prediction of radionuclide transfer in temperate environments(1994).
- [3] Gavrilesco M., Pavel, L. V. and Cretescu, I. Characterization and remediation of oils contaminated with uranium. J. Hazard. Mater. 163, 475-510 (2009).
- [4] Hakonson-Hayes A. C., Fresquez P.R., Whicker F.W., Assessing potential risk from exposure to natural uranium in well water. Journal of Environmental Radioactivity, Elsevier, 59, 29-40 (2002).
- [5] Jha S. et al. at al. Environmental Rn levels around an Indian U complex, Journal of Environ. Radioactivity, 48 (2000) 223-234.
- [6] Venkatraman K., Shastry, S. and Srinivasan, M. N., 1971, Jaduguda: Certain observations regarding uranium and base metals mineralization, Proc. Ind. Nat. Sci. Academy, vol.37 A. No.2 (1971).
- [7] Quindos Poncela, L.S, Fernandez Navarro, P.L., Gomez, J., Arozamena, Rodenas, Palomino, C., Sainz., C., Martin Matrranz, J.L. and Arteche, J. Population dose in the vicinity of old Spanish uranium mines. Sci. of Total Environment. 329. pp. 283-288 (2004).

- [8] Tripathi R. M., Sahoo S. K., Jha V. N., Kumar Rajesh, Shukla A.K, Puranik V.D. and Kushwaha H. S., Radiation dose to members of public residing around uranium mining complex, Jaduguda, Jharkhand, India. *Radiation Protection Dosimetry*, pp1-8 (2010).
- [9] UNSCEAR-2000. Sources, Effects and Risks of Ionizing Radiations, UNSCEAR 2000 Report to the General Assembly, with Scientific Annexes, UNSCEAR, United Nations, New York (2000).
- [10] ICRP-65, International Commission on Radiological Protection for Protection against radon at home and at work. *Ann ICRP* 23(2), ICRP publication 65, Pergamon Press, oxford (1993).
- [11] Steck D. J., Field R.W., Lynch C.F. Exposure to Atmospheric Radon. *Environ. Health Perspect.* 1999; 107:123–127.
- [12] Vaupotič J., Kobal I., Križman M.J. Background Outdoor Radon Levels in Slovenia. *Nukleonika.* 2010; 55:579–582.
- [13] Wu Q., Pan Z., Liu S., Wang C. Outdoor Radon Concentration in China. *Nukleonika.* 2016; 61:373–378. doi: 10.1515/nuka-2016-0062
- [14] Žunic Z. S., Yarmoshenko I.V., Birovljev A., Bochicchio F., Quarto M., Obryk B., Paszkowski M., Čeliković I., Demajo A., Ujić P., et al. Radon Survey in the High Natural Radiation Region of Niška Banja, Serbia. *J. Environ. Radioact.* 2007; 92:165–174. doi: 10.1016/j.jenvrad.2006.11.002.
- [15] Wasikiewicz J. M., Daraktchieva Z., Howarth C.B. Passive Etched Track Detectors Application in Outdoor Radon Monitoring. *Perspect. Sci.* 2019; 12:100416. doi: 10.1016/j.pisc.2019.100416.
- [16] Gunning G.A., Pollard D., Finch E.C. An Outdoor Radon Survey and Minimizing the Uncertainties in Low Level Measurements Using CR-39 Detectors. *J. Radiol. Prot.* 2014; 34:457–467. doi: 10.1088/0952-4746/34/2/457.
- [17] Oikawa S., Kanno N., Sanada T., Ohashi N., Uesugi M., Sato K., Abukawa J., Higuchi H. A Nationwide Survey of Outdoor Radon Concentration in Japan. *J. Environ. Radioact.* 2003; 65:203–213. doi: 10.1016/S0265-931X (02)00097-8.
- [18] Kümmel M., Dushe C., Müller S., Gehrcke K. Outdoor <sup>222</sup>Rn-Concentrations in Germany—Part 1—Natural Background. *J. Environ. Radioact.* 2014; 132:123–130. doi: 10.1016/j.jenvrad.2014.01.012
- [19] Sarrou I., Pashalidis I. Radon Levels in Cyprus. *J. Environ. Radioact.* 2003; 68: 269–277. doi: 10.1016/S0265-931X (03)00066-3.
- [20] Zhuo W., Furukawa M., Guo Q., Shin Kim Y. Soil Radon Flux and Outdoor Radon Concentrations in East Asia. *Int. Congr. Ser.* 2005; 1276: 285–286. doi: 10.1016/j.ics.2004.10.002.
- [21] Shweikani R., Hushari M. The Correlations between Radon in Soil Gas and Its Exhalation and Concentration in Air in the Southern Part of Syria. *Radiat. Meas.* 2005; 40: 699–703. doi: 10.1016/j.radmeas.2005.06.025.
- [22] Özen S. A., Celik N., Dursun E., Taskin H. Indoor and Outdoor Radon Measurements at Lung Cancer Patients' Homes in the Dwellings of Rize Province in Turkey. *Environ. Geochem. Health.* 2018; 40:1111–1125. doi: 10.1007/s10653-017-9991-9.



# Thermodynamic and Kinetic Studies on the Pyrophoricity of Uranium Flakes

Saparya Chattaraj\* and P. Srinivasan

Health Physics Division, Bhabha Atomic Research Centre, Trombay, Mumbai – 400085, India

Volume 1, Issue 5, October 2024

Received: 11 September, 2024; Accepted: 25 October, 2024

DOI: <https://doi.org/10.63015/7N-2442.1.5>

\*Correspondence Author - [saparya@barc.gov.in](mailto:saparya@barc.gov.in)

**Abstract:** The objective of this work was to arrive at quantitative estimates of pyrophoricity of uranium in different geometries. The major source of heat generation was identified to be exothermic chemical reactions of uranium with moist air. Time evolution of temperature was studied for uranium considering 3D conduction and convection heat loss routes using Finite Element Analysis. Auto ignition temperature for uranium flakes was quantified using heat balance equation and was found to be around 500 K. Excess heat generation rates needed to cause auto ignition of uranium flakes at room temperature were also estimated. The major sources of excess heat leading to its ambient ignition could be attributed to friction and other exothermic chemical reactions of process impurities in uranium.

**Keywords:** Pyrophoricity, Uranium flakes, Finite element method, Geometry dependence

**1. Introduction:** Fossil fuels take several thousand years to get formed. However, its rate of consumption is very rapid. Considering the current energy crisis, it has been felt that the nuclear fuel can be considered to be an appropriate alternative. The conventional fuel used for the nuclear reactors is uranium (U) in several forms viz. metallic, oxide etc. Different nuclear reactors use uranium in different forms as a fuel for an optimized power profile. U is mined and is processed before it can be used as nuclear fuel for use in reactor. Spent fuel removed from a reactor, after it has reached the end of its useful life, can be reprocessed to recover valuable fissile materials.

An ‘open nuclear fuel cycle’ means direct disposal of the spent fuel from the reactor and a ‘closed nuclear fuel cycle’ includes reprocessing of the spent fuel for recovery and reuse of valuable fissile materials. India has a poorer reserve of U than many other countries; so, closed nuclear fuel cycle is adopted here for proper utilization of the resources.

The ‘front end’ of the nuclear fuel cycle includes, U mining, milling, conversion and fuel fabrication.

Handling/processing of spent nuclear fuel is carried out in ‘back end’ of the nuclear fuel cycle which includes, spent fuel storage, reprocessing, U and Pu recycling, spent fuel disposal and waste management.

Both the front end and the back end processes involve storage and handling of U in various forms. U is subjected to mechanical operations like machining, cutting and metallurgical operations like melting and casting into different shapes and sizes. Also storage and handling of U in finely divided powder forms is a common requirement during processing.

It is observed that U in finely divided forms is highly pyrophoric even at ambient conditions. ‘Pyrophoricity’ is a property of a material used to describe how easily it ignites at ambient conditions. Thus there exists a potential for fire accidents in the nuclear facilities which deal with U in various forms especially in form of fine powders and turnings. Moreover, U could attain high temperature due to internal self-heating and hence demands proper ventilation in storage areas. From a radiological perspective it may be noted that the fine air suspended particles formed during burning can cause inhalation hazards due to the toxicity.

USDOE Report, ANS, 1994 suggested a description of cause, effect and preventive measures of metallic fires [1]. It states that spontaneous combustion is the ignition of a combustible material caused by the accumulation of heat from oxidation reactions. The extent of pyrophoricity mainly depends on the following factors viz. the specific surface area of the reacting metal, concentration of moisture and other vapors in air, temperature, oxygen concentration and presence of protective oxide layer.

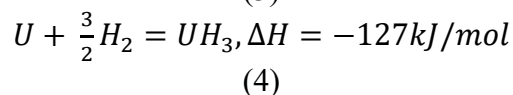
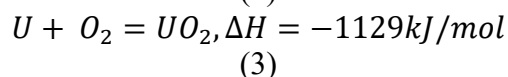
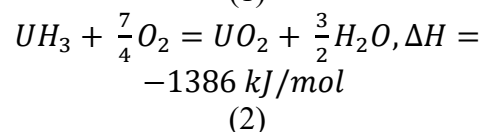
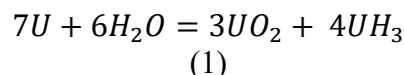
In case the rate at which the heat is generated, via oxidation, is larger than that of heat being removed through thermal radiation, convection and conduction the material could ignite spontaneously. Ignition temperature and the specific area of the pyrophoric substance are two important factors of concern. As a best practice, inflammable materials are not stored in contact with radioactive substances.

Special techniques are to be adopted towards extinguishing the fire in case of any emergency associated with fire in radioactive material. Eutectic mixture of Ba, K and Na (commercial name: ANSUL powder) is the commonly used fire extinguisher in case of fire involving U in metallic form.

The first source of heat generation for pyrophoricity that can be thought of is radioactive decay heat due to U (considering Nat. U) and its progeny. The progeny concentration of the decay products can be calculated using the Bateman Equation [2]. The second source of heat leading to pyrophoricity of U is the exothermic chemical reactions when exposed to the ambient environment. The rate and exothermicity of the reactions are to be studied for a better understanding of the pyrophoricity phenomena and the design of engineering controls for U-storage systems. Studies show that the heat generation due to radioactive decay is insignificant in comparison to the heat generation due to chemical reactions [3]. Hence, for this study we have focused on heat generation by chemical reactions only.

Guyadec et al in 2009, proposed a mechanism for spontaneous ignition of U powders [3].

This includes a set of exothermic reactions which take place when the same is exposed to the ambient conditions.



Totemeier in 2000 suggested that the kinetics of oxidation and corrosion of U are characterized in terms of the specific reaction rate (k) [4]. This constant is related either to the weight gain of the specimen per unit area or the amount of metal reacted per unit area related by an equation,

$$\frac{\Delta W}{A} = kt^n \quad (5)$$

Where,  $\Delta W$  is weight gain of the specimen after reaction or mass of the metal reacted, A is the reacting surface area of the material, 't' is the time, 'n' is the empirical exponential factor.

The two principal methods for the estimation of the specific reaction rate are as follows,

- (i) Continuous measurement of the specific mass of the specimen which is exposed to the oxidizing environment, gravimetrically.
- (ii) Amount of gas reacted for closed systems can be estimated using pressure sensing devices like manometer.

The modes of gaseous oxidation reactions of U in environment are segregated into three main groups viz. i) reaction with oxygen and dry air, ii) reaction with water vapor and iii) reaction with moist air (i.e. moisture and oxygen). U on reaction with oxygen forms a superstoichiometric  $UO_2$ . For temperatures below  $400^\circ\text{C}$ , the initial kinetics was found to be linear quadratic rather than linear. A subsequent transition to higher linear rate is generally observed. This final linear rate of oxidation is pertinent with respect to long term storage. The initial parabolic rate law

commonly observed for U oxidation in air suggests that the rate limiting step of the initial U oxidation process is the diffusion of oxygen ions through the growing oxide lattice. The transition to linear oxidation rate is related to the onset of oxide cracking, with the linear rate controlled by diffusion of oxygen ions through the oxide layer whose thickness remains constant throughout the further oxidation process. The mechanism of U oxidation by water vapour is similar to the dry air oxidation mechanism. The first step is the adsorption of water molecule on the oxide surface. Winer et al (1987) postulated that the oxidation occurs via dissociation of water molecule via hydrolysis reaction [5]. In case of oxidation of U in moist air, oxygen has an inhibitory effect. Addition of oxygen considerably lowers the rate of the U-water vapour reaction. Ritchie et al in 1986 showed that the reaction rate increases as water vapour is added to U-oxygen system up to relative humidity of 1-2% [6]. In the range of 2%-90% relative humidity, the reaction rate is constant. Above 90% relative humidity, the reaction rate again increases.

McGillivray et al in 1994 performed a detailed investigation on the oxidation of U-oxygen-water vapour system [7]. They developed a model based on Langmuir monolayer adsorption isotherm in the temperature range of 115°C to 350°C and a water vapour pressure range of 0-47 kPa. Their experimental results concluded that the reaction of U with water vapour predominates over all the other possible reaction routes. On increasing the water vapour pressure, the specific reaction rate increases. Moreover, from the heat of the reaction consideration we see that the uranium hydride oxidation has the highest exothermicity. Thus, for a conservative estimate of pyrophoricity due to chemical reaction, we choose this pathway for an in depth analysis.

The most common method to characterize the pyrophoric nature of uranium is the burning curve method [8]. In this method the specimen and furnace temperatures are recorded as a function of time. When the specimen ignites i.e. the oxidation reaction becomes self-

sustaining the specimen temperature increases drastically. The ignition temperature is determined as the specimen temperature curve deviates from the furnace temperature curve. Ignition temperature can also be estimated from the shielded ignition test. In this test, the specimen is heated in an inert atmosphere till the furnace reaches a specified temperature. Then an oxidizing atmosphere is admitted and the specimen temperature is noted as a function of time. If the test temperature is higher than the specimen ignition temperature, the specimen will ignite with a corresponding dramatic change in temperature. Else the self-heating to oxidation will be very feeble. The most important parameter for estimating pyrophoricity of a material is the ignition temperature of that specimen. It is the temperature at which the heat generation rate is more than that of the heat loss, thus leading to drastic rise in temperature. Thus, estimation of ignition temperature of U in different forms and geometries was an important exercise to do.

Plys et al in 2000 suggested a basic model for the estimation of pyrophoricity of U fines in spent fuel [9]. The model considers heat generation due to chemical reactions and dissipation due to conduction and convection. They coined a term called the ignition parameter (B), whose value gives an idea of pyrophoricity. B is basically defined as the ratio of heat generation to that of the heat dissipation. If  $B > 1$ , the system is pyrophoric and for  $B < 1$ , the system is not pyrophoric.

However, the model by Plys et al doesn't consider the effect of the extent of diffusion in the oxide layer formed at initial phase of oxidation. Kanouff et al in 2013 proposed an 'ionic diffusion oxidation' model of U for the low temperature oxidation of U exposed to air [10]. The model is based on the diffusion of oxygen ions through oxide film driven by the electrostatic potential generated between the metal and the adsorbed oxygen ions. The value of the diffusion coefficient (D) is defined as,

$$D = 4. a^2. v. \exp\left(-\frac{W}{k_b \cdot T}\right) \quad (6)$$

where,  $a$  = Lattice parameter i.e. distance between two U atoms in the crystal,  $v$ = Vibrational frequency of O atoms in  $UO_2$ ,  $W$  = Activation energy for chemical diffusion of  $O_2$  in U,  $T$ = Ambient temperature,  $k_b$ = Boltzmann constant

This formula was adapted to estimate the diffusion coefficient for oxygen in U matrix.

Then the depth till which the moisture penetrates into the U-matrix was determined using the solution of Fick's Second Law of Diffusion for the case where the surface is in contact with an infinite long reservoir of fixed concentration of solute.

$$\frac{C_s - C_x}{C_s - C_0} = \text{erf} \left( \frac{x}{2\sqrt{Dt}} \right) \quad (7)$$

where,  $C_s$  = surface concentration of solute,  $C_0$  = initial concentration of solute in the solid,  $x$  = distance from the surface,  $D$  = diffusivity of solute and  $t$  = time

The most prominent heat loss mechanism for a large body is conduction. It is a method of heat loss due to internal molecular collisions [11]. Fundamental equation for non-steady state conduction is,

$$\nabla^2 T + \frac{1}{\kappa} Q_v - \frac{1}{\rho c_p} \frac{\partial T}{\partial t} = 0 \quad (8)$$

where,  $\kappa = \frac{k}{\rho \cdot c_p}$ ,  $k$  = conductivity of U,  $\rho$ = density of U,  $c_p$  = specific heat capacity,  $Q_v$  = volumetric heat generation rate

First term takes care of the heat diffusion (the Fickian term), second term caters for the heat generation in the body and third term takes care of the temporal behavior of heat loss.

**2. Computational Details:** Initially, a benchmarking exercise was carried out to verify the agreement of the FEM based software with traditional methods to study heat transfer. The results are presented in the supplementary section [13].

Convection is a more prominent method of heat loss for flakes and turnings, where air can flow through the cavities and remove the heat.

$$q = h \cdot A \cdot (T_s - T_a) \quad (9)$$

where,  $q$ = heat generation rate,  $h$ = coefficient of convection,  $A$ = Area of the body,  $T_a$ = Air temperature,  $T_s$ = surface temperature

Radiation is less prominent. But for a condition when the metal is about to burn, it will play a significant role. Again this method of heat loss will be encountered in metallic fines and chips.

The governing equation is,

$$q = \sigma \cdot \epsilon \cdot A \cdot (T_s^4 - T_a^4) \quad (10)$$

where,  $\sigma$  = Stefan-Boltzmann Constant,  $\epsilon$  = Emissivity of the surface

The time evolution of temperature in different geometries of U was studied using a Finite Element Method (FEM) based software. The FEM analysis generally converts a partial differential equation to a set of algebraic (or at most ordinary differential) equations which are solved through a variational technique that makes the method robust. Moreover, it can be applied to systems with irregular shapes [12].

Herein we have presented the conservative estimates of the rise in temperature and ignition temperature of U in different geometries (especially flakes) and in different conditions, using basic thermodynamics and kinetic equations considering relevant chemical reactions. The results of this study provide upper bound estimates of pyrophoricity of uranium in different forms, which could be utilized for safe storage and handling.

The thermal analysis module of the software was used to study the 3D chemical heat generation, conduction and convection losses in the most vulnerable geometries of U. Three cuboids of different dimensions as shown in *Figure 1* were considered for the study [14].

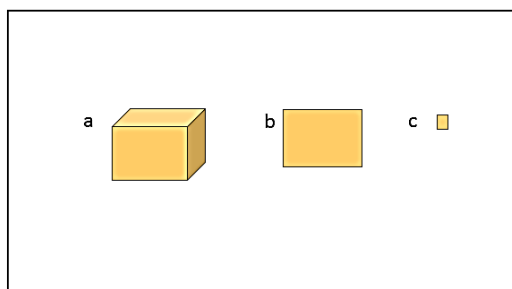


**Figure 1. Representative models of a (a)cuboidal block, (b)sheet and a (c)flake of U.**

It is assumed that the heat generation rate on the outer surface area is nearly equal to the volumetric heat generation rate in the outermost reacting layer. This assumption is supported by the fact that the reacting depth obtained from ionic diffusion oxidation model is nearly four orders lesser than that of the thinnest dimensions considered for different geometries. The volumetric heat generated rate is defined as,

$$Q_v = (A_s/V).k_0.\Delta H.\exp(-T_E/T) \tag{11}$$

where, ‘ $A_s$ ’ is the surface area, ‘ $V$ ’ is the volume, ‘ $k_0$ ’ is the specific reaction rate, ‘ $\Delta H$ ’ is the heat of  $UH_3$  oxidation reaction, ‘ $T_E$ ’ is the normalized activation energy of the same reaction and ‘ $T$ ’ is the ambient temperature.

The values of the relevant parameters are obtained from Pearce correlation (Pearce, 1989) as it matches with the storage condition. Pearce correlation in the given condition are as follows [15],

For relative humidity < 100%,  $UH_3$  oxidation reaction route and  $T < 192^\circ C$ ,  $k_0 = 1.023 \times 10^5 \text{ kg/m}^2/\text{s}$ ,  $T_E = 11490 \text{ K}$  and  $n = 0.3$ .

The reacting depth ( $d$ ) was used as obtained from Eqns. 6 & 7. Volume under consideration can be defined as the product of the surface area ( $A_s$ ) and the reacting depth.

At 313K the volumetric heat generation rate comes out to be,

$$Q_v = \left(\frac{1}{d}\right).k_0.\Delta H.\exp\left(-\frac{T_E}{T_m}\right) = 3970 \text{ Jm}^{-3}\text{s}^{-1} \tag{12}$$

Thus the areal heat generation rates on all surfaces is assumed to sufficiently account for the heat generation due to chemical reactions. Heat losses are simulated by providing

convective boundary conditions on all the surfaces. For a restrictive study, for heat loss by air convection the convective heat transfer coefficient was taken as  $10 \text{ Wm}^{-2}\text{K}^{-1}$ .

In FEM, the material model is created by specifying the conductivity, specific heat capacity and density of U. Conductivity ( $k$ ) =  $27.5 \text{ Wm}^{-1}\text{K}^{-1}$ , Specific Heat ( $C_p$ ) =  $117.23 \text{ Jkg}^{-1}\text{K}^{-1}$ , Density ( $\rho$ ) =  $19,000 \text{ kgm}^{-3}$

Hexagonal meshing is chosen for the FEM calculations as it gives the best approximation to solid block geometries.

A transient thermal analysis is carried out to see the temperature evolution in a time range of  $10^5 \text{ s}$  (~ a day). 100 numbers of stepwise iterations were carried out for optimum computation efficiency.

Employing a simplistic approach, the auto-ignition temperature of U flakes was estimated using heat balance equation.

**Heat generation due to chemical reactions = Heat loss due to convection + Heat loss due to radiation**

$$Ak_0 \exp\left(-\frac{T_E}{T}\right)\Delta H = hA(T_s - T) + \sigma \epsilon A(T_s^4 - T^4) \tag{13}$$

where ‘ $T_s$ ’ is the surface temperature and rest of the symbols have their usual meanings.

When we plot the heat generation rate due to reactions, heat loss rate due to convection and radiation, heat loss due to pure convection and heat loss due to pure radiation vs. temperature in the same plot, we arrive at the steady state temperatures from the intersection points.

Further, the excess heat generation rates ( $\frac{Q}{A}$ ) needed to cause ignition at room temperature were estimated using the following equation,

$$k_0.\Delta H.\exp\left(-\frac{T_E}{T_m}\right) + \frac{Q}{A} = h.(T_m - T_s) + \sigma.\epsilon.(T_m^4 - T_s^4) \tag{14}$$

and their probable sources are discussed in subsequent sections.

**3. Results & Discussions:** Using the Ionic Diffusion Oxidation Model and substituting the values of the parameters in Eq. 7, we get a plot of how deep the moisture penetrates into

the U-matrix when exposed to the ambient moisture for different time ranges.

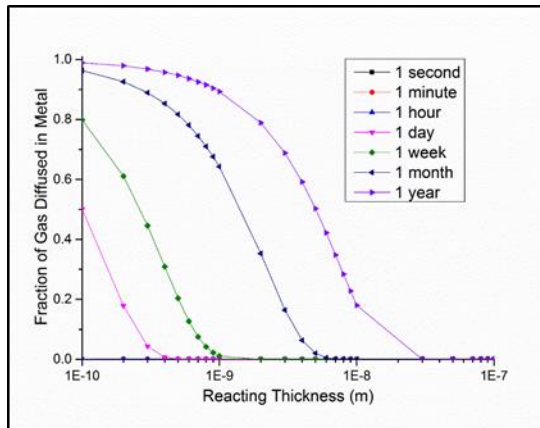


Figure 2. Plot of fraction of solute gas diffused into the metal with varying reacting thickness

Figure 2 shows that for a long term storage of about one year, moisture diffuses up to a thickness of  $0.1\ \mu\text{m}$ . This conservative estimate of reacting thickness was used for further studies to simulate extended storage periods. Extent of diffusion for time ranges viz. seconds, minutes and hours are negligible. The output from the FEM analysis i.e. the rise in temperature of U considering the three different geometries as a function of time is presented in a consolidated graphical form in Figure 3.

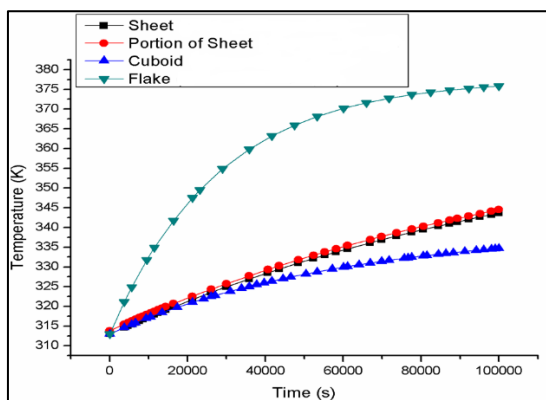


Figure 3. Plot of temperature evolution of U in different geometries

It is observed from Figure 3 that in the given model, the rise in temperature is steepest for the thinnest geometry i.e. the flake, followed by sheet and then a cuboid. This is because the only mode of predominant heat loss is convection for a flake. Thus, the heat generated

by chemical reactions is not quickly dissipated leading to the steep rise in temperature.

When we plot the heat generation rate due to reactions, heat loss rate due to convection and radiation, heat loss due to pure convection and heat loss due to pure radiation vs. temperature in the same plot (using Eqn. 13), we arrive at the steady state temperatures from the intersection points. Any temperature higher than the steady state temperature will have heat generation larger than heat loss, indicating the onset of auto-ignition phenomenon.

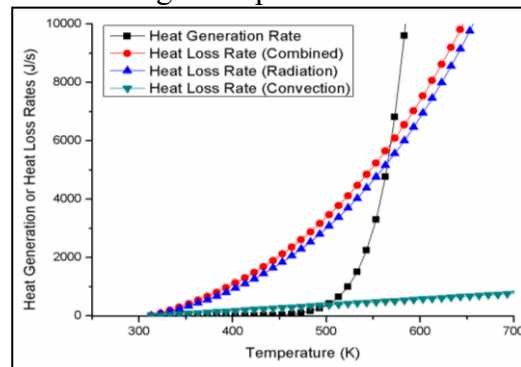


Figure 4. Plot of heat generation or heat loss rates vs. temperature

For the most conservative estimate, the heat loss only by convection was considered. The above equation was further solved numerically to obtain the steady state temperatures for the U-flakes.

Table 1: Table for Steady State Temperature achieved for Different Heat Loss Modes

Heat Loss Type	Steady State Temperature (K)
Combined Loss	569
Radiation	566
Convection	501

From Table 1 it is seen that the ignition temperature for flakes is much higher than ambient temperature ( $\sim 300\ \text{K}$ ). Thus a significant amount of other heat source is required for U to auto-ignite at room temperature. Also, larger exposed surface area to volume ratio, will render larger heat generation.

The excess heat generation rates needed for auto-ignition at different ambient temperatures are given in Table 2.

**Table 2: Table for Excess Heat Generation Rates Needed for Auto-Ignition at Different Ambient Temperatures**

Ambient Temperature (K)	Steady State Temperature (K)	Excess heat generation rate per unit area ( $\text{Jm}^{-2}\text{s}^{-1}$ )
298	502	3169
303	502	3121
308	501	3071
313	501	3018

The results in Table 2 depict, significant amount of additional heat source is required for uranium to auto-ignite at room temperature. Also, larger the exposed surface area to volume ratio, higher will be the heat generation. The major sources of heat leading to pyrophoricity may be in physical or chemical form. Friction during processing might be one of physical forms of heat generation. Contamination in U with other process related chemical species can lead to exothermic reactions, which can add up to the heat input.

Presence of chemical impurities and other physical phenomena could supply enough energy to cross the activation barrier for uranium oxidation reaction which might lead to a rise in temperature, finally causing ignition. These explanations will be useful to corroborate with the observed pyrophoricity behaviour of uranium compounds in various storage-handling conditions and to design the appropriate engineered control measures. Further specific studies using known concentration of chemical impurities in uranium will help in arriving at impurity-specific heat generation rates to suit various processing conditions in facilities.

**4. Conclusions:** Pyrophoric behaviour of U flakes is studied using a finite element based technique. It has been observed that the thin geometries are associated with the steep rise in

temperature. Quantitative estimates of the steady state temperatures for ignition of flakes are obtained. Important insights into the mechanism of pyrophoricity is also attained i.e. the pyrophoric behaviour of uranium flakes is mainly due to the exothermic reactions it undergoes with moist air; which can be further aggravated in the presence of other heat sources like friction, chemical contamination etc. [16]

**Acknowledgements:** Authors are thankful to Shri D. P. Rath, Dr. Ashokkumar P., Dr. S.K. Jha and Dr. D.K. Aswal, Health Physics Division, Health, Safety & Environment Group, BARC, Mumbai for their encouragement and constant support during this work.

**Conflict of Interest:** Authors declare No conflicts of interest.

## 5. References:

- [1]. Primer on Spontaneous Heating and Pyrophoricity, *DOE-HDBK-1081-94*, 1994, U.S. Department of Energy
- [2]. H. Bateman, The solution of a system of differential equations occurring in the theory of radioactive transformations, *Proc. Cambridge Philos. Soc.*, 15, 1910, V, 423–427
- [3]. F. Le Guyadec, X. Génin, J. P. Bayle, O. Dugne, A. Duhart-Barone, C. Ablitzer, Pyrophoric behaviour of uranium hydride and uranium powders, *J. Nucl. Mater.*, 396, 2010, 294-302
- [4]. T.C. Totemeier, Characterization of uranium corrosion products involved in a uranium hydride pyrophoric event, *J. Nucl. Mat.*, 278(2-3), 2000, 301-311
- [5]. K. Winer, C.A. Colmenares, R.L. Smith, and F. Wooten, Interaction of water vapor with clean and oxygen covered Uranium surfaces, *Surface Science*, 67, 1987, 183
- [6]. A.G. Ritchie, A Review of the Rates of Reaction of Uranium with Oxygen and Water

Vapour at Temperatures Up to 300°C, *J. Nucl. Mat.*, 102, 1981, 170-182

[7]. G. W. McGillivray, D.A. Geeson, R.C. Greenwood., Studies of the Kinetics and Mechanism of the Oxidation of Uranium by Dry and Moist Air, *J. Nucl. Mat.*, 208, 1994, 81-97

[8]. C.W. Solbrig, J.R. Krsul, and D.N. Olsen, Pyrophoricity of Uranium in long term storage environments, *DOE Spent Nuclear Fuel-Challenges and Initiatives*, 1994, ANS

[9]. M.G. Plys, and B. Malinovic, IWTS Metal-Water Reaction Rate Evaluation, *FAI/99-26*, 2000, Fauske & Associates, Inc., Burr Ridge, IL

[10]. M. P. Kanouff, P. E. Gharagozloo, M. Salloum, A. D. Shugard, A multiphysics numerical model of oxidation and decomposition in a uranium hydride bed, *Chem. Eng. Sci.*, 91, 2013, 212-225

[11]. J.M Abbott, H.C Smith, M.M. Van Ness, *Introduction to Chemical Engineering Thermodynamics* (7th ed.). ,Boston Montreal: McGraw-Hill, 2005

[12]. D. Baguley, and D. R. Hose, *How to Plan a Finite Element Analysis*, 1994

[13]. T. J. Dekker, "Finding a zero by means of successive linear interpolation", in *Constructive Aspects of the Fundamental Theorem of Algebra*, London: Wiley-Inter Science, 1969

[14]. P. Srinivasan and A. K. Ray., Radiological Shielding and Pyrophoric condition analysis of storage of metal uranium ingots at designated storage area, RISP, Hall-6, *Design Report*, 2011

[15]. R.J. Pearce, *CEGB Report RD/B/6231/R89*, Central Electricity Generating Board, Berkeley Nuclear Laboratories, UK, 1989,

[16]. S. Chattaraj, *Assessment of Pyrophoric Behavior of Uranium Flakes for Safe Storage and Handling*, Homi Bhabha National Institute, Mumbai, India, 2016



# CNS&E

Current Natural  
Sciences &  
Engineering

[www.cnsejournals.org](http://www.cnsejournals.org)

e-ISSN

3048-460X

CNS&E Journal papers are widely available in Google Scholar, Research Gate and in other citation platforms.



CNS&E Journal assigns DOIs to published articles for international citation.

The journal uses Turnitin software to ensure originality and it provides readers with reliable, plagiarism-free scientific research.

Globally  
Visible

Peer  
Reviewed

A  
Comprehensive  
Interdisciplinary  
Partially Open  
Access  
Journal

Easy  
Submission,  
Quick  
Publication  
in 40 days

**CNS&E Editorial Board Comprises of Globally Renowned S & T Luminaries & Advisory Support from World Top Institutes' Leaders**

Current Natural Sciences & Engineering (CNS&E), a bimonthly journal, publishes new, innovative and cutting-edge research in:

- Natural Sciences
- Health Science
- Nuclear science
- Agricultural Science
- Environmental Science
- Nanomaterials
- Hydrogen Energy
- Net Carbon Zero
- Industrial R&D
- Engineering & AI

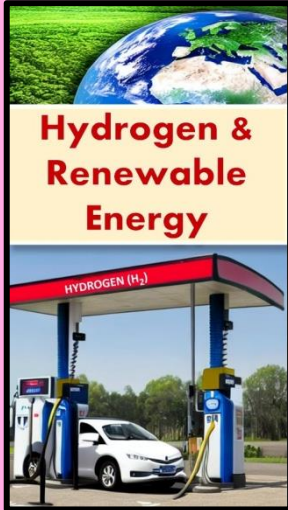
**No Article Processing  
Charges !!!**  
For 3 months

**The Most  
Valuable & Biggest  
Journal on  
New Science  
from India**

**A Unique Platform to Boost your Research Impact Globally !**

# CNS&E

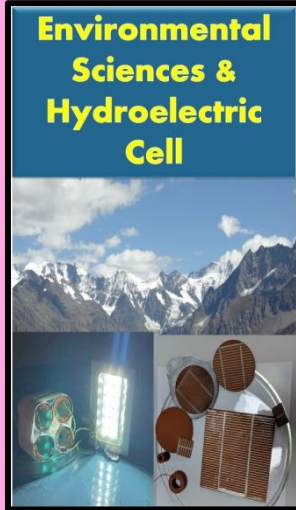
Current Natural  
Sciences &  
Engineering



**Hydrogen & Renewable Energy**

HYDROGEN (H<sub>2</sub>)

A collage featuring a green globe, a hydrogen fuel station with a car, and a blue hydrogen tank.



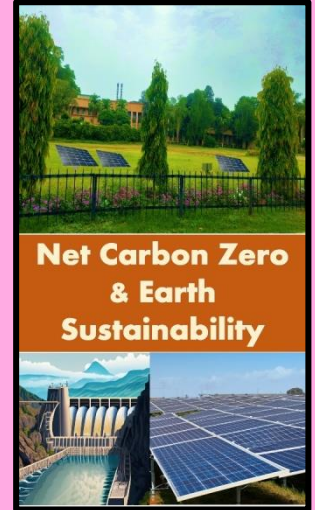
**Environmental Sciences & Hydroelectric Cell**

A collage showing a snowy mountain range, a hydroelectric dam, and various scientific instruments like a microscope and a fan.



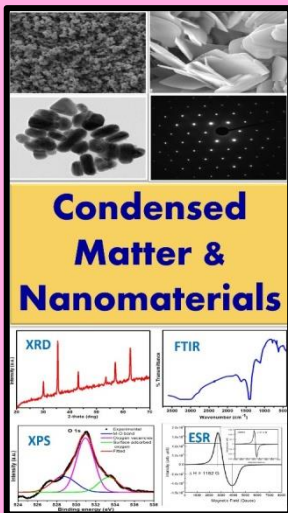
**Artificial Intelligence Convergence in S&T**

A collage featuring a robotic hand, a futuristic AI head, and a server room.



**Net Carbon Zero & Earth Sustainability**

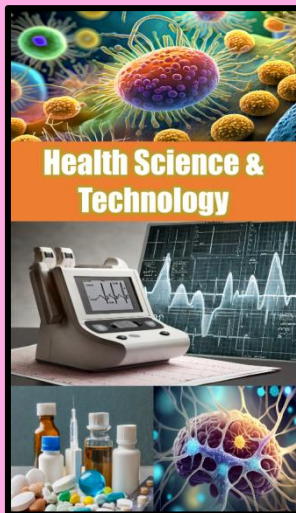
A collage showing a green landscape with solar panels, a dam, and a large solar farm.



**Condensed Matter & Nanomaterials**

XRD FTIR XPS ESR

A collage of microscopic images, chemical structures, and scientific graphs.



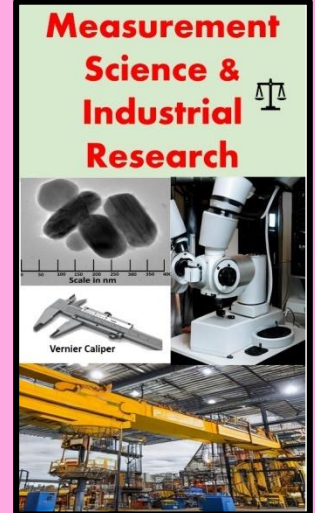
**Health Science & Technology**

A collage of colorful cells, a medical device, and a person in a hospital bed.



**Nuclear Science: Health & Society**

A collage of a nuclear atom, a particle detector, and a medical scanner.



**Measurement Science & Industrial Research**

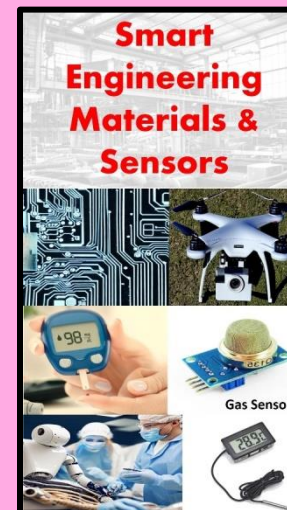
Scale in nm Vernier Caliper

A collage of industrial machinery, a microscope, and a scale.



**Digital & Sustainable Agriculture**

A collage of a farm with digital icons, a tractor, and a field with irrigation.



**Smart Engineering Materials & Sensors**

Gas Sensor

A collage of a circuit board, a drone, a gas sensor, and a person in a lab.